Doctoral Thesis

A study on enhancement of wetting resistance in membrane distillation (MD) by engineering the physical morphology and modifying the surface energy through chemical fluorination

Hyung Kae Lee

Department of Urban and Environmental Engineering
(Environmental Science and Engineering)

Ulsan National Institute of Science and Technology

2021

A study on enhancement of wetting resistance in membrane distillation (MD) by engineering the physical morphology and modifying the surface energy through chemical fluorination

Hyung Kae Lee

Department of Urban and Environmental Engineering
(Environmental Science and Engineering)

Ulsan National Institute of Science and Technology

A study on enhancement of wetting resistance in membrane distillation (MD) by engineering the physical morphology and modifying the surface energy through chemical fluorination

A thesis/dissertation submitted to UNIST
in partial fulfillment of the
requirements for the degree of
Doctor of Philosophy

Hyung Kae Lee

18/06/2021 of submission

Approved by
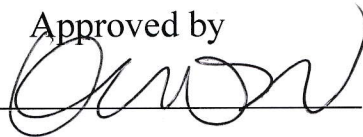
_____

Advisor

Young-Nam Kwon

A study on enhancement of wetting resistance in membrane distillation (MD) by engineering the physical morphology and modifying the surface energy through chemical fluorination

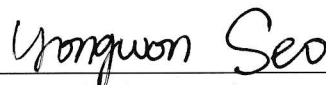Hyung Kae Lee

This certifies that the thesis/dissertation of Hyung Kae Lee is approved.

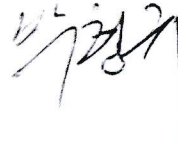18/06/2021 of submission

_____
Advisor: Young-Nam Kwon

_____
Yongwon Seo: Thesis Committee Member #1

_____
Changsoo Lee: Thesis Committee Member #2

_____
In-Chul Kim: Thesis Committee Member #3

_____
Hyung-Gyu Park: Thesis Committee Member #4

Abstract

Currently, water treatment is required to provide clean water worldwide. Among many studies for water treatment, membrane distillation (MD) is one of the emerging technologies. The MD is a process that utilizes the temperature difference between the high-temperature feed solution and the low-temperature permeate solution, and the vapor generated due to this temperature difference passes through the membrane and then finally condenses to become a high-quality distillate. Less thermal energy is required for the generation of vapor because of the temperature difference, and almost 100% of non-volatile contaminants can be removed. However, if the generated vapor condenses inside of the pores, the membrane becomes wet. After the pores are wet, the feed solution can pass directly, reducing the removal rate and reducing the lifetime of the membrane.

To solve this wetting problem, many studies are focus on the hydrophobicity of the membrane. For this, many types of hydrophobic polymers were applied. Mainly used hydrophobic polymers include polypropylene (PP), polytetrafluoroethylene (PTFE), polyvinyl chloride (PVC), and polyvinylidene fluoride (PVDF). However, there is a limit to the hydrophobicity a material can exhibit. Therefore, various studies have been conducted to improve the hydrophobicity of membranes to overcome the limitation. However, various previous studies still need improvement in performance decline, fouling, and wetting issues. First, coating methods that have been widely used to date have weaknesses such as poor performance and poor stability. Next, as a new method to increase hydrophobicity, the method of increasing hydrophobicity by applying a pattern on the surface is in the spotlight. However, this method has a problem in that it is difficult to make a pattern and fouling easily occurs due to an increase in roughness.

To address the performance decline and poor stability in the coating method, the PVDF membrane was modified through four steps: pore expansion by a plasma treatment, hydroxylation of the membrane by the Fenton reaction, generation, and growth of nanoparticles (NPs) on the hydroxylated functional groups in pores, and hydrophobic modification using fluorine chemical. The membranes modified by the methods proposed in this study did not lose their hydrophobicity and maintained the flux over a significantly longer period MD test. The PVDF membrane modified by hydrophobic NPs attached inside enlarged pores exhibited a minimized flux reduction and significantly higher antiwetting stability. Sonication was also applied to test the stability of the NPs grown from the PVDF membrane. This result support that NPs grown from the hydroxyl functional group on PVDF enhance the stability.

For overcoming the further performance change, a lot of research is being conducted on patterned membranes as a new technology, but it has the disadvantages such as difficulty to prepare a

patterned membrane and fouling issue because of pattern on the surface. To overcome the issues in patterning studies, the template was used for easy fabrication of patterned membrane, and low surface energy was achieved polymerization of hydrophobic chemical on the membrane. To prepare the pattern surface, a polyvinylidene fluoride-co-chlorotrifluoroethylene (PVDF-CTFE) membrane was poured on a template having a specific structure. It has been found that patterned membranes with hierarchical microstructures are more hydrophobic than those with flat surfaces. It was also confirmed that the patterned membranes have high resistance in wetting in direct contact membrane distillation (DCMD) showing stable performance over a longer period compared to membranes with flat surfaces. However, the patterned membrane has the problem of rapid performance decline during fouling testing due to the deposition of foulants. In this study, the fouling issue was solved through polymerization with 1H, 1H-perfluorooctyl methacrylate (FOMA) which makes membrane have low surface energy. After surface polymerization with FOMA, it was confirmed that the superhydrophobic patterned membrane showed any performance decline in the DCMD process with foulants such as humic acid (HA), alginic acid (AA), and bovine serum albumin (BSA). In addition, it was confirmed that it did not get wet for more than 7 days in the actual DCMD process due to the higher hydrophobicity due to the lower surface energy as well as the rough surface due to the patterned surface.

For the last, a new approach to prevent wetting of the membrane was investigated. As the reason for the wetting in the MD process, the vapor generated by the temperature difference between feed and permeate solution is condensed inside of the pores. To prevent this phenomenon, as a next-generation technology to prevent wetting, the internal temperature of the membrane increased by heating to prevent the vapor from condensing inside the pores. To achieve the heating membrane, a PVDF membrane was prepared using a copper mesh as a substrate which has good thermal conductivity, and it was possible to prevent wetting by transferring heat during the MD. Sweep gas MD (SGMD) was used to confirm the prevention of wetting through heating of the membrane. In the case of proceeding without applying heat, it was found that the membrane gets wetted so that feed solution passes through dramatically, whereas when the temperature of the membrane was increased by applying heat, it was confirmed that the membrane was not wetted over 2500 min. Furthermore, to enhance the thermal conductivity of the membrane, carbon nanofiber (CNF) was added into the dope solution before fabrication. With CNF, heat can be transferred more efficiently so that wetting could be prevented over 3500 min in SGMD.

Contents

List of Figures

VII

List of Tables

Nomenclature and Abbreviation

AA	**Alginic acid**
AGMD	**Air gap membrane distillation**
ATR-FTIR	**Attenuated total reflectance Fourier-transform infrared**
ATRP	**Atom transfer radical polymerization**
BiBB	**α-Bromoisobutyryl bromide**
BSA	**Bovine serum albumin**
CA	**Contact angle**
CA	**Cellulose acetate**
CNF	**Carbon nanofibers**
CTA	**Cellulose triacetate**
CVD	**Chemical vapor deposition**
DCM	**Dichloromethane**
DCMD	**Direct contact membrane distillation**
DMAc	**Dimethylacetamide**
DS	**Draw solution**
DS	**Draw solution**
DVB	**Divinylbenzene**
FAS	**1H, 1H, 2H, 2H-perfluorooctyltriethoxysilane**
FO	**Forward osmosis**
FOMA	**1H,1H-perfluorooctyl methacrylate**
FS	**Feed solution**
HA	**Humic acid**
Hema	**2-hydroxyethyl methacrylate**

ICP	International concentration polarization
Jw	Flux
MD	Membrane distillation
MED	Multi-effect distillation
MSF	Multi-stage flash distillation
MVC	Machine vapor compression distillation
NIPS	non-solvent induced phase separation
NPs	Nano particles
PA	Polyamide
PAL	Palygorskite
PAN	Polyacrylonitrile
PE	Polyethylene
PET	Polyethylene terephthalate
PFDA	Perfluorodecyl acrylate
PMDETA	Pentamethyldiethylenetriamine
PP	Polypropylene
PPFDA	Poly-(1H, 1H, 2H, 2H-perfluorodecyl acrylate)
PS	Polystyrene
PSF	Polysulfone
PTFE	Polytetrafluoroethylene
PVC	Poly vinyl chloride
PVDF	Polyvinylidene fluoride
PVDF-CTFE	Poly (vinylidene fluoride-co-chlorotrifluoroethylene)
PVDF-HFP	Poly vinylidene fluoride-co-hexafluoropropylene
RO	Reverse osmosis

SDS	**Sodium dodecyl sulfate**
SEM	**Scanning electron microscopy**
SF	**Salt flux**
SF	**Salt flux**
SGMD	**Sweep Gas Membrane Distillation**
SW	**Sea water**
TEA	**Triethanolamine**
TEOS	**Tetraethyl orthosilicate**
TEOS	**Tetraethylorthosilicate**
TEP	**Triethyl phosphate**
TFC	**Thin film composite**
TIPS	**Thermal-induced phase separation**
UF	**Ultrafiltration**
VIPS	**Vapor-induced phase separation**
VMD	**Vacuum Membrane Distillation**
XPS	**X-ray photoelectron spectroscopy**

Chapter. 1

Introduction

1. Introduction

1.1 Water treatment technology using membrane

Because of the population increasing, the consumption of clean water has been increasing continuously [1]. The population doubled from 1900 to 1995, but the water demand increased by six times [2]. The increase in industrial and agricultural activities also contributes to the increasing water consumption. Moreover, freshwater such as river water and groundwater, which are sources of clean water, are being contaminated. Seawater desalination is one of the widely used methods for obtaining clean water [3-5]. In the Middle East, distillation is an important process that is used to obtain clean water via the evaporation and subsequent condensation of pure water vapor [6]. Although distillation does not require high pressure, it requires high thermal energy. Moreover, it is disadvantageous due to its slower production speed compared to that of other methods [7]. Reverse osmosis (RO) is another technology of seawater desalination [8, 9]. In recent decades, the largest seawater RO plant (SWRO) in Israel has been the most studied technology. SWRO plant produces approximately 590 Mm3/y of water, which is equivalent to approximately 80% of the total industrial and domestic needs of Israel [10]. However, RO requires a significantly high pressure to overcome the osmotic pressure of seawater and allow pure water to pass through the semipermeable membranes [11].

Recently, the membrane distillation (MD) method has gained increasing attention owing to its different advantages compared to that of the distillation and RO techniques [12-14]. In the MD process, a semipermeable barrier is interposed between the feed and permeate solutions. Pure water vapor is produced on the feed side because of the temperature differences between the two solutions. Subsequently, the vapor from the feed solution passes through the membrane and condenses in the permeate solution. The pores in the membrane provide a path for the vaporized water molecules to pass through [15]. MD has several advantages over other water treatment methods. Although MD uses the partial vapor pressure difference caused by the temperature difference, the process requires a low energy consumption as it is not required to increase the temperature of the feed solution to the boiling point. When waste heat is available, the operation cost of MD becomes smaller than that of the water treatment method using pressure as a driving force. In addition, when the MD is applied to freshwater, wastewater, and seawater treatments, pure water vapor leaving the rest of inorganic and nonvolatile organic materials in the feed side is transferred to the permeate side; therefore, the process can have a considerably high salt rejection.

1.2 Problem statement of MD process

Considering the nature of the separation process, which requires separation of the vapor from the mixed solution using a membrane, the membranes used in the MD must consist of hydrophobic materials [16]. When the vapor passes through the pores of the membrane during the operation, the temperature difference across the membrane can cause condensation of the vapor in the membrane pores. Hydrophobic materials employed in the MD process include polypropylene (PP), polyethylene (PE), polytetrafluoroethylene (PTFE), and polyvinylidene fluoride (PVDF) [17]. Among them, PVDF is a widely used material in MD owing to its high chemical durability, mechanical strength, and thermal stability. As the condensed vapor fills the membrane pores, the feed solution including various salts and particular materials passes the membrane through the wet pores, causing a sharp decrease in rejection. In this stage, the osmotic and operation pressures across the membrane, not the vapor pressure, lead to migration of the solution through the membrane, which will not further act as a semipermeable barrier.

Numerous studies have been performed to prevent wetting phenomena in the MD process [18]. The studies on the development of superhydrophobic membranes with contact angles of (or larger than) 150° employed a physical method of increase in the roughness of the membrane surface and chemical method modifying the surface with nonpolar and low-energy materials [19]. Coating, mixing, layer-by-layer structures, electrospinning, and chemical vapor deposition (CVD) have been proposed to increase the hydrophobicity of the membrane. Efome et al. carried out experiments to improve the performance and hydrophobicity of a vacuum MD membrane by preparing the membrane with a mixed dope solution of hydrophobic SiO2 particles and polymer [20]. Prince et al. carried out an experiment with a polymer solution containing PVDF and nanoclay to form a membrane with a removal rate of 99.97% and a contact angle of 154º through electrospinning [21]. Lia et al. added hydrophobically modified SiO_2 nanoparticles (NPs) into a dope solution for electrospinning to obtain a superhydrophobic membrane [22]. Zhang et al. dispersed hydrophobic SiO_2 particles in toluene and sprayed them onto the membrane surface [23]. Through this method, a membrane with a rough surface and large contact angle was obtained. Similarly, Zhang et al. [24] modified the surface of PVDF to superhydrophobic by coating SiO_2 NPs and hydrophobic modification using perfluorooctyltrichlorosilane. Superhydrophobicity was also achieved by Xianfeng [25] by casting a PVDF solution and gelation of the surface through quenching. In addition, a superhydrophobic membrane with a contact angle larger than 150° could be formed through the deposition of poly-(1H, 1H, 2H, 2H-perfluorodecyl acrylate) (PPFDA) on a PVDF membrane using the CVD method [26].

However, in the previous studies, the mixing of the hydrophobic material could affect the performance of the membrane due to the additionally spiked material, which could affect the formation

of pores or membranes and could change the membrane structure [27]. In addition, when a dope solution is prepared by mixing with a hydrophobic material, the added materials are surrounded and coated by a polymer solution, leading to a loss of hydrophobicity of the materials. In the case of membrane preparation through gelation, undesirable pore changes occur in the gelation and drying processes [28]. In the method of spraying with hydrophobic particles dispersed in a solvent, the stability between the sprayed particles and membrane surface becomes low in a long-term operation and thus the hydrophobicity can be lost. In the case of electrospinning, the shape and structure of the membrane can be significantly changed by the ambient humidity or conductivity during the application of a voltage in the spinning stage [29].

To further increase hydrophobicity, various studies have been conducted. Fluorine-based chemicals are widely used for fabricating hydrophobic membrane surfaces. Wei et. al. has performed CF_4 treatment for a polyethersulfone membrane using plasma radiation [30]. Through plasma treatment, the hydrophobicity of the membrane surface has improved with a contact angle up to 120º. However, it is not easy to exceed a contact angle of 150º, the standard for superhydrophobicity, using only the chemical modification method. Liu et al. have created a patterned cellulose surface by pressing a metal mesh on the cellulose membrane and engraving the pattern [17]. Such a patterned membrane followed by a chemical modification showed a superhydrophobicity behavior with a contact angle of more than 150˚. Similar research has been performed by Huang et al., creating a uniform structure on PTFE membrane using a nanoimprinting technique under high pressure [31]. After patterning the surface, the membrane was further modified by coating hydrophobic TiO_2 nanoparticles. However, coating with TiO_2 particles decreased the performance due to pore blocking. In addition, particles were not stably maintained on the membrane surface. The patterned surface has been also created using a spacer imprinting method [32-34]. A patterned spacer was carefully placed on a polymeric solution to create a certain structure during the coagulation step and imprint the pattern on the membrane. The size and shape of the pattern could be easily changed using various spacers. However, using spacers has limitations because spacers with higher thickness are much larger than nano or micro size. The lithographic technique is another patterning method. Lee et al. have fabricated a membrane with a prism-shaped patterned structure on the surface using a mold made by lithographic technology [18].

1.3 Objects of this study

Firstly, omniphobic PVDF membranes were prepared, and the performances and long-term stabilities were evaluated under the condition of direct-contact membrane distillation (DCMD). Omniphobic NPs were dip-coated on the PVDF membrane surface prepared by non-solvent induced phase separation (NIPS). To enhance the stability of the NPs on the surface, a membrane was prepared by a method involving the Fenton-reaction, formation of NPs, and their hydrophobic modification. The Fenton-reaction was used to form -OH functional groups on the PVDF membrane surface where tetraethyl orthosilicate (TEOS) grew to SiO_2 NPs [35-37]. The omniphobic modification was then completed through the reaction of the surface of SiO_2 with 1H, 1H, 2H, 2H-perfluorooctyltriethoxysilane (FAS), thereby forming a superhydrophobic membrane. Finally, to minimize the flux reduction from the modification and maximize the stability during the operation, the membrane pores were expanded by a plasma treatment [38] and NPs were grown in the expanded pores, followed by modification of the NPs with FAS. The performances of the prepared superhydrophobic membranes were compared with those of the pure PVDF membrane. For the stability measurement, sonication and recycling test were carried out.

Secondly, a poly(vinylidene fluoride-co-chlorotrifluoroethylene) (PVDF-CTFE) patterned membrane was fabricated using a templet made up of aluminum which had micro sized structures on the surface. Furthermore, this PVDF-CTFE was modified with 1H,1H-perfluorooctyl methacrylate (FOMA) through atom transfer radical polymerization (ATRP) to achieve low surface energy [39, 40]. PVDF-CTFE was chosen because the Cl functional group in the polymer chain could form a bond with other chemicals. To evaluate the fouling issue of the prepared membrane, humic acid (HA), alginic acid (AA), and bovine serum albumin (BSA) were chosen as representatives of humic substances, polysaccharides, and proteins, respectively [41-44]. They are components of natural water sources. This study can be used as fundamental research for combining chemical and surface engineering to enhance wetting and fouling resistance against various foulants to improve the overall MD performance.

Finally, as a new approach to prevent the wetting in MD, condensation of vapor causing the wetting was prevented by raising the temperature of the membrane. Many studies have been conducted to increase the hydrophobicity of the membrane to prevent wetting in MD, but as a fundamental solution, in this study, membrane temperature was maintained higher than the feed solution temperature which could prevent condensation of the vapor. To achieve this, the copper mesh was used as a substrate to prepare a membrane that has thermal conductivity. With this thermal conductive membrane, it was possible to increase the temperature of the membrane by directly applying heat during MD. Through this, the vapor condensation could be prevented longer period. In addition, due to the high temperature

inside the membrane, the movement of the vapor was accelerated, resulting in improved performance. Furthermore, to further improve the thermal conductivity inside the membrane, heat transfer could be improved by adding CNF to the dope polymer. The heat transferred to the copper mesh was able to transfer heat more effectively to the membrane through the CNF spread inside the polymer and prevent the wetting for a longer time.

Background

2. Background

2.1 Basic theory of the membrane

2.1.1 Fabrication of membrane

2.1.1.1 non-solvent induced phase separation (NIPS)

The NIPS method is one of the simplest and most frequently used methods used to cast membranes. This method uses the principle that when a solvent and a nonsolvent contact, they exchange with each other and form pores like in Figure 2.1 [45]. This principle was first introduced by Kesting to fabricate porous membranes [46]. The membrane prepared by exchanging this solvent and non-solvent is mainly used to prepare microfiltration membranes or ultrafiltration membranes, and many commercially available membranes are being prepared through this method.

To prepare a membrane through the NIPS method, first, a polymer solution was prepared by dissolving into the solvent. After the polymer solution becoming a homogeneous state, the polymer solution was fabricated into the required shape (flat or hollow fiber type) and then immersed into the non-solvent [47]. When polymer solution is contacted with non-solvent, an exchange occurs between the solvent and non-solvent, which will lead to the composition. As a result, the solubility limit of the solvent is exceeded, and finally, the polymer will be precipitated causing by liquid-liquid separation. Simultaneously, the non-solvent starts to occupy the place where the solvent was, and pores are formed. The pores are formed in two structures according to the difference in the exchange rate between the solvent and the non-solvent. First, exchange occurs very fast because of high interaction between solvent and non-solvent, the finger-like structure generated from the surface and finally an asymmetric membrane is formed [48]. The membranes prepared in this way are frequently used in the field of RO or UF. Conversely, if the exchange between solvent and nonsolvent occurs slowly, the symmetrical membrane with a sponge-like structure is formed [49].
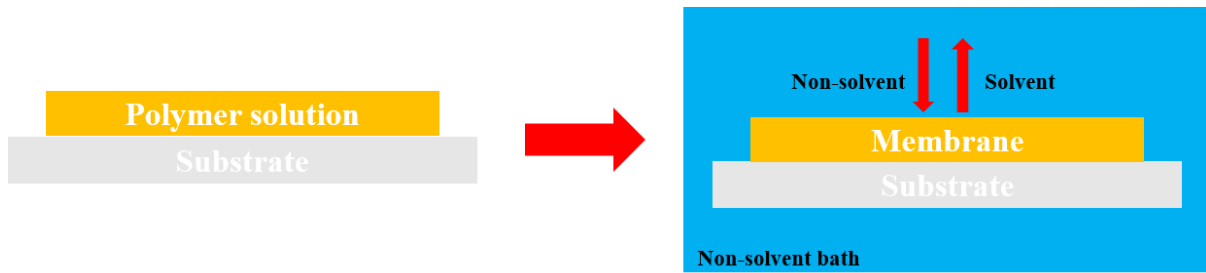
Figure 2. 1 Exchange between solvent and non-solvent in NIPS process.

2.1.1.2 Thermal-induced phase separation (TIPS)

The fabrication of membrane using NIPS described in 2.1.1.1 is widely used because it is simple, but because of the exchange between solvent and non-solvent, membranes have relatively large pores size. In addition, since the amount of polymer that can be dissolved in a solvent is limited, a high-concentration polymer solution cannot be prepared. Because of this low polymer concentration, the membrane prepared by the NIPS method has low mechanical strength. To overcome this large pore size and low mechanical strength, another technique has been conducted. TIPS method is one of the fabricating methods which can solve the problems that the NIPS method has. In the TIPS process, the polymer solution is prepared with higher concentration by applying heat in which the polymer can be dissolved in a solvent more than at room temperature. This hot polymer solution will form a membrane caused by the phase separation through cooling (Figure 2.2). Therefore, in the TIPS process, the solidification and cooling conditions are very important factors for pore forming of the membrane [50]. As the dissolved polymer cools at a high temperature, it forms crystals. If the cooling rate is slow, the crystallization proceeds slowly, which is a good condition for quartz growth. Conversely, if the cooling rate is fast, small quartz is formed. The TIPS process, in which such a high-concentration polymer solution forms a membrane through heat exchange, has the advantage of having high mechanical strength and strong chemical resistance. However, it should maintain high heat during casting, and it is difficult to control the size of pores compared to NIPS.

Figure 2. 2 Membrane fabrication caused by temperature difference in TIPS process.

2.1.1.3 Vapor-induced phase separation (VIPS)

It was first reported by Zsigmondy and Bachmann in 1918 and then developed by Elford in 1937. Since then, VIPS has been established as a representative method for producing polymer membranes along with NIPS and TIPS [51]. Compared to NIPS, a characteristic of VIPS is that the non-solvent phase is gaseous (Figure 2.3). Since the non-volatile non-solvent is originally contained in the volatile solution, evaporation during the control process results in a non-solvent concentration. This is a method using the fact that phase separation is achieved through the ingestion of non-solvent rather than solvent effluent, and the polymer is finally precipitated from the casting solution to form a membrane. Due to this manufacturing method, the polymer membrane prepared by VIPS has the advantage of pore control through a relatively easy process. Therefore, membranes manufactured by VIPS are widely used for a variety of applications. For example, porous membranes are used for water filtration, and high-density membranes are usually applied for gas separation. In terms of materials, PVDF membranes made through VIPS are also used for protein adsorption, and PS membranes can be efficiently used for MD. However, membranes made with VIP are still limited for commercial use.
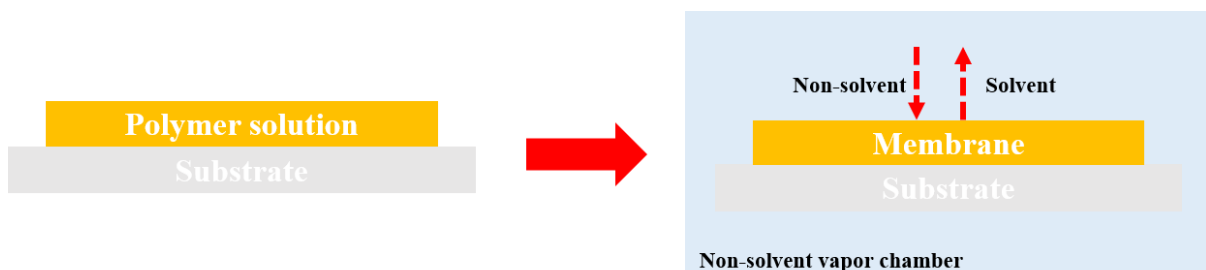
Figure 2. 3 Solvent-non-solvent exchange in vapor chamber during VIPS process.

2.1.2 Type of membrane

2.1.2.1 Flat-sheet type

The flat-sheet type membrane is the most widely used type of membrane, and its preparation is simpler than the hollow fiber described in the next section [52]. First, to prepare a flat membrane,

prepare a support layer. Research without a support layer is also being conducted, but when a membrane is made using the only polymer, the mechanical strength is weak, so a support layer is generally used for long-term experiments. At this time, non-woven or woven fabric is generally used as the support layer. In the case of the fabric used as the support layer, various materials are used, and since the porosity of the support has a great influence on the performance of the membrane, performance evaluation using various support layers is also underway. After fixing the support layer on the glass plate, the polymer solution was poured onto the substrate and spread the polymer solution to a certain thickness. At this time, a certain thickness can be applied using a spin coater or casting knife to spread the polymer solution to a certain thickness on the support layer. After that, it can be put in a coagulation bath to form a membrane. Much research has been done to alter the coagulation fluid and alter the pore shape and size of the membrane as described in 2.1.1.1. The prepared flat membrane is used to fabricate a module for water treatment. At this time, to increase the degree of packing of the module, a flat membrane is manufactured through various methods.

2.1.2.2 Hollow fiber type

There is a hollow fiber membrane in the shape of a straw, which is a different type of membrane from the flat membrane introduced earlier. Due to this shape, hollow fiber modules generally exhibit a large surface area per unit volume [53]. The hollow fiber module has a packing capacity of up to $500 - 9000 \ m^2/m^3$, providing higher productivity per unit volume compared to flat membranes. In addition, the hollow fiber is mechanically self-supporting and has excellent flexibility, so it is easy to manufacture modules for various fields. To make such a hollow fiber membrane, a tool called a spinneret is first used to create a shape. The prepared polymer solution passes through the spinneret to form a straw shape. By flowing a non-solvent inside and outside the hollow fiber membrane, it causes precipitation and maintains the shape to form the membrane. The inside of the hollow fiber thus formed is called the lumen side and the outside is called the shell side. The pore structure of the membrane varies depending on the nonsolvent if the NIPS method is used as the flat membrane and depends on the cooling temperature if the TIPS method is used.

As described above, the hollow fiber membrane has the advantage of having a large surface area per unit volume and easy handling. To overcome these shortcomings, various studies are being conducted in recent years, such as a technology of applying a support layer to a hollow fiber and improving the performance by forming a structure on the surface.

2.2 Various water treatment technology using membrane

2.2.1 Distillation

Seawater desalination is the most widely used technique to produce clean water. Distillation has been started use since the 4th century BC. As modern desalination systems, it has been established in the late 19th century. Since the 1950s, desalination systems in the Middle East have grown even bigger as the demand for clean water has increased due to population growth. As a basic principle, it is a method to obtain clean water by evaporating seawater and collecting only the vapor like in Figure 2.4. Representatively, it could be classified into MSF (Multi-stage Flash Distillation), MED (Multi-Effect Distillation), and MVC (Machine Vapor Compression Distillation) methods [54].
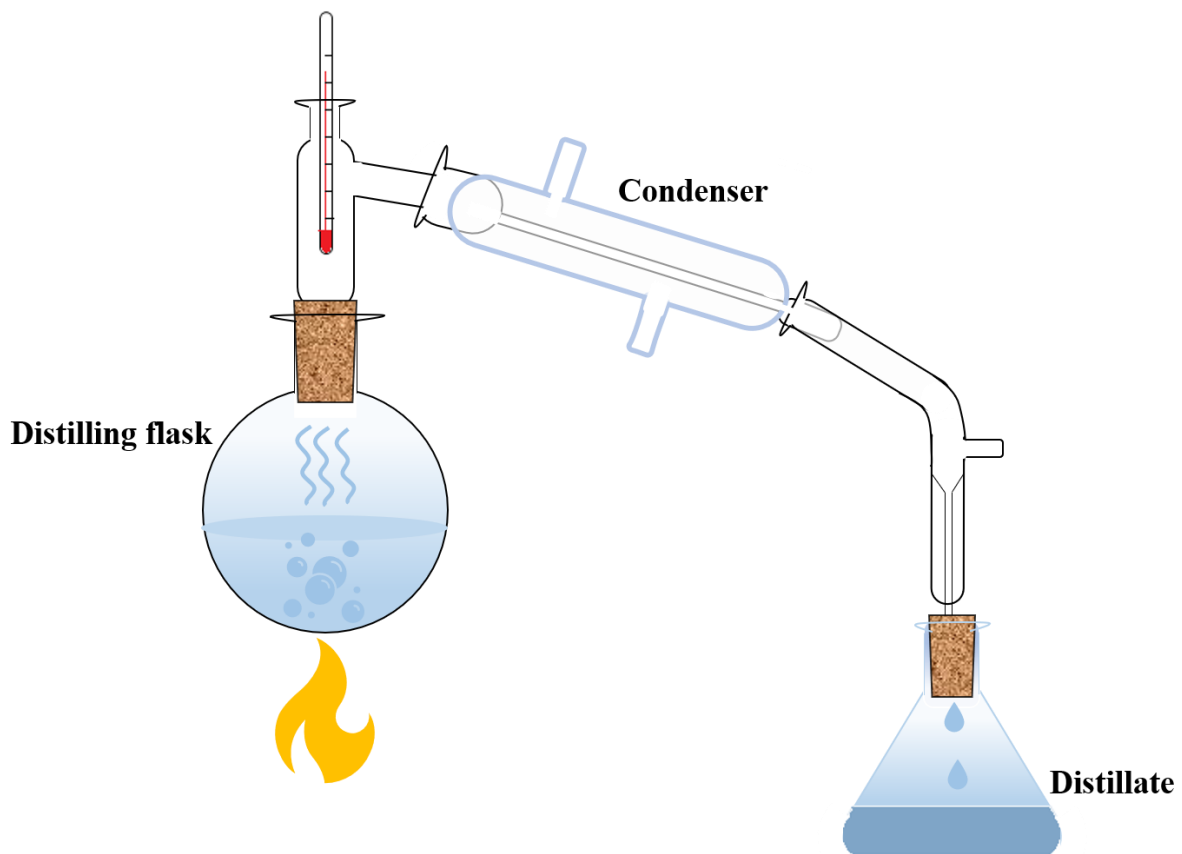
Figure 2. 4 Schematic diagram of distillation process.

2.2.2 Forward osmosis (FO)

FO is a membrane water treatment technology that utilizes natural osmotic pressure [55]. When salty water is purified through the membrane, the difference of two solutions on both sides of the membrane generate osmotic pressure (Figure 2.5). The different solutions used in FO are classified into concentrated draw solution (DS) and feed solution (FS). The difference in osmotic pressure between these two solutions causes clean water to flow from FS to DS. As water passes from FS to DS, the diluted DS is concentrated again to recycle the extraction solute and produce purified water. The disadvantage of FO is the international concentration polarization (ICP), which promotes reduced water flux due to the structural properties of the membrane. Therefore, the number of studies related to improving both the active and support layers of FO membranes is increasing in the field of application.
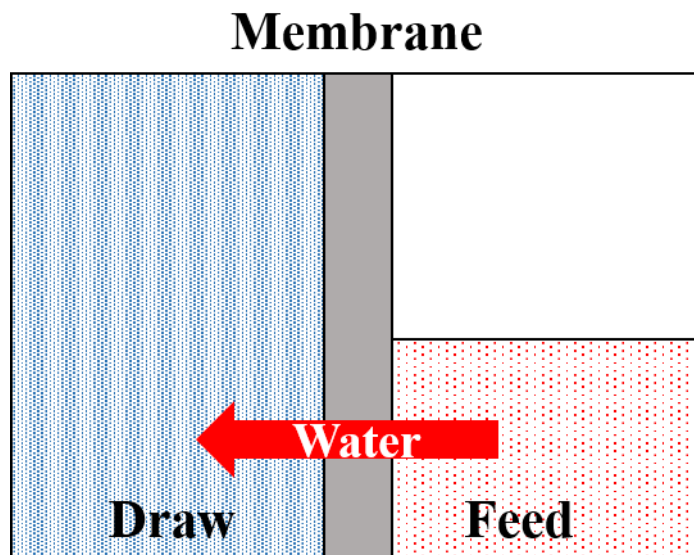
Figure 2. 5 Draw and feed solution for FO system.

2.2.3 Reverse osmosis (RO)

The distillation process has disadvantages like high thermal energy for evaporation and low production efficiency. Therefore, various studies have been conducted to solve these shortcomings using membranes. Among many technologies, RO has been widely used for seawater desalination (Figure 2.6). Regarding RO, research has been conducted since 1985 [56]. Cadotte focused on

composite RO membranes by conducting research on the materials of membranes used in RO. The RO membrane using the chemical properties of cellulose acetate (CA) has the advantage of a very high salt removal rate (98%) so that many studies had been conducted in 1950, but the disadvantage of low performance due to the problem of small pores could not be solved. Therefore, research on making RO membranes using Cellulose triacetate (CTA), a material that can withstand in a wide range of pH and temperature, has been conducted [57]. It was considered an excellent material because it has high chemical and biological resistance, but it did not solve the problem of a sharp decrease in performance due to serious compaction at a high pressure of 30 bar. Therefore, although RO membranes using CA were manufactured after that, their vulnerability to microbial contamination, durability, and limited application range were still problems to be solved.

To solve the CA problem, Richter and Hoehn first started the study of hollow fiber manufacturing using an asymmetric membrane using polyamide (PA) [58]. PA has achieved great commercial success as a hollow fiber form that is significantly more durable and stable than CA and can be efficiently packaged. However, PA was found to be ozone and chlorine for a week, so more research was needed. Asymmetric membranes using polypiperazine-amides were also studied in another attempt to fabricate membranes with similar performance to CA and resistance to chlorine attack [11]. Although polypiperazine-amide membranes were found to have good chlorine resistance, they exhibited relatively low rejection rates (<95%).

A lot of research is being done to solve the problem of RO, and recently, as an innovative method to solve this problem, a method of making a thin membrane complex membrane (TFC) membrane produced through two steps has been developed [59]. It is a membrane having a large pore polysulfone (PSF) support layer and a thin barrier layer and has a high removal rate and performance. TFC was first developed by Francis, and the PSF used as the support layer was chosen as the material for the support layer because it is resistant to compression and resonant fluxes. Also, the material was an excellent candidate for a backing layer because it was durable in acidic conditions. Furthermore, since PSF has resistance to alkali, more various modifications could be attempted. The first attempt is to synthesize aliphatic and aromatic diamines. However, this reforming method loses the high salt removal rate that TFC membranes have. In another attempt, Cadotte found that high removal rates could be achieved using aromatic acyl halides and monomeric aromatic amines [60]. Using these two chemicals has great advantages over other methods as no acid acceptors or surfactants are required. The acyl halide used here is easy to polymerize and crosslink, and this crosslinked aromatic polyamide TFC RO membrane has been extensively studied and was widely used until the 1980s.
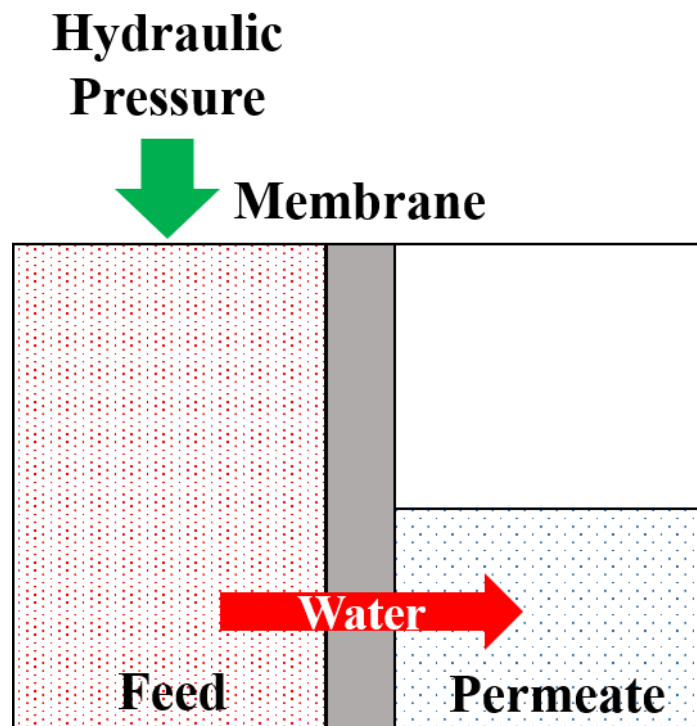
Figure 2. 6 Water treatment using hydraulic pressure in RO.

2.2.4 Membrane distillation (MD)

MD has been studied as a third-generation desalination technology that is different from the desalination technology introduced earlier [61]. MD which is a thermally driven separation process purifies using vapor volatilized by the temperature difference between feed and permeate solution. Because of this temperature difference, MD has the advantage of high thermal energy efficiency because it does not require energy to boil the feed solution. This MD process was first studied by Bodell in 1963 [62]. The MD system which Bodell conducted, a silicone membrane was used which is difficult to confirm the shape or condition of the pores. He used the vacuum to generate vapor more efficiently, but as a result, the membrane tube was broken, and normal operation could not be confirmed. Later, in 1967, Weyl conducted research on MD to improve water purification efficiency in seawater desalination [63]. A flux of 1 LMH could be obtained using a PTFE membrane (3.2 mm thick, pore size 9 μm), but it did not receive much attention because it was significantly lower than the RO process with a flux of 5 to 75 LMH at that time. In the 1960s, he first published on the basic theory of distillation and DCMD [64]. Since then, research on MD has been actively conducted, and additional studies have been conducted to understand the module design and temperature and concentration polarization phenomena for MD

[65]. In addition, for commercial use of MD, an experiment was conducted to fabricate and apply Membrane manufactured by The Swedish Development Co. as a module. Since then, MD has been applied in many fields and various studies have been conducted, and it has been shown that in 1997 there was an increase of about 2 times compared to 1990.

2.3 Various type of MD
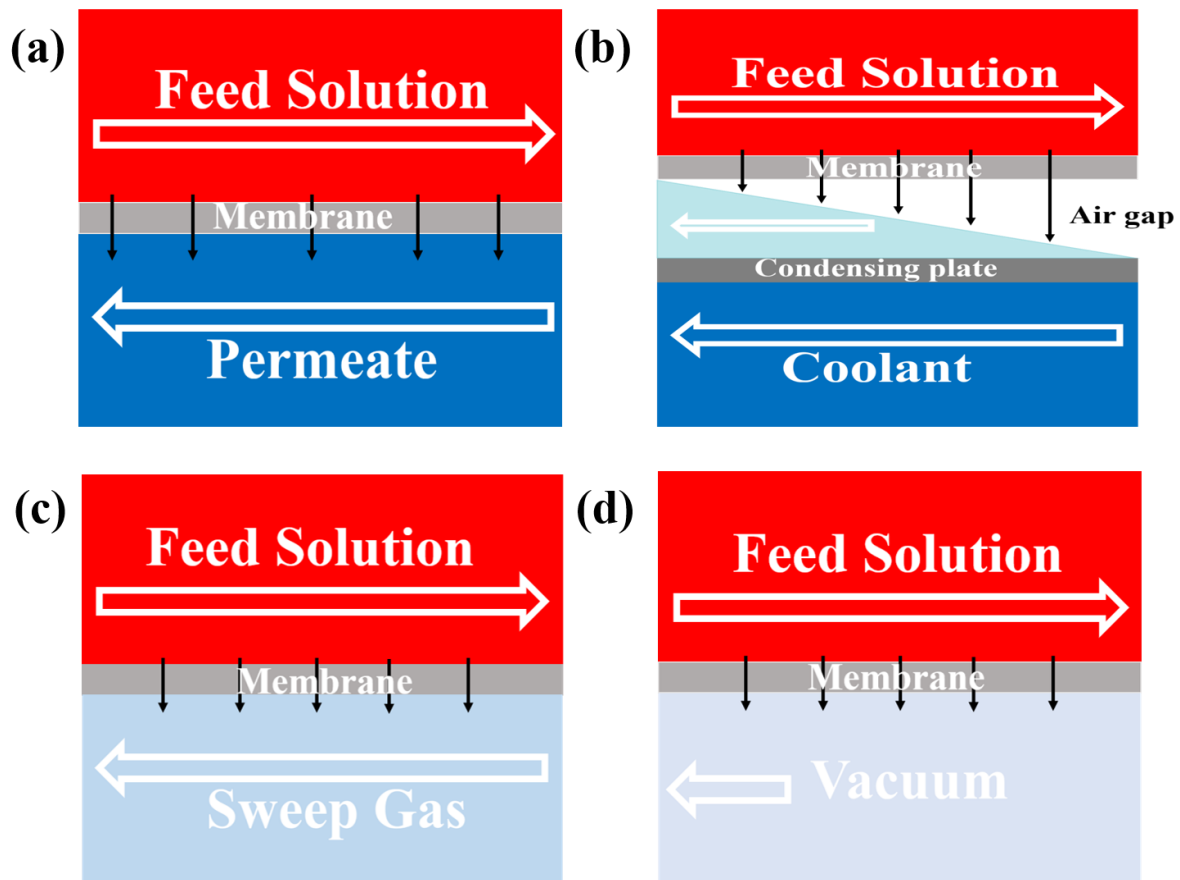
Figure 2. 7 Schematic diagram of (a) DCMD, (b) AGMD, (c) SGMD, and (d) VMD.

2.3.1 Direct Contact Membrane Distillation (DCMD)

DCMD has been studied because of its easy installation compared to other MD processes [66]. As shown in Figure 2.7 (a), the hot feed solution is in direct contact with the hot membrane side. On the opposite side, a cold permeates solution flows in direct contact, and water vapor is generated in the feed solution due to the temperature difference between the two solutions. The generated vapor moves to the permeate side through the pores due to the pressure difference across the membrane, and as a result, it is condensed by the permeate solution. Since only the generated vapor can pass through, the membrane used in MD uses a hydrophobic material, so the feed solution cannot penetrate the membrane. As mentioned above, DCMD is a simple method and is widely used in various fields such as the food industry, desalination process and aqueous solution concentration. However, the biggest disadvantage

of DCMD is that the feed solution and permeate solution are in contact with the membrane, so heat loss is large due to conduction.

2.3.2 Air gap Membrane Distillation (AGMD)

To reduce heat loss caused by direct contact between feed and permeate solution, the air layer is created between the permeate side of the membrane and the cold condensing plate, and the vapor generated from the feed solution is penetrated and finally condensed on the cold condensing plate which will be collected into the separate tank (Figure 2.7 (b)). Because of the gap between the membrane and the cold condensing plate, heat loss is lower compared to DCMD. However, since the driving force for evaporating the feed solution is water vapor generation by pure thermal evaporation, there is a disadvantage that the flow rate is relatively low. In this process, feed temperature, flow rate, concentration, and degassing are important factors.

2.3.3 Sweep gas Membrane Distillation (SGMD)

Another MD method is SGMD using sweep gas (Figure 2.7 (c)). As you can see in the picture, SGMD is a method to induce evaporation by flowing an inert gas to the side of the membrane [67]. It is a useful method for removing volatile compounds because it uses gas, so heat loss is small, and because it flows continuously, the mass transfer coefficient is high. Also, as the speed of the sweep gas increases, the concentration polarization decreases, and the performance improves. However, this method does not receive much attention compared to DCMD because it has the disadvantage that the sweep gas must be continuously circulated, and a considerable cost is required to re-condensate the evaporated flowing vapor.

2.3.4 Vacuum Membrane Distillation (VMD)

VMD is the least studied method compared to other MD processes [68]. As a basic principle of MD, unlike obtaining a clean permeate by re-condensing the vapor generated due to the temperature difference between two solutions, VMD is a method to induce evaporation of the feed solution by applying a vacuum to the permeate (Figure 2.7 (d)). The vapor evaporated in this way is condensed in

the condenser outside the module and collected. Therefore, compared to other MD processes, VMD has high performance to directly induce evaporation and has advantages of low heat loss because the capacitor is separated. However, relatively few studies have been conducted because of the disadvantages that complex technology is required to operate it and high cost is required to apply a vacuum. However, since it is a method that uses direct evaporation through the vacuum, it is widely used in the process of treating raw water containing volatile substances. As a representative example, a lot of research is in progress as a process for separating ethanol. In Bandini's study [69], VMD was also found to be about 10 times more efficient in ethanol separation than AGMD.

2.4 Statement of MD

2.4.1 Basic concept of MD

MD is a thermally driven separation process in which a specific component of a high-temperature mixed solution, which is in contact with one side of a hydrophobic membrane, evaporates and transports through the membrane in the form of vapor and condenses on the other side at a low temperature [64]. This process separates the specific component from the mixed feed solution. When the MD is applied to freshwater, wastewater, and seawater treatments, pure water vapor leaving the rest of inorganic and nonvolatile organic materials in the feed side is transferred to the permeate side; therefore, the process can have a considerably high salt rejection. MD has several advantages over other water treatment methods. Although MD uses the partial vapor pressure difference caused by the temperature difference, the process requires a low energy consumption as it is not required to increase the temperature of the feed solution to the boiling point. When waste heat is available, the operation cost of MD becomes smaller than that of the water treatment method using pressure as a driving force.

Considering the nature of the separation process, which requires separation of the vapor from the mixed solution using a membrane, the membranes used in the MD must consist of hydrophobic materials. Hydrophobic materials employed in the MD process include polypropylene (PP), polyethylene (PE), polytetrafluoroethylene (PTFE), and polyvinylidene fluoride (PVDF). Among them, PVDF is a widely used material in MD owing to its high chemical durability, mechanical strength, and thermal stability.

2.4.2 Weakness of MD

When the vapor passes through the pores of the membrane during the operation, the temperature difference across the membrane can cause condensation of the vapor in the membrane pores (Figure 2.8) [70]. As the condensed vapor fills the membrane pores, the feed solution including various salts and particular materials passes the membrane through the wet pores, causing a sharp decrease in rejection. In this stage, the osmotic and operation pressures across the membrane, not the vapor pressure, lead to migration of the solution through the membrane, which will not further act as a membrane.
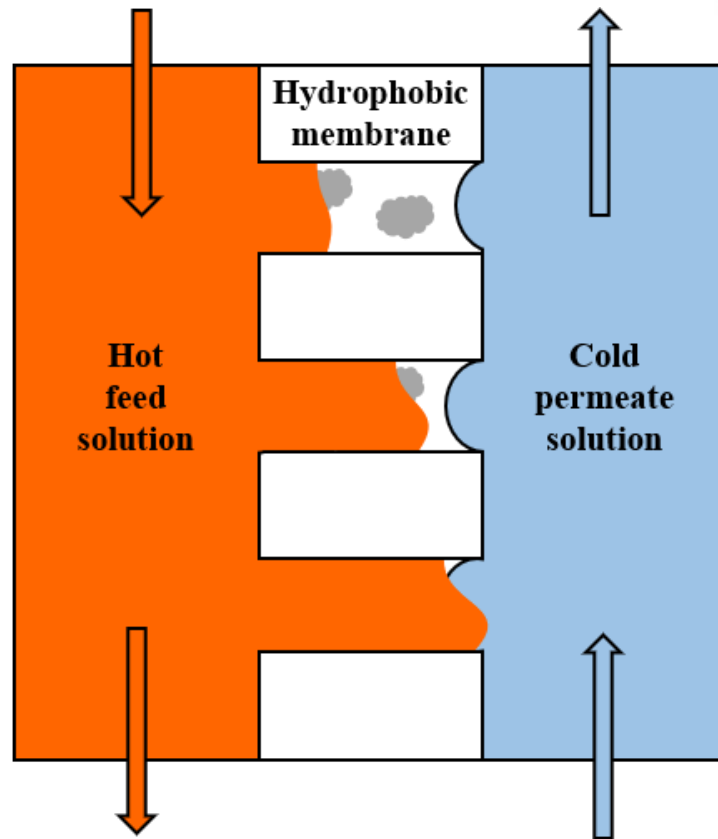
Figure 2. 8 Wetting mechanism in MD system.

To solve this wetting problem, hydrophobic materials have been used for fabricating the membrane. As shown in Figure 2.9, many MD studies started to increase rapidly from the year 2000. However, research to prevent wetting has recently received a lot of attention and has been conducted.
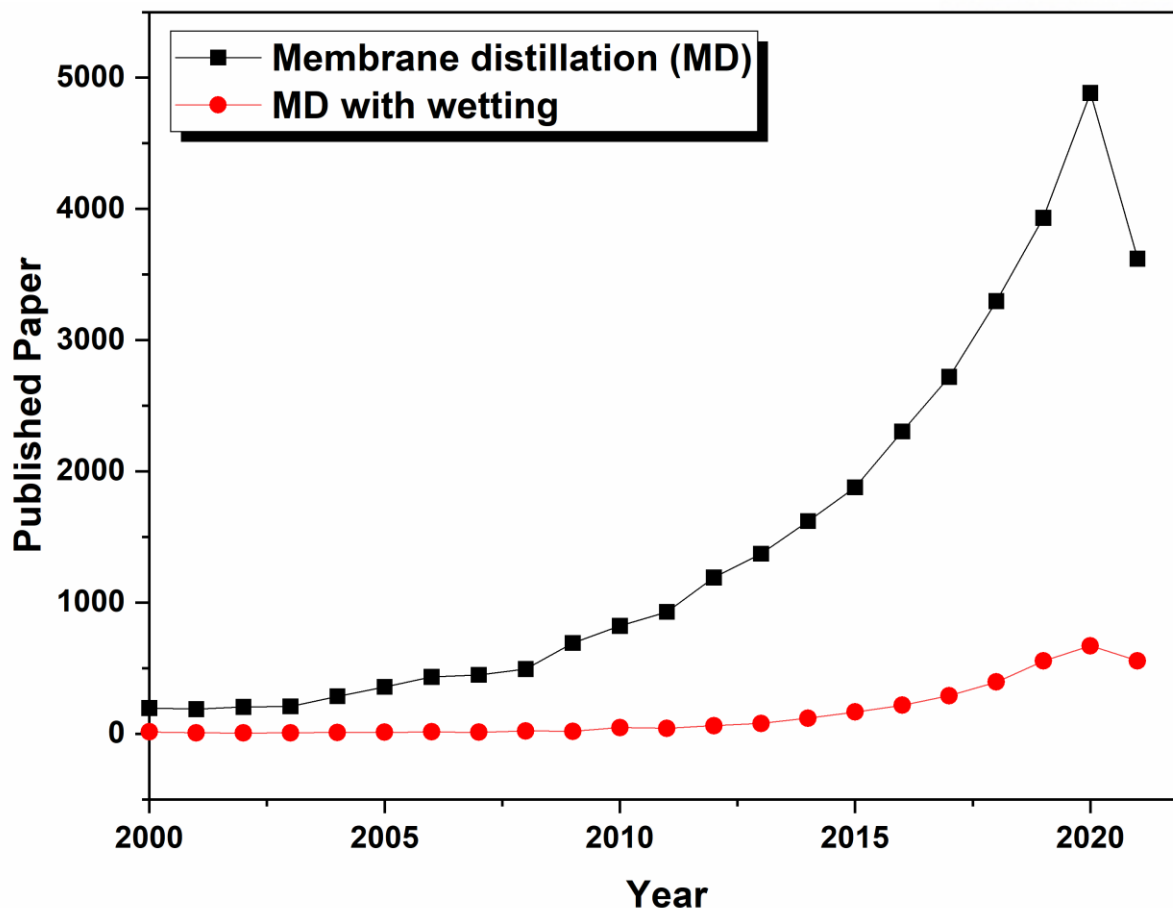
Figure 2. 9 Publication trend for MD and wetting.

2.4.3 Various technique for enhancement of membrane hydrophobicity/omniphobicity

Various studies are conducted to improve hydrophobicity which is water repelling property during MD. Furthermore, an omniphobic surface that repels both water (i.e., hydrophobic) and low surface tension liquids such as oil (i.e., oleophobic) has been studied [71].

Omniphobic surfaces can be prepared by creating surfaces with low surface tension and fine reentrant structures, which together promote the existence of metastable Cassie-Baxter states for liquid-solid-vapor interfaces. To achieve this hydrophobic/omniphobic surface, several types of modification on the membrane have been studied.

2.4.3.1 Additive

It is a very simple method used to modify the membrane, and the membrane can be prepared by adding additional hydrophobic material to a polymer solution. PTFE is a frequently used material. PTFE is a highly hydrophobic polymer and is also used as a material for membranes. Even though PTFE is hydrophobic, it has a disadvantage which is difficult to fabricate as a membrane due to its excellent durability. Therefore, very high pressure is required to make PTFE into a membrane, and it is very difficult to make a desired pore shape or size. For this reason, PTFE, which has high hydrophobicity, is used as an additive using nano particles. In addition, SiO_2 particles are easy to prepare on a lab scale and are easy to modify the surface. Because of these advantages, SiO_2 particles are widely used as additives by preparing a hydrophobic material through additional hydrophobic chemicals and modification from OH functional groups on the surface. Several types of additives for hydrophobicity and CA values are introduced in Table 2.1. However, the method of modifying the membrane using this additive has the disadvantage that the pores of the membrane can be changed, compared to very easy. Additives can change the size or shape of pores due to interaction when casting mixed with a dope solution, which makes direct comparison with membranes prepared without additives difficult. In addition, when additives are added to the polymer solution, the hydrophobic properties of its own are buried in the polymer, making it difficult to expect full modification performance.

Table 2. 1 Type of additive in studies.

Polymer	Concentration (wt%)	Additive	Concentration (wt%)	Contact angle (°)	Ref
PVDF	11	SiO$_2$	3	97	[72]
PSF	25	FPA	3	>150	[73]
PS	10	PS	4	151	[74]
PVDF	15	PTFE	12	151	[75]
PVDF	20	Silica	10	163	[76]
PVDF-co-HFP	18	Graphene	10	162	[77]

Membrane	Concentration	Additive		Contact angle	Ref
PVDF	12	Clay	8	154	[21]
PVDF	12	Graphene Platelet powder	20	151	[78]
PVDF-co-HFP	20	Carbon nanotube	3	>150	[79]
PVDF	15	Silver nanoparticles	2	151	[80]
PVDF	13	MOF	5	133	[81]

2.4.3.2 Coating

Like additive modification, as a widely used modification process, there is a coating method in which a hydrophobic material is attached to the surface of the prepared membrane. As a method of attaching a material having hydrophobicity to the surface of the membrane, it is a method of making the surface hydrophobic by putting the prepared membrane in a solution in which the hydrophobic material is dispersed. This is very simple and does not affect the performance of the membrane itself, making it a widely used modification method compared to additives (Table 2.2). The coated membrane shows high hydrophobicity due to the hydrophobic material on the surface. However, the hydrophobic material can be detached from the surface during actual operation and the membrane is gradually losing its hydrophobicity. To solve this problem, many methods have been studied for a more stable hydrophobic surfaces. Typically, PDMS is used as a method of attaching hydrophobic particles to the surface using a material having strong adhesion to the surface.

Table 2. 2 Various coating materials for hydrophobicity of membrane.

Membrane	Concentration (wt%)	Coating materials	Coating method	Contact angle (°)	Ref
PTFE	-	P(PFDA-co-	Dip-coating	149	[82]

				EGDA)	
PTFE	10	PVA	Electrospinning	148 (oil)	[83]
Regenerated cellulose 100kDa	-	MWCNT	Filtration in stirred UF unit	109.1	[84]
Cellulose	-	Lignin; nano-silica	Dip-coating	155º	[85]
PTFE/PET pore size 0.22μm	-	Fluorinated palygorskite (PAL)	Spraying	163.9º	[86]
PAN	8.5%	Nanocluster Ag	Chemical deposition	156.7º	[87]

In the case of the coating material introduced above, it is generally in the form of a solution. Furthermore, various studies are being conducted on coating using particles to achieve hydrophobic or omniphobic surfaces by forming a nano/micro size of structure on the surface. Among them, research using SiO_2 particles is being actively conducted compared to studies using other particles because of mild conditions and easy modification. In addition, the particle size can be variously adjusted according to the conditions for synthesizing. As shown in Tables 2.3 and 2.4, a typical reaction is started using TEOS to prepare SiO_2 particles, and the desired particle size can be created by changing various conditions such as solvent, catalyst, and temperature. As solvents (DI and EtOH), the larger the amount of DI, the smaller the particle size is formed. On the other hand, with increasing the amount of ammonia as a catalyst, the particle size increases. Furthermore, the catalyst can be selected with an acid solution like HCl, H_2SO_4, nitric acid, or acetic acid. By changing the catalyst, the pH of the solution is changed which leads to the change of particle size. In addition, it can be seen in Table 2.4 that the particle size decreases as the temperature increases. Because of these various advantages like the convenience of size control or mild condition for synthesis, SiO_2 particles are frequently applied for increasing hydrophobicity/omniphobicity of the membrane. However, this coating modification also has a disadvantage such as the sharp flux decline because of the pores clogging and losing hydrophobicity during the MD process because of low interaction between particles and membrane surface.

Table 2. 3 Size difference of silica nanoparticles with solvent.

Material	Solvent		Catalyst (ml)	Size (nm)	Ref
TEOS (ml)	DI (ml)	EtOH (ml)			
200	400	500	50 (NH$_4$OH)	300	[88]
200	500	500	50 (NH$_4$OH)	200	[88]
200	700	500	50 (NH$_4$OH)	100	[88]
18	6.4	20	36 (Acetic acid)	150	[89]
6.9	-	15	0.5 (NH$_4$OH)	93	[90]
6.9	-	15	1 (NH$_4$OH)	162	[90]
6.9	-	15	1.5 (NH$_4$OH)	214	[90]
1	-	50	10 (NH$_4$OH)	320	[91]
1.5	-	50	3 (NH$_4$OH)	110	[92]
1	45	20	10 (NH$_4$OH)	740	[93]

1	4	-	4 (Acetic acid)	2000	[94]
8	35	100	1 (Nitric acid)	190	[95]
8	35	100	1 (HCl)	310	[95]
8	35	100	1 (H_2SO_4)	277	[95]

Table 2. 4 Silica nanoparticles generation with different temperature.

Material	Solvent		Catalyst	Temperature	Size	Ref
TEOS	DI	EtOH		(°C)		
0.045 (mol/L)	3	8	14 (NH_4OH)	30	372	[96]
0.045 (mol/L)	3	8	14 (NH_4OH)	50	345	[96]
0.045 (mol/L)	3	8	14 (NH_4OH)	70	324	[96]
8 (ml)	35	100	-	100	175	[95]
8 (ml)	35	100	-	650	154	[95]

2.4.3.3 Chemical grafting

27

Unlike the previous methods, chemical grafting can change the membrane properties which will make the membrane surface hydrophobic without physical changes. To prevent wetting during MD, the membrane is synthesized with hydrophobic chemicals from the specific functional group. Typically, a polymer having a Cl functional group such as PVC has the advantage of being very easy to modify using radical polymerization kwon as ATRP. However, in the case of a polymer without a functional group capable of such synthesis, chemical modification is difficult, and studies using various methods are being conducted to solve this problem (Table 2.5). Typically, plasma or Fenton-reaction was applied for polymerization. Both modification methods can produce radicals on the membrane even without the specific functional group. However, in the case of such chemical grafting, as described above, an additional process is required, and wastewater is generated during the process.

Table 2. 5 Chemical grafting using several types of methods.

Membrane	Grafting materials	Grafting method	Contact angle (º)	Ref
Ceramic	Fluorinated silanes	Condensation	150	[97]
PET	Polypentafluorostyrene	Plasma	102	[98]
Ceramic	Perfluorodecyltriethoxysilane	Condensation	160	[99]
Zirconia	Hydroxyethyl acrylate	Condensation	140	[100]
PVDF	N-octyltriethoxysilane	Plasma	121	[101]
Zirconia	Perfluorodecyltriethoxysilanes	Condensation	180	[99]
PEG	Styrene	Radical polymerization	-	[102]
Bamboo flour	Methyl methacrylate	Radical polymerization	128	[103]
PP	HEMA; GMA	ATRP	179	[104]
PET	Triethoxyvinylsilane	Photoinduced graft polymerization	104.9	[105]
PVC	Poly ethyl acrylate	Free radical graft copolymerization	95.4	[106]
PVDF	CNT	Covalent bonding	131	[107]

2.4.3.4 Plasma treatment

Plasma treatment is a dry process that involves physical modification of pores as well as modification of functional groups on the surface of the membrane. Basically, plasma treatment is used to impart desired properties to a surface or to enlarge pores on a surface. During plasma treatment, the monomers on the membrane surface evaporate to form radicals, so most of them start under vacuum conditions. This is because water molecules present in the atmosphere can react with the membrane during plasma treatment and attach to hydroxyl functional groups. When the hydrophobic materials such as CF_4 spread on the surface with plasma, the reaction starts from the generated radicals (Table 2.6). This reaction takes place only on the surface, and since it is a reaction using radicals, it can be reacted very quickly. This plasma treatment method makes it possible to easily synthesize various monomers on the surface of the membrane, but it has disadvantages in that expensive machines are required for synthesis and the environment is difficult to control and if the pretreatment process (vacuum stage) is not proper, the immediate reaction can cause unwanted synthesis such as dust particles or other substances.

Table 2. 6 Hydrophobic modification using plasma treatment.

Polymer	Plasma materials	Contact angle	Ref
PES	CF_4	125	[108]
Nylon	CF_4	135	[108]
PVDF	CF_4	101	[109]
poly (L-lactide)	CF_4	116	[110]
Si	C_4F_8	112	[111]
PAN	Perfluorodecyl methacrylate	132	[112]
PVDF	O_2, CF_4	117	[113]
PVDF	CF_4	162	[114]
Poly-L-lactic acid	CF_4	135	[110]
Polyacrylonitrile (PAN)	CF_4	148	[115]

2.4.3.5 Chemical vapor deposition (CVD)

CVD technique is a strong tool for fabricating microporous membranes or thin SiO_2 films by modifying inorganic materials. In general, CVD which involves gaseous reactants is performed on the surface of a heated substrate. CVD is a technology capable of structural control on a nano scale, and for MD processes, it can be used to create a hydrophobic membrane by dip coating a typical organosilane-based solution like in Table 2.7. With CVD modification, the chemical can cover the rough surface uniformly compare with the physical modification method. However, there are many parameters to consider implementing a CVD process, such as the type, concentration, boiling point, time, and volume of the organosilane. Therefore, it is a technology that is difficult to set, but it has the advantage of being able to form a very thick coating layer through the CVD method and that it can be modified simultaneously by using various materials of interest.

Table 2. 7 CVD process with various hydrophobic materials.

Polymer	Concentration (wt%)	CVD materials	Contact angle (º)	Ref
Bamboo non-woven fabric	-	Hexafluorobutyl acrylate	>150	[116]
PA6(3)T	22	PPFDA	151	[117]
PVDF/ZnO	-	Perfluorooctyltriethoxysilane	151	[118]
PP	-	Heptadecafluorodecyl acrylate	154	[119]
PAN	8	Divinylbenzene DVB	149	[120]
Millipore Isopore	-	Perfluorodecyl acrylate (PFDA) divinylbenzene (DVB)	122	[121]

Polymer					
PVDF	5	Methyltrichlorosilane	141	[122]	
Cotton fabric		Aniline	156	[123]	

2.4.3.6 Patterning the membrane surface

Although many modification methods have been applied to fabricate the membrane with high hydrophobicity to prevent wetting during MD, among them, a technique that creates a pattern on the surface of the membrane is newly applied for increasing the roughness of the surface (Table 2.8). The common method to create the pattern is using a mold that has a specific structure itself and then a patterned membrane can be fabricated using the NIPS method, in which a polymer solution is poured on the mold and soaked in a coagulation bath [124]. However, while the NIPS process, the exchange between solvent and non-solvent acts as an important factor in the formation of pores. For this reason, the pores on the side where the polymer solution contact with the mold are formed very small, and the surface pores on the opposite side directly in contact with the coagulation solution are formed very large. Because of the small pore size on the pattern side, the patterned membrane fabricated with the NIPS process has poor performance. To overcome this problem, various studies have been conducted, for example, the imprinting technique which can be obtained a certain structure on the active layer directly [125]. The imprinting technique which can be applied on a fabricated membrane physically changes the surface structure by applying the pressure so that it can be done simply compare with the mold method. As another technique, the VIPS method was applied to fabricate the homogenous patterned membrane. [126]. Even though this method also uses a mold, it is possible to form a pore with a very uniform size by inducing phase separation between evaporating water and the solvent as explained in 2.1.1.3. Like in Table 2.8, various type of research is being conducted to increase hydrophobicity by forming a pattern on the membrane surface, the patterned membrane has a certain disadvantage which is the fouling. On the rough surface, fouling can easily accumulate which leads to performance decline during the MD process [124]. To solve this fouling problem on the patterned membranes, various studies have been conducted to achieve low surface energy through additional modification on patterned membranes such as the modification methods introduced in previous sections.

Table 2. 8 Several types of pattern surface on membrane

Polymer	Structure	Size	Patterning method	Contact angle	Ref

31

				(º)	
PTFE	parallel line	Widths of 606 nm, Heights of 100 nm	Nanoimprinting	125	[125]
Cellulose	Pillar	Widths of 349.5 nm, Heights of 70.7 nm	Pressing	130	[127]
PDMS	Square microchannel	Widths of 50 nm	Lithography	112	[128]
OSTE	Square microchannel	Widths of 40 nm, Heights of 80 nm	UV	115	[129]
PP	Hemisphere	Micro size	Deposition	113	[130]
PDMS	Cluster	3 µm	Electrostatic atomization	91.3	[131]
PVDF	Corrugated	Micro size	Bubbling	106	[132]
Nafion	Microchannel	Width is 19 µm, Height of 20 µm	Hot embossing	-	[133]
PVDF	Square pillar	Micro size	Imprinting	154	[134]

Wetting resistance:

NPs growing

Abstract

In this study, modifications of polyvinylidene fluoride (PVDF) membranes were carried out to improve both hydrophobicity and stability through four steps: pore expansion by a plasma treatment, hydroxylation of the membrane by the Fenton reaction, generation, and growth of nanoparticles (NPs) on the hydroxylated functional groups in pores, and hydrophobic modification. The membranes modified by the methods proposed in this study did not lose their hydrophobicity and maintained the flux over a significantly longer period. The PVDF membrane modified by hydrophobic NPs attached inside enlarged pores exhibited a minimized flux reduction and significantly higher antiwetting stability.

3.1 Materials and Methods

3.1.1 Materials

PVDF polymer (Solef 1015/1001) was purchased from Solvay. Triethyl phosphate 99.5% (TEP) used as a solvent was purchased from Sigma. Methanol (99.5%), ethanol (95%), and n-hexane (99%) were purchased from Daejeong. Tetraethylorthosilicate (TEOS) (99%), FAS (97%), and $NH_3 \cdot H_2O$ (28%) were purchased from Sigma to synthesize the NPs and provide hydrophobic NPs. $FeSO_4 \cdot 7H_2O$ (99.5%), H_2O_2 (30%), and H_2SO_4 (95%) were purchased from Sigma for the Fenton reaction. Sodium dodecyl sulfate 98% (SDS) was purchased from Sigma as a surfactant to accelerate the membrane wetting during the DCMD operation. All the reagents were used as received without further purification.

3.1.2 Preparation of membrane

A dope solution was prepared by dissolving PVDF polymer (15 wt%) in a triethyl phosphate (TEP) solvent (85 wt%) [135]. The dope solution was purged with nitrogen gas for 30 min to remove air bubbles trapped in the solution. Subsequently, the solution was mechanically stirred at 80ºC for 24 h to obtain a homogeneous solution. Subsequently, the solution was cooled down at room temperature. The polymer dope solution was cast on a polyethylene terephthalate (PET) substrate wrapped on a glass plate with a casting knife with a thickness of 150 μm, and then the solution cast on the PET was immediately put in an ethanol bath. After the immersion for 12 h, the membrane was taken out and immediately soaked in methanol for 1 h, in 1-hexane for 1 h, and then taken out. The membrane was dried in an oven at a temperature of 60ºC.

3.1.3 Modification of membrane

3.1.3.1 Membrane surface modification by the dip-coating method

SiO_2 NPs were prepared using TEOS, modified with FAS, and then introduced onto the surface

of the PVDF membrane by the dip-coating method to form a hydrophobic membrane surface. For the preparation of the SiO_2 NPs, 1 mL of TEOS was mixed with 25 mL of ethanol (denoted as solution A). As a second solution (solution B), 25 mL of ethanol were mixed with 10 mL of $NH_3 \cdot H_2O$. When the prepared solutions A and B were mixed and reacted for 12 h, SiO_2 NPs with uniform sizes were formed. The hydrophobic modification of the NPs was carried out by adding 1% FAS to the prepared SiO_2 NP solution. The modification was carried out through a reaction between the OH group of SiO_2 and ethoxysilane functional group of FAS. After the formation of the hydrophobic NPs, the surface of the PVDF membrane was modified by dipping the membrane into the NP solution. To investigate the difference in the degree of modification according to the dip-coating time, the coating time was varied in the range of 0.5 to 4 h.

3.1.3.2 Modification by NP growth on the membrane surface

SiO_2 NPs were grown on the membrane surface to obtain a hydrophobic membrane with an improved stability. A dried PVDF membrane was placed together with 1.4 g of $FeSO_4 \cdot 7H_2O$, 6 g of H_2O_2, 50 mL of ethanol, and 50 mL of deionized (DI) water in a reactor. By purging with nitrogen gas for 30 min, the temperature of the solution in the reactor was increased to 50°C, at which the Fenton reaction was carried out in the reactor for 1 h. During the Fenton reaction of ferrous ions and hydrogen peroxide, OH functional groups could be formed on the PVDF membrane surface by the oxidizing power of the $\cdot$OH radicals generated from the Fenton reaction. After the reaction was completed, the membrane was taken out, washed with H2SO4 and DI water, and then dried using methanol and n-hexane.

When TEOS reacts with the OH functional groups generated on the PVDF surface, NPs grow at the hydroxylated groups and increase their sizes. 50 mL of ethanol were poured onto the hydroxylated surface of the PVDF membrane, and then 1 mL of TEOS was added and stirred. After a sufficient stirring, 10 mL of an $NH_3 \cdot H_2O$ solution were added to enable the NP growth. The growth time was varied (4, 6, and 12 h) to compare the hydrophobic properties according to the degree of particle growth. After the growth reaction of the particles was completed, 1% FAS in 50 mL of the ethanol solution was poured and stirred for 12 h for the hydrophobic modification of the NPs. The modified membrane was then taken out and dried.

3.1.3.3 Plasma treatment to increase the surface pore size and further omniphobic

modification

To control the surface pore size of the prepared PVDF membrane, an atmospheric plasma equipment (A.P.P. Co., Ltd.) was used. A dried membrane was attached to the stage of the plasma apparatus using O_2 and Ar gases. The distance between the surface of the membrane and head of the plasma apparatus was set to approximately 0.3 cm. The surface was exposed at 150 W for 60 s. The PVDF membrane with the increased pore size by the plasma treatment was hydrophobically modified according to the method in Section 3.1.3.2.

3.1.4 Characterization

The surfaces and morphologies of the pure and modified PVDF membranes were investigated by scanning electron microscopy (SEM). The membranes, consecutively immersed in methanol and n-hexane and dried in an oven at 60°C for 24 h, were fixed on a sample holder with a carbon double sticky tape and their surfaces were coated with Pt. The Pt coating was carried out using a turbo-pumped high-resolution chromium sputter coater (K575X, EMITECH, Lohmar, Germany) for 1 min at 2×10^{-3} mbar and 20 mA. All the samples were observed at a magnification of 5000.

Attenuated total reflectance Fourier-transform infrared (ATR-FTIR) spectroscopy was used to evaluate the changes in chemical properties resulted from the modification of the membrane surface. The PVDF membrane was analyzed using a diamond ATR crystal. Prior to the analysis of the membranes, the instrument was purged with nitrogen for 24 h. The spectra were measured at a resolution of 4 cm^{-1} in the range of 600 to 4000 cm^{-1}. The OMNIC software (version 8.1) was used as a spectrum analysis program.

Chemical properties were confirmed using an X-ray photoelectron spectroscopy (XPS, Thermo Fisher, UK) with Kalpha (1486.6 eV). In XPS analysis, a double-focusing hemispherical analyzer was used. The pass energy was measured in a vacuum as 50 eV with a binding energy step size of 0.1 eV.

To evaluate the hydrophobicity of the pure and modified membrane surfaces, their contact angles were measured using a Phoenix 300 Plus instrument (Surface & Electro Optics Co. Ltd., Korea). The surface contact angle was measured using the sessile drops method. For comparison of the pure PVDF membrane with the superhydrophobic PVDF membranes, two coupons were used for each membrane type; the contact angle was measured 20 times per coupon, and then the values were averaged.

The thickness of the membrane was measured using a Digital thickness gauge (Mitutoyo, Japan). Thickness was measured 10 times and then averaged.

For pore size measurement, PMI's pore size measuring device (CFP-1500AEL) was used. The wet up/dry up method was used to measure pore size distribution and mean pore size. Before measurement, all membranes were prepared in wet condition and mounted on the instrument cell. Starting at 0 psi, the pressure was gradually increased until 50 psi. Pressure recorded the section where the first bubble point is taken, and then measure the wet-up state by measuring the flow rate in real time. After finishing wet up measurement, pressure was decreased and then the pore size distribution could be measured by checking the flow rate in the dry up state.

3.1.5 DCMD performance test

An operation in the DCMD mode was carried out to evaluate the performances and antiwettabilities of the membranes. Membrane samples were mounted in a cell with an effective area of 4×6 cm^2, the feed and permeate solutions flowed counter-currently along the membrane. The feed solution of 1 M NaCl at 70°C was circulated along the membrane surface using a gear pump at 1 Lmin^{-1}. As a permeate solution, DI water maintained at 25°C was also circulated by contacting the other membrane surface using a gear pump at 1 Lmin^{-1}. To maintain the feed concentration after the start of the operation, DI water was added to the feed solution with an amount equal to that of the produced permeate. After 2 h of operation, for comparing the omniphobicity between the membranes, SDS was spiked in the feed to 0.2 mM, and then 0.2 mM of SDS were added every 30 min. Therefore, the SDS concentration in the feed was gradually increased to accelerate the wetting [136]. The flux was calculated using the change in weight of the permeate over the operated time, as shown in Eq. 1. In addition, the salt flux (SF), which is the amount of salt passing from the feed to the permeate per unit area and time, was calculated using Eq. 2.

$$J_w = \frac{\Delta \text{ weight}}{\Delta \text{ time} \times \text{effective membrane area} \times \text{water density}} \left(\frac{\text{L}}{\text{m}^2\text{h}} \text{ (LMH)} \right) \qquad \text{Eq. (1)}$$

$$SF = \left(\frac{\Delta C_p \, \Delta V_p}{\Delta \text{ time} \times \text{effective membrane area}} \right) \left(\frac{\text{g}}{\text{m}^2\text{h}} \text{ (GMH)} \right) \qquad \text{Eq. (2)}$$

where ΔC_p and ΔV_p are the changes in concentration and volume of the permeate, respectively.

3.1.6 Stability test of the modified membranes

The hydrophobic stability of the membrane after the hydrophobic modification was investigated using ultrasonic equipment (Cole Parmer Co.). A 3×3 cm^2 membrane was immersed in 100 mL of an ethanol solution for complete wetting, followed by sonication for 30 min with an energy of 288000 J. After the sonication treatment, the stability of the membrane was evaluated by the remaining number of particles on the surface through SEM and CA. For the further stability comparison, weight of the NPs was measured using certain size of membrane. Virgin, dip-coating, and plasma + growth membranes were prepared with 1 x 1 cm^2 of size. Then, the weight of each membrane was measured 3 times for exact comparing. Finally, to verify the stability in actual MD process, plasma + growth membrane was applied for 5 times separately without any treatment and then flux and SF were calculated.

3.2 Results and Discussion

3.2.1 Morphologies of the pure and surface modified PVDF membranes
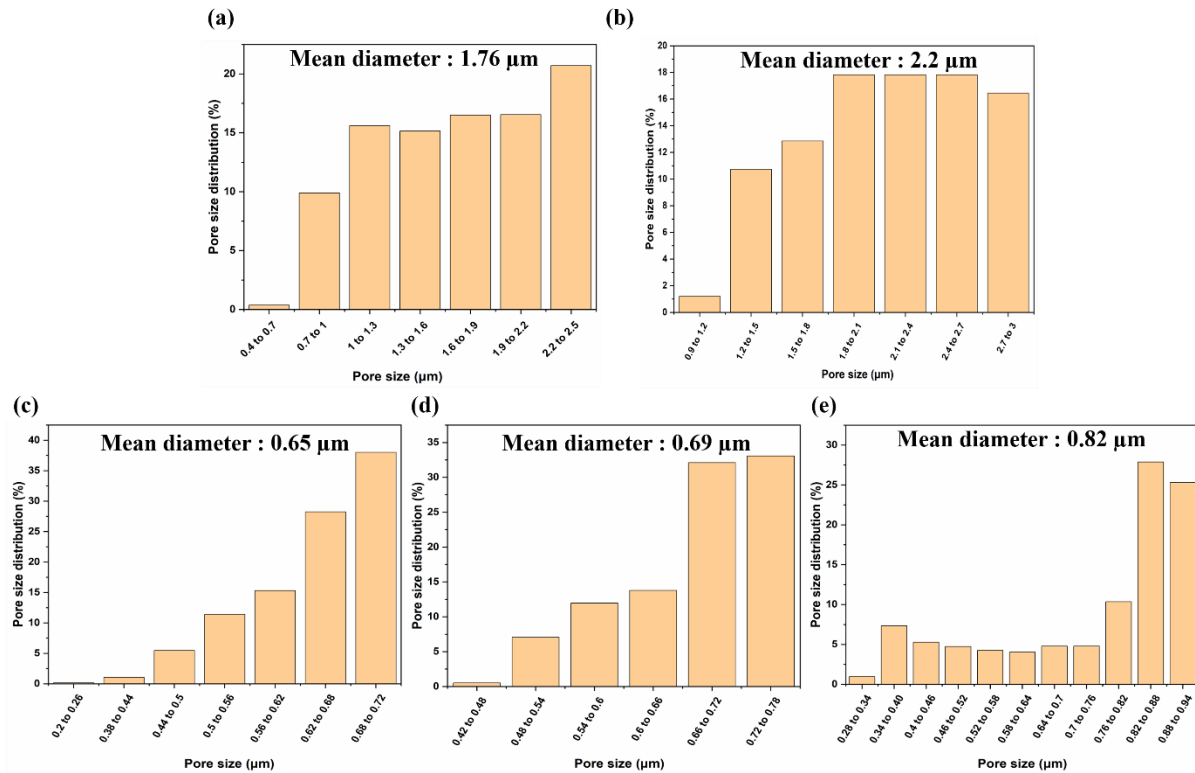
Figure 3.1 Pore size distribution and mean diameter of (a) pure PVDF, (b) PVDF after plasma treatment, (c) dip-coating 4 h, (d) no plasma + growth 12 h, and plasma + growth 12 h.

The pore size distribution and mean diameter were measured to confirm the change of pore according to the modification. As can be seen in Figure 3.1 (a), pure PVDF has a mean diameter of 1.76 μm. Figure 3.1 (b) shows that the value increased to 2.2 μm after plasma treatment. In the case of the modification by dip-coating 4 h, the mean diameter of 0.65 μm is shown in Figure 3.1 (c). This is because the hydrophobic NPs accumulate on the surface and the first bubble point is observed when the pressure is increased to measure the pore size and it seems to be measured at a smaller value than the pore size of the membrane itself. In the case of Figure 3.1 (d) using the no plasma + growth 12 h method, it can be confirmed that 0.69 μm. This is due to the growth of NPs, which can be seen as filling the pore with NPs and reducing the pore size. As a method to solve this problem, plasma treatment was applied on the membrane. Effect of plasma treatment is confirmed in Figure 3.1 (e) that the pore size of 0.82 μm which is larger than no plasma + growth 12 h membrane.
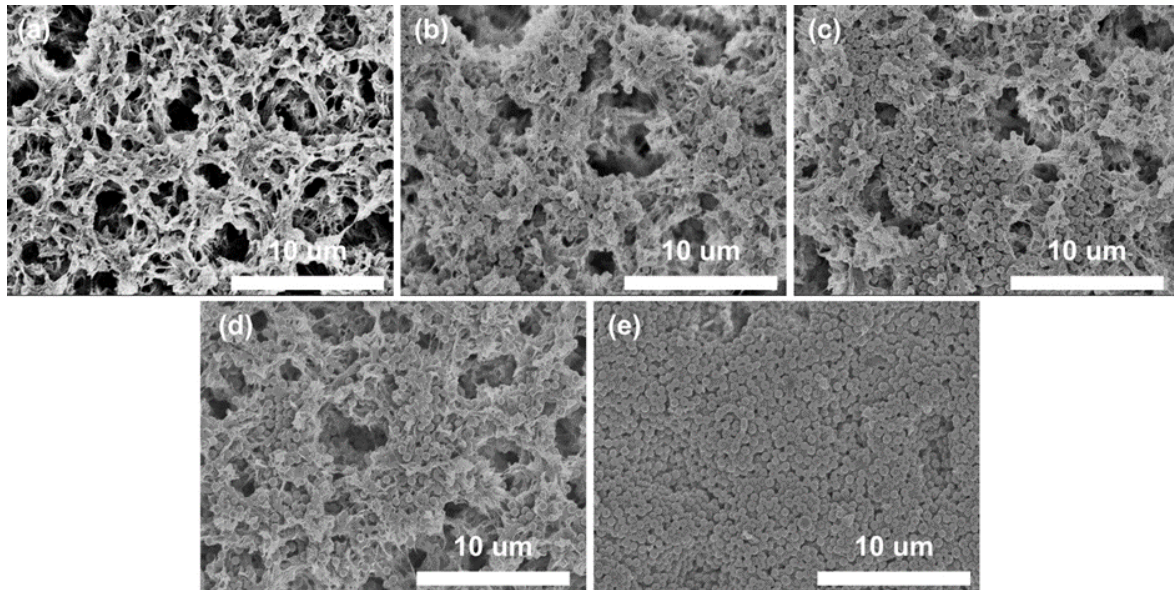
Figure 3.2 SEM surface images of the membranes modified using the dip-coating method over coating times of (a) 0, (b) 0.5, (c) 1, (d) 2, and (e) 4 h.

To verify membrane pore changes visually, the surface morphologies of the membranes were investigated after the dip-coating modification with SEM. SiO_2 NPs prepared from TEOS were surface-modified with FAS. The pure PVDF membrane was then immersed in the solution containing the hydrophobic NPs. Figure 3.2 shows the surface changes with the increase in the coating time. Figure 3.2 (b) shows hydrophobic SiO_2 NPs with sizes of approximately 500 nm on the surface of the PVDF membrane after 0.5 h of coating. A larger number of NPs were observed on the surface when the coating time was increased to 2 h (Figure 3.2 (d)). When the coating time was increased to 4 h, the membrane surface was fully covered with NPs (Figure 3.2 (e)).
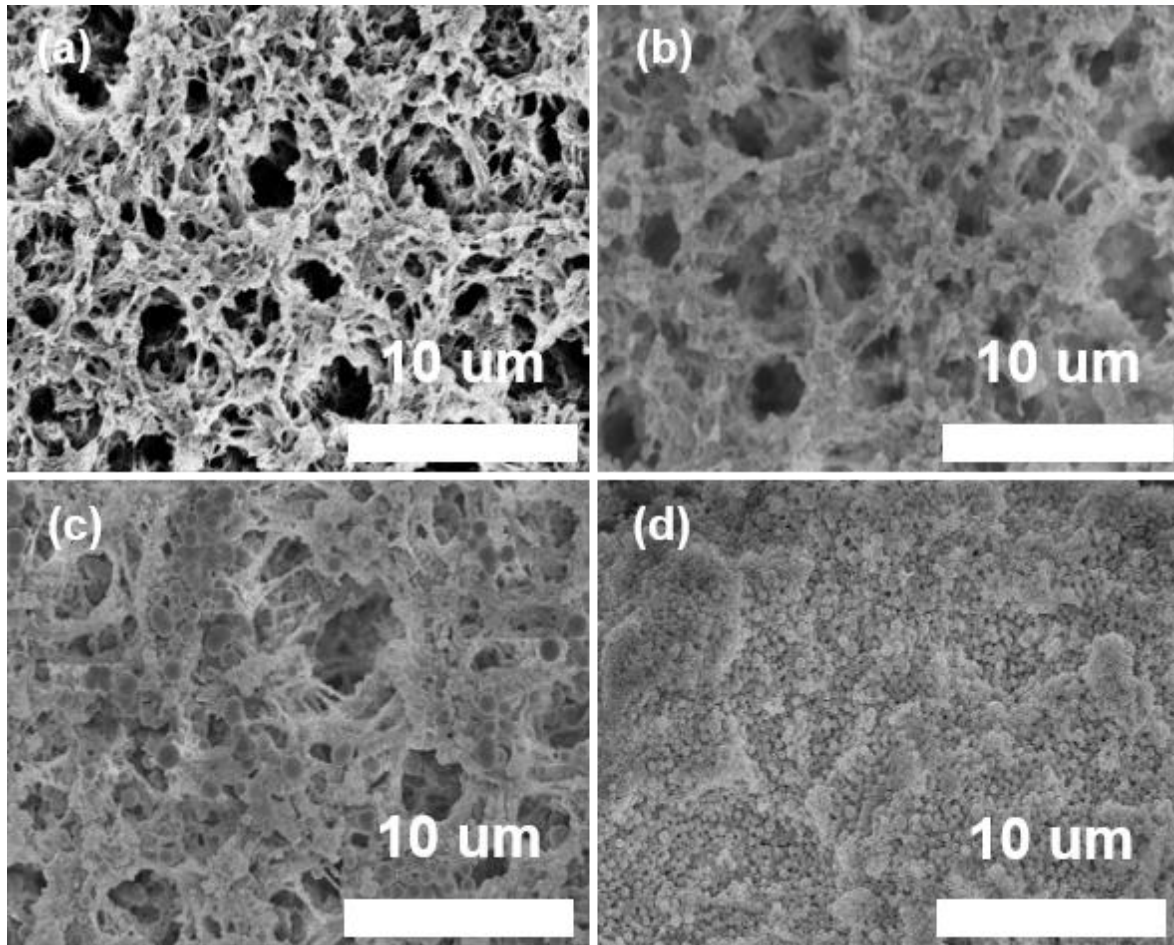
Figure 3.3 SEM surface images of the membranes modified by the NP growth on the hydroxylated membrane surface with different growth times of (a) 0, (b) 4, (c) 6, and (d) 12 h (without plasma pretreatment).

To improve the stability of the NPs on the membrane surface, NPs were grown from the membrane surface. Figure 3.3 shows the surfaces of the membranes modified by the Fenton-reaction which leads to OH functional groups on the membrane surface. From this OH functional group, SiO_2 NPs grew, and subsequent reaction of the NPs with FAS had been done. The SEM image showing the NPs grown for 4 h on the surface of the PVDF membrane reveals that the particles were not completely grown and had various sizes, which shown smaller than 500 nm (Figure 3.3 (b)). When the growth (reaction) time increased to 6 h, the sizes of the SiO_2 particles on the membrane surface increased, more particles were grown on the surface, and more membrane pores were blocked by the NPs (Figure 3.3 (c)). With 12 h of growing time, the particles almost covered the surface with various size (Figure 3.3 (d)). Because of growing procedure, NPs has various size which is totally different compare with dip-coating method (Figure 3.2). When NPs were synthesize only using TEOS, SiO_2 NPs showed uniform size (around 500 nm) because TEOS reacted only each other. However, with the membrane after Fenton-

reaction, OH functional group on the membrane also involved in the NPs synthesis which leads to the various size of NPs. Even though SiO_2 NPs can be prepared with various size after changing the synthesizing condition, growing procedure with OH functional group induce the size variation automatically so that surface can have nano/micro structure itself which will increase omniphobicity effectively.
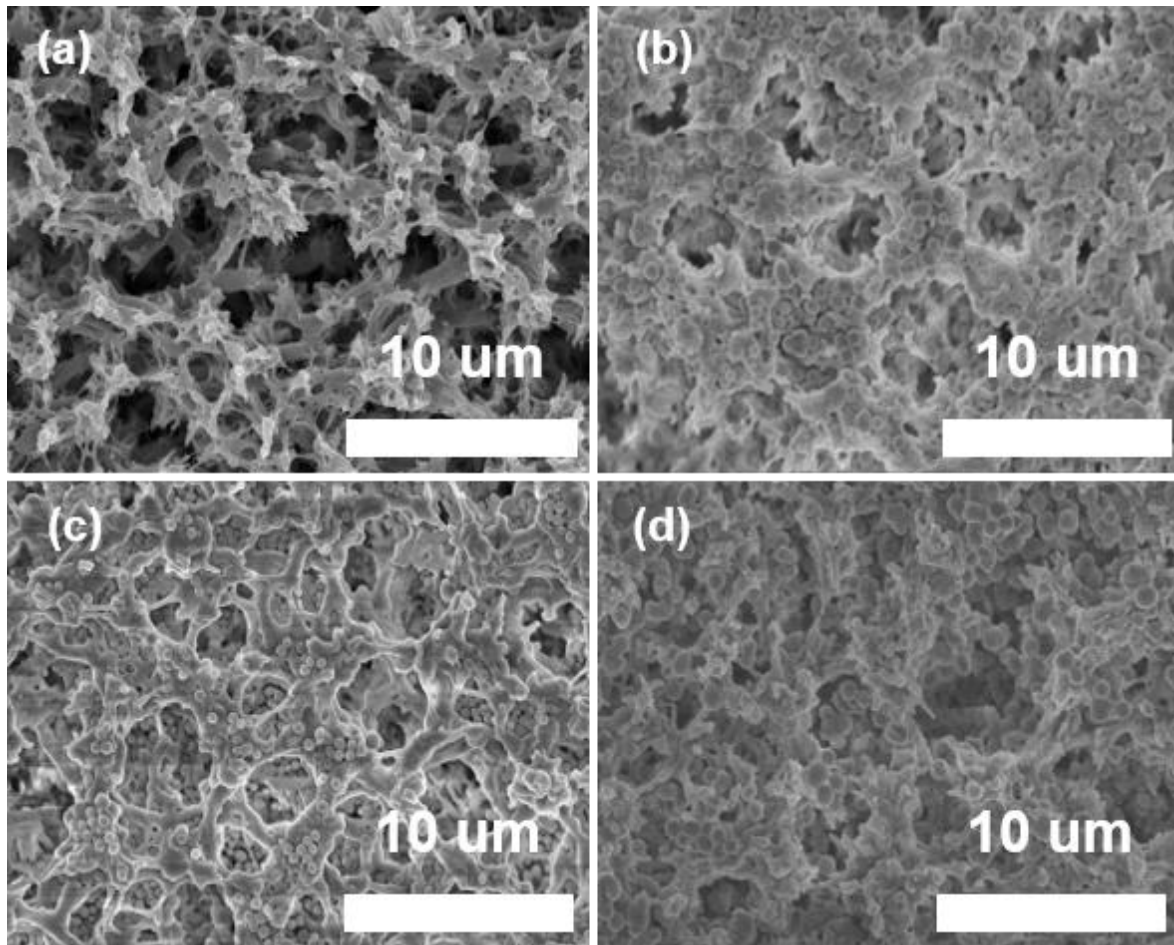
Figure 3.4 Figure. SEM surface images of the membranes modified by the NP growth on the hydroxylated membrane surface with different growth times of (a) 0, (b) 4, (c) 6, and (d) 12 h (with the plasma pretreatment).

To maximize the stability of the NPs and enhance the performance, the pores of the membrane were expanded by the plasma treatment. The membrane was then modified using the previously described NP growth method. As shown in Figure 3.4 (a), the surface pores of the plasma-treated membrane were larger than those of the pure PVDF (Figure 3.2 (a)). With growing time of 4 h (Figure 3.4 (b)), the NPs were grown not only on the membrane surface but also inside the enlarged pores. After

6 h of growing (Figure 3.4 (c)), SiO_2 particles were more abundant on the surface and inside, and after 12 h (Figure 3.4 (d)), the surface and pores were covered and filled with NPs. This shows that after the plasma treatment, the NPs grew not only on the surface but also inside the membrane, providing a high stability of the modified membrane during the long-term operation and enhanced performance because of enlarged pore size. Furthermore, the SiO_2 NPs were synthesized in various size like in Figure 3.3. Same as before, OH functional group acted as starting point of SiO_2 synthesis.
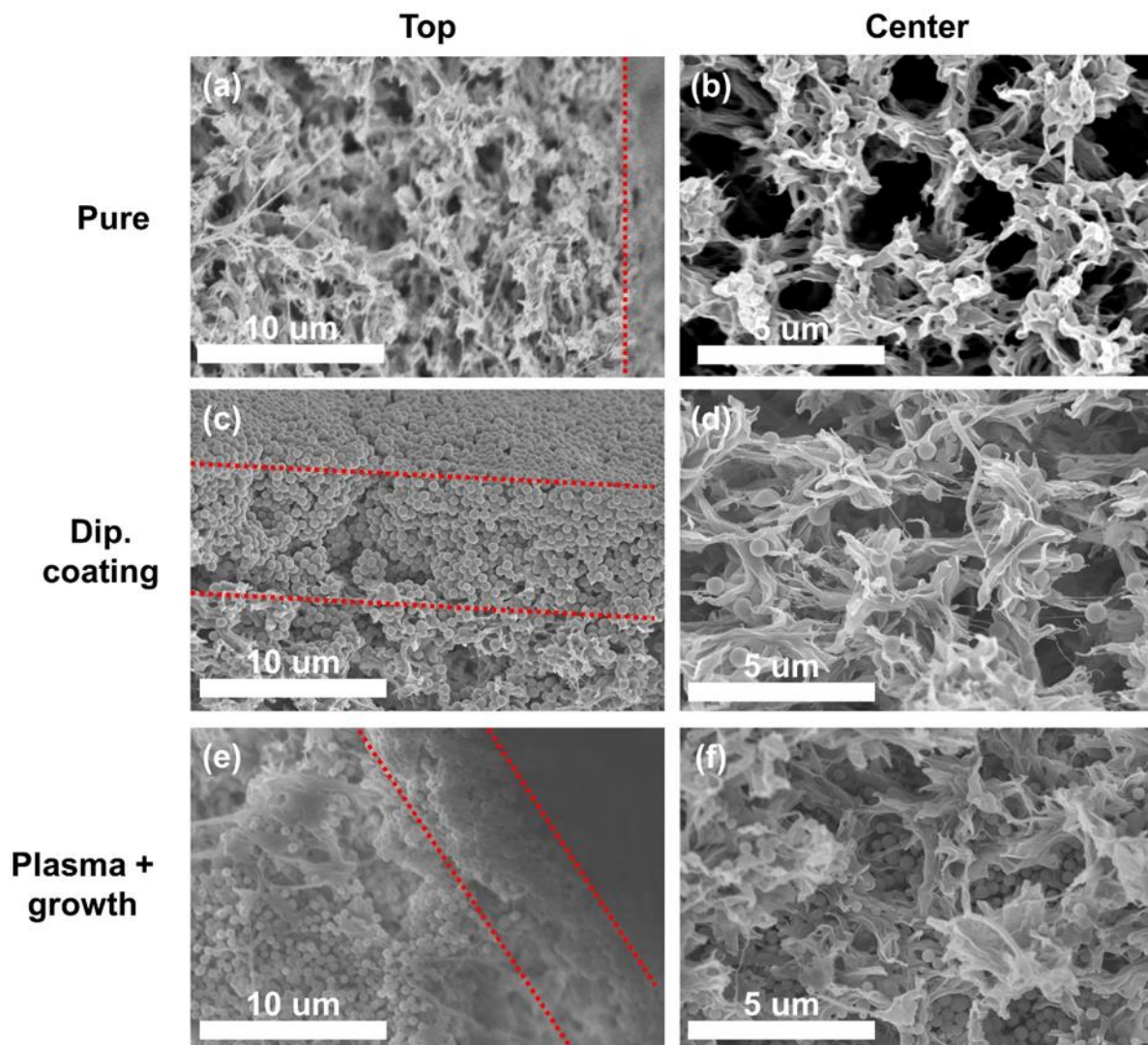
Figure 3.5 Cross-section images of (a) pure PVDF (top), (b) pure PVDF (center of membrane), (c) dip-coating 4 h (top), (d) dip-coating 4 h (center of membrane), (e) plasma + growth 12 h (top), and (f) plasma + growth 12 h (center of membrane).

We also measured cross-section images to identify NPs that were growing in the pore, and then

we compared with the above result. Pure PVDF membrane shows a sponge-like structure (Figure 3.5 (a, b)). After the dip-coating 4 h modification, NPs are accumulated on the surface of the membrane like a layer (Figure 3.5 (c)). However, in the middle part of the membrane, there is very small number of NPs found in Figure 3.5 (d). In the case of dip-coating, it is confirmed that the particles do not penetrate the sponge-like structure because it only covers the surface. In plasma + growth 12 h case, NPs were growing in the inner pores as compared to dip coating (Figure 3.5 (e, f)).
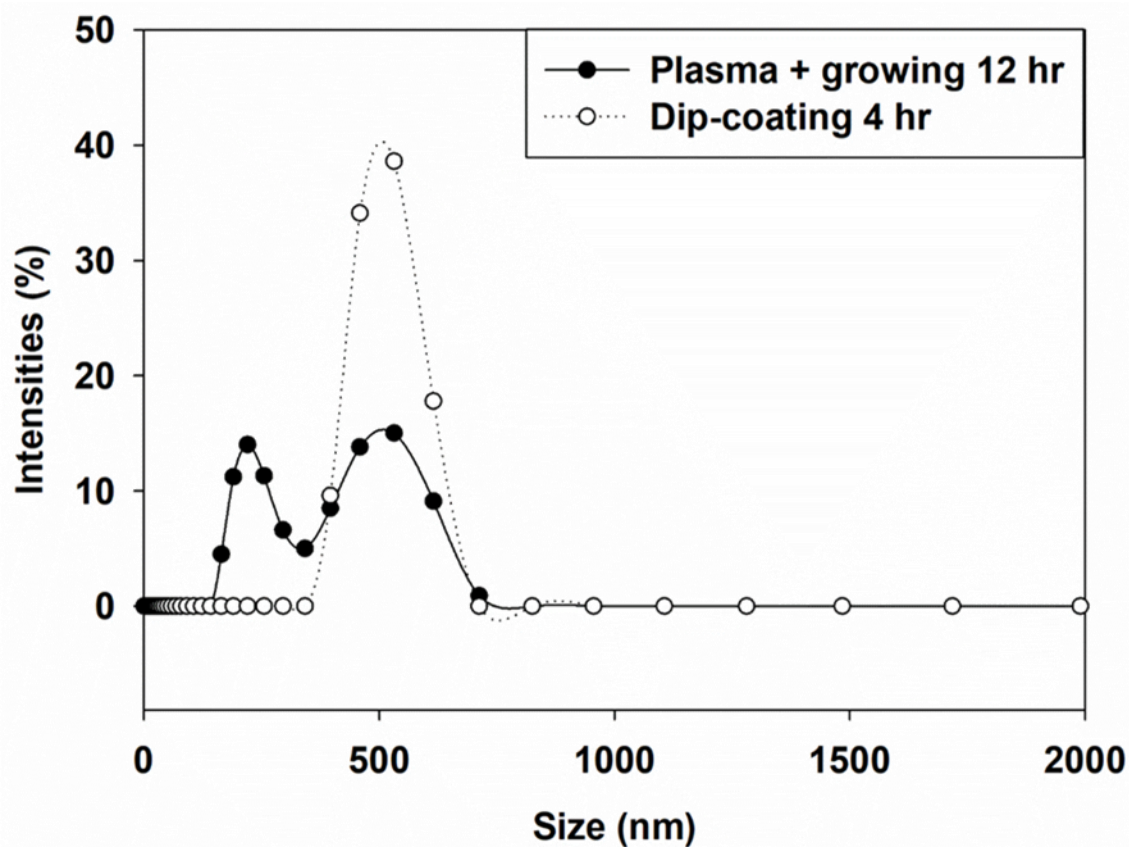
Figure 3.6 Size distribution of SiO₂ NPs from dip-coating 4 h and plasma + growth 12 h membranes.

To analyze the size of the NPs, size distribution analysis was conducted (Figure 3.6). For the NPs from dip-coating method and plasma method, membrane after modification was prepared and sonicated in the EtOH to get the NPs in the solution. After sonication, detached NPs were dispersed in the EtOH which was used for distribution analysis. In the case of dip-coating, NPs were formed before coating and the membrane was covered after hydrophobic modification (Figure 3.2). From the results of the size distribution analysis, it can be confirmed from the Figure 3.6 that it has a constant particle size about 500 nm. In the case of plasma + growth method, we can confirm visually that the size of

particles on the surface is not constant by SEM (Figure 3.4). The particles grow from the surface and are not constant depending on the surface position of the membrane. As a result of size distribution, it spreads to 300 ~ 600 nm.
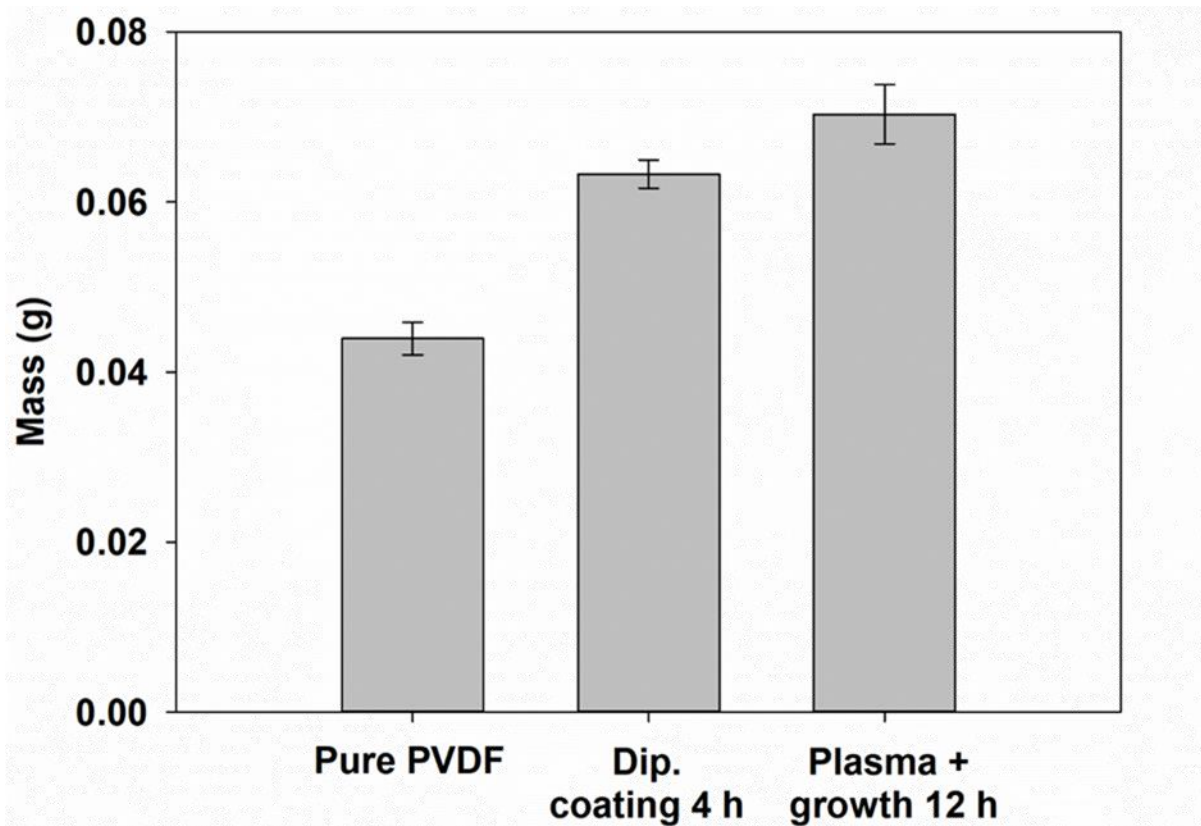
Figure 3.7 Mass increasement of pure, dip-coating 4 h, and plasma + growth 12 h membranes.

Furthermore, In the case of the content of NPs, it is difficult to measure accurately, so we will explain the change of membrane weight and cross-section analysis as an indirect method (Figure 3.7). Pure PVDF, dip-coating 4 h, and Plasma + growth 12 h membranes were prepared at 1 × 1 cm, respectively, and the degree of NPs on (or in) the membrane was indirectly shown through the increase in weight. Figure 3.7 shows 0.044 g for pure membranes. In the case of dip-coating 4 h, 0.063 g was observed, which is about 40% higher than that of the pure PVDF membrane. In the case of plasma + growth 12 h, it was explained that NPs grow inside the pores so that there are more particles. As can be seen in the Figure 3.7, more weight change is observed (0.07 g, 60% increase) than coating.

3.2.2 FTIR spectroscopy, XPS, and contact angle measurements of the pure and surface
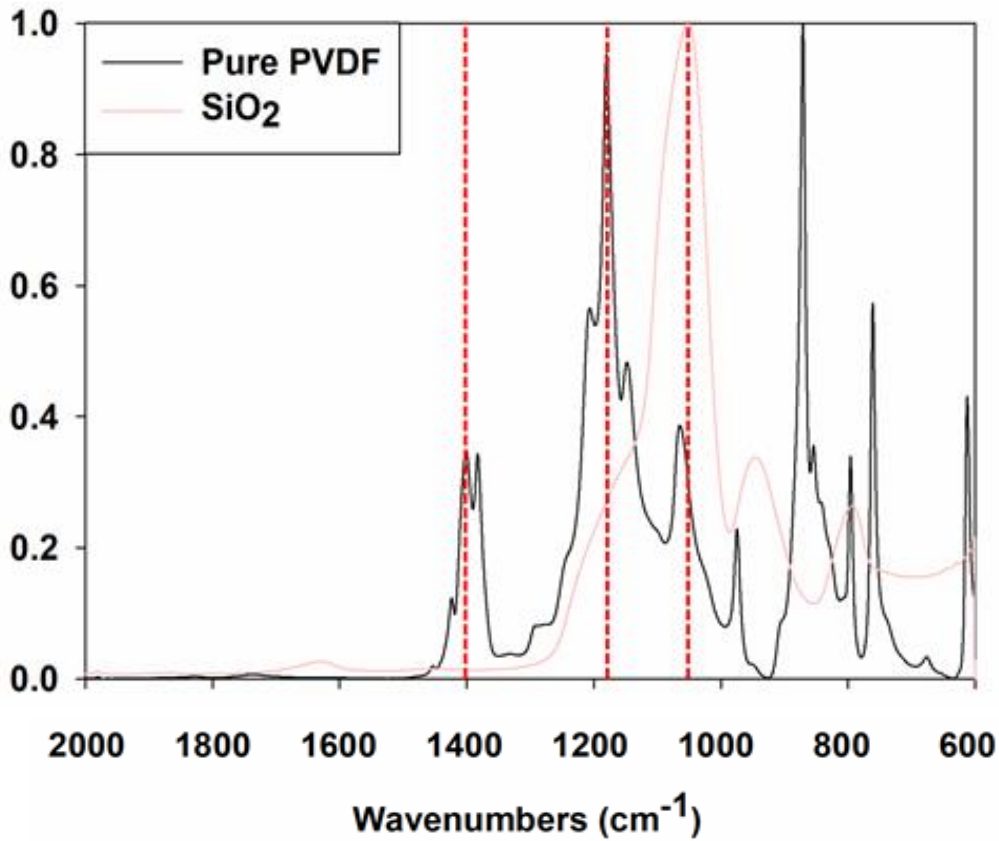
Figure 3. 8 FTIR spectra of pure PVDF and SiO₂ NPs.

The changes in the chemical characteristics of the membranes originated from the surface modification were investigated using FTIR spectroscopy. Figure 3.8 shows the changes in FTIR spectra with the increases in the coating and growth times in the coating and NP growth methods, respectively. The PVDF membrane exhibited characteristic peaks around 1400 cm^{-1} associated with -CH$_2$ and peaks around 1180 cm^{-1} associated with -CF$_2$ [137]. NPs are composed mainly of Si–O–Si bonds, and thus their FTIR spectra showed broad peaks around 1050 cm^{-1} [138].
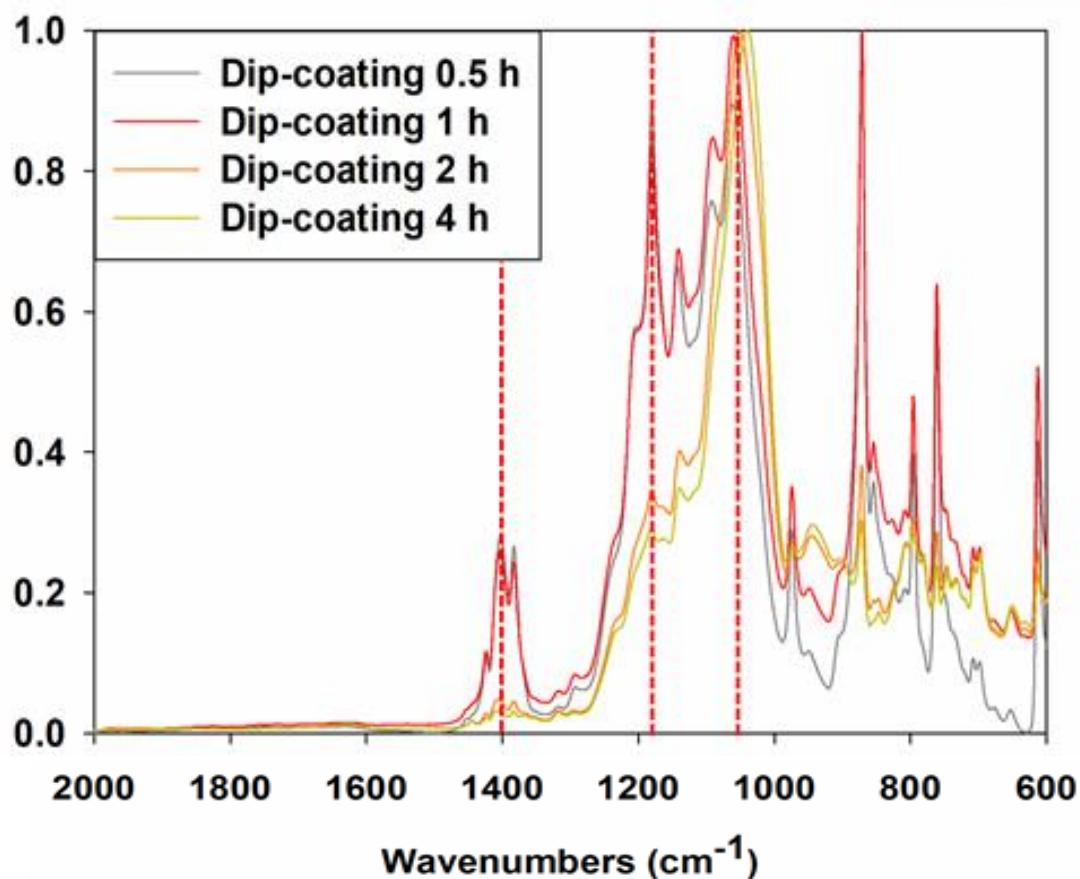
Figure 3. 9 FTIR spectra of membranes modified by the dip-coating method for 0.5, 1, 2, and 4 h.

As the NPs covered the membrane surface after the coating (Figure 3.9), the Si–O–Si peak gradually increased overwhelming the PVDF peak at 1180 cm^{-1}, which was relatively buried at 1050 cm^{-1}. After the 4 h of coating, the FTIR spectra of the modified membrane were like that of the pure NPs, which implies that the membrane surface was almost completely covered by the NPs.
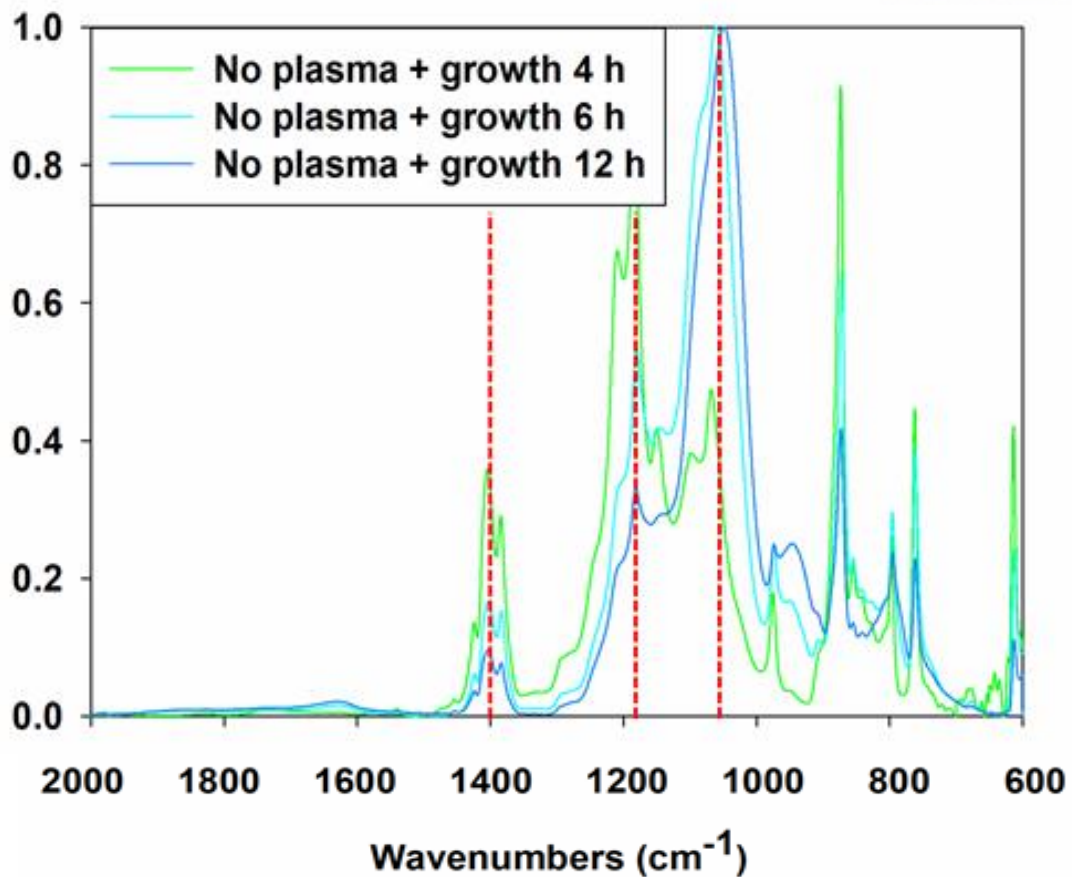
Figure 3. 10 FTIR spectra of the membranes modified by the NP growth method for 4, 6, and 12 h (without plasma pretreatment).

The membranes modified by the NP growth on their surfaces (Figure 3.10) exhibited decreased PVDF peaks at 1400 and 1180 cm^{-1} with the increase in the growth time, as in the case of the coating method. This was attributed to the faster deposition of PVDF through the grown NPs on the surface. This tendency also occurred in the modified membrane after the pores were enlarged through the plasma treatment.
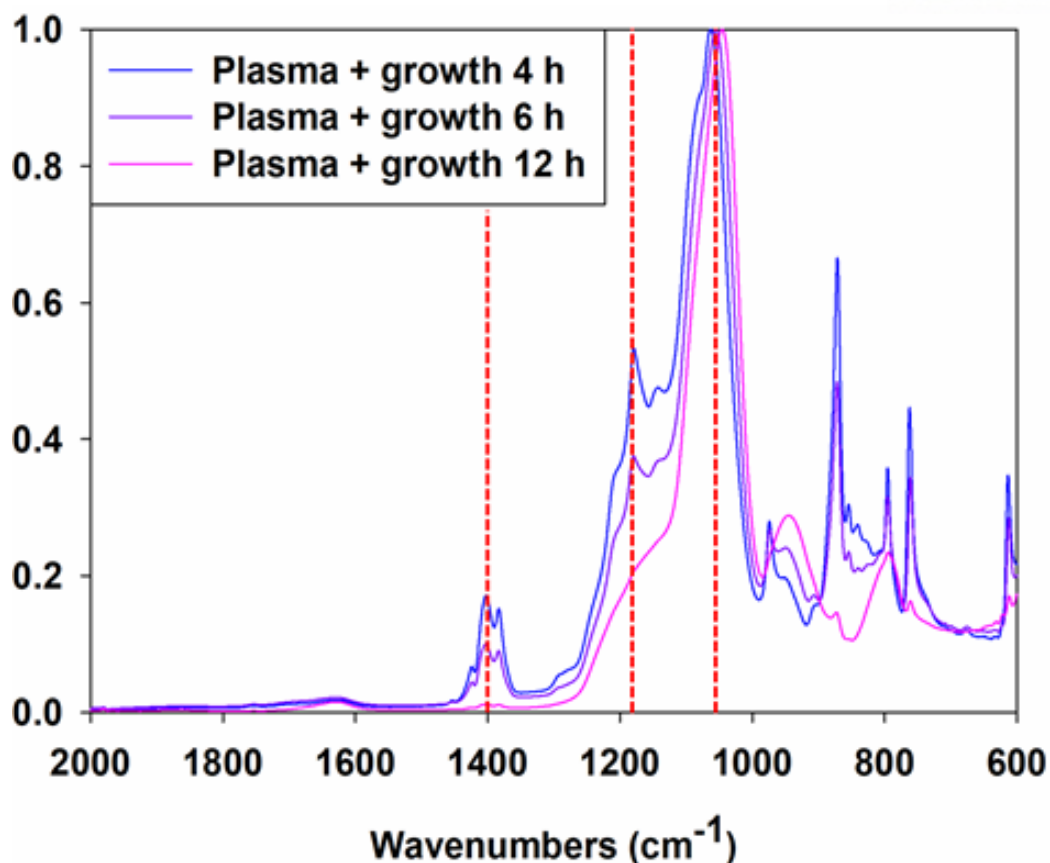
Figure 3. 11 FTIR spectra of the membranes modified by the NP growth method for 4, 6, and 12 h (with the plasma pretreatment).

The PVDF peak gradually disappeared with increasing growing time, and thus almost the same peak as that of the NPs was observed for the growth time of 12 h (Figure 3.11). The comparison of the FTIR spectra at the growth time of 12 h with and without the plasma pretreatment shows that the FTIR spectrum of the membrane after the plasma treatment is more like that of the NPs. When the pore size was increased, the NPs were accumulated from the inside of the pores and thus more NPs were exposed to the feed side of the membrane [139].
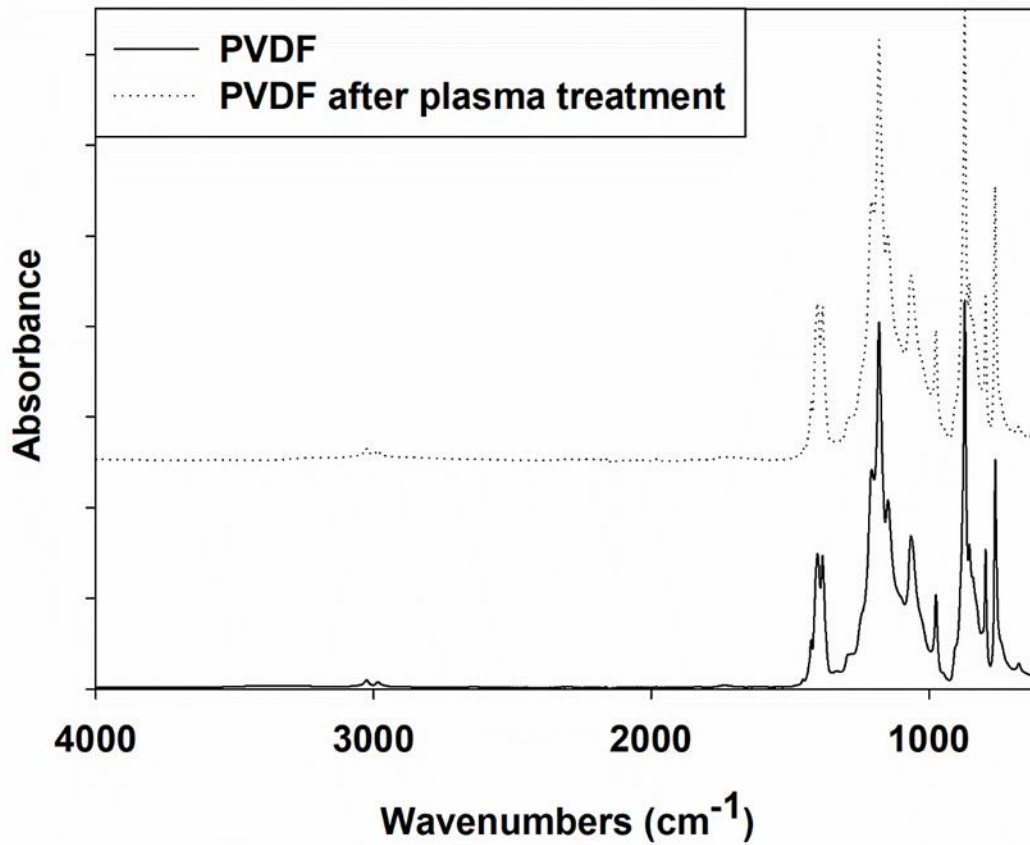
Figure 3. 12 FTIR spectra of the pure PVDF, dip-coating 4 h after sonication, and plasma + growth 12 h after sonication.

  Through the plasma treatment, the change of surface after treatment of pure PVDF membrane was confirmed FTIR. As shown in Figure 3.12, it was confirmed that there was no chemical change on the surface of the membrane through FTIR. This seems to be the result of proving that the plasma treatment did not cause any chemical change. Therefore, the FTIR spectra confirmed the chemical changes in the membrane surfaces upon the modification.

	C	O	Si
Pure PVDF		Area % C1s 37.34% F1s 62.57%	
PVDF after Fenton-reaction		Area % C1s 32.81% F1s 34.89% O1s 32.3 %	
Plasma + growth 12 h		Area % C1s 6.55% F1s 17.02% O1s 48.85 % Si2p 27.58%	
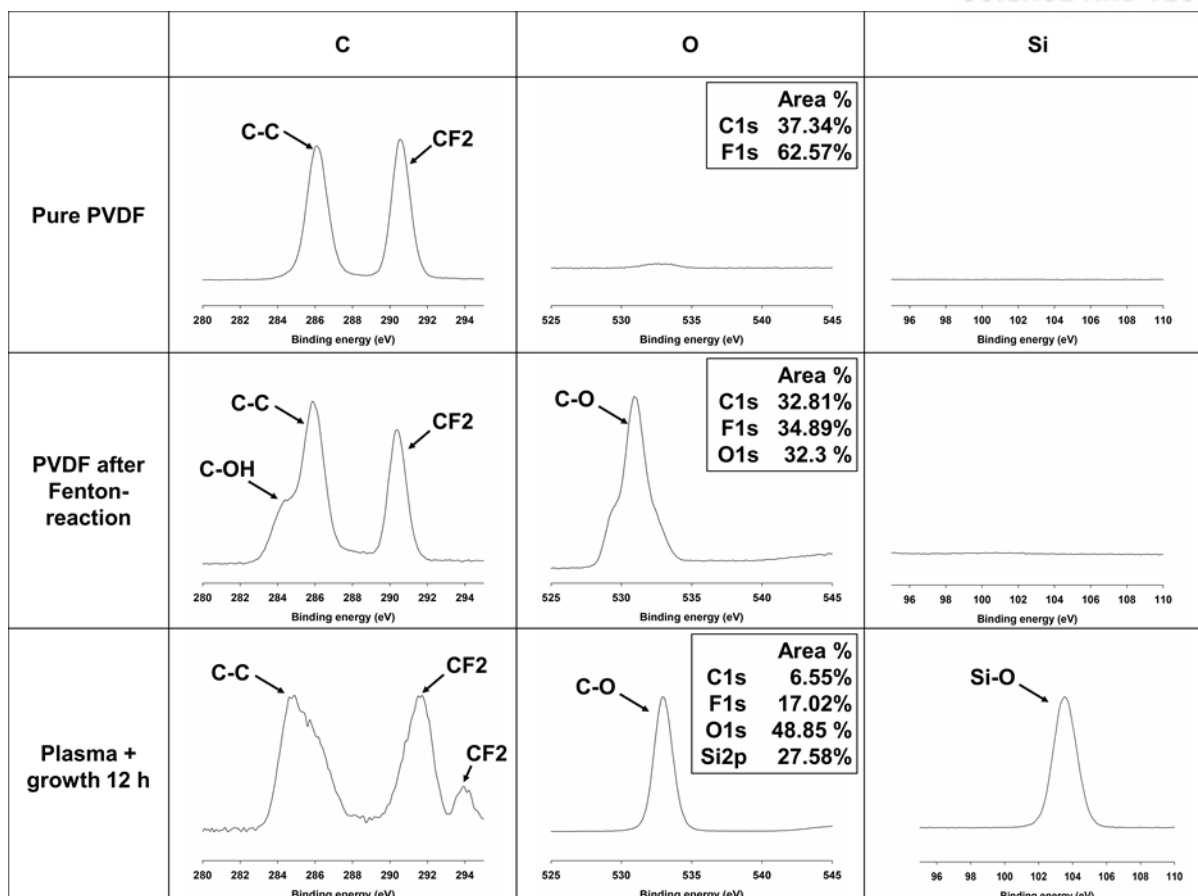
Figure 3. 13 XPS spectra of C1s, F1s, O1s, and Si2p of membranes. (a) pure PVDF, (b) PVDF after Fenton reaction, (c) plasma + growth 12 h.

XPS was measured to confirm the chemical change before and after the modification of the membrane. As can be seen in the Figure 3.13, only PVDF can detect C-C (286 eV) and CF_2 (291 eV) peaks. After the Fenton-reaction, OH bonds are formed on the surface, and a new peak of C-OH (284 eV, 531 eV) is found. Thereafter, because of the formation of particles through the growth treatment, a new Si-O (104 eV) peak was observed on the surface, thereby confirming the particles on the surface.

With FTIR and XPS results in Figure 3.8 to 3.13, it was confirmed that the membrane surface was successfully modified by chemical modification with Fenton-reaction, plasma treatment and growing procedure.
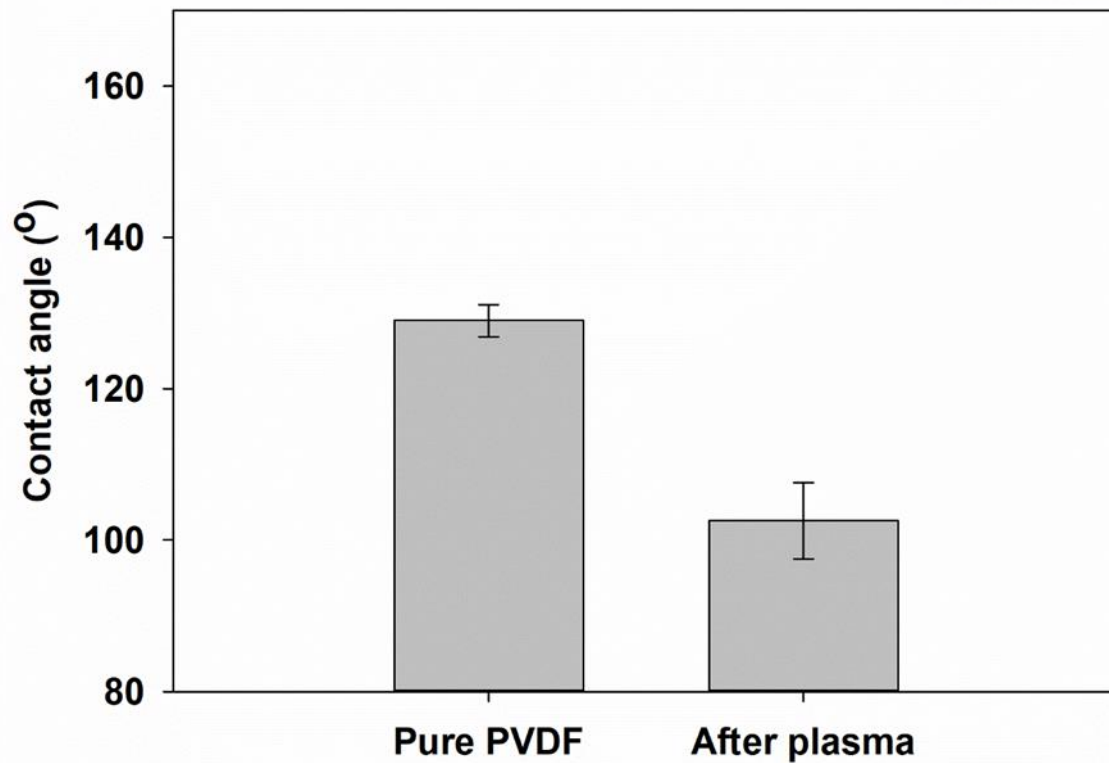
Figure 3. 14 CA measurement of pure PVDF membrane and after plasma treatment.

To verify the effect of plasma on hydrophobicity, pure membrane was compared with plasma treated membrane. The CA value of the membrane was slightly decreased after plasma treatment (Figure 3.14). The decrease in the contact angle, even without the chemical change of the surface like in Figure 3.12, can be seen as the enlargement of the surface pore size. As the pore size of the surface increased, the decrease of CA could be confirmed.
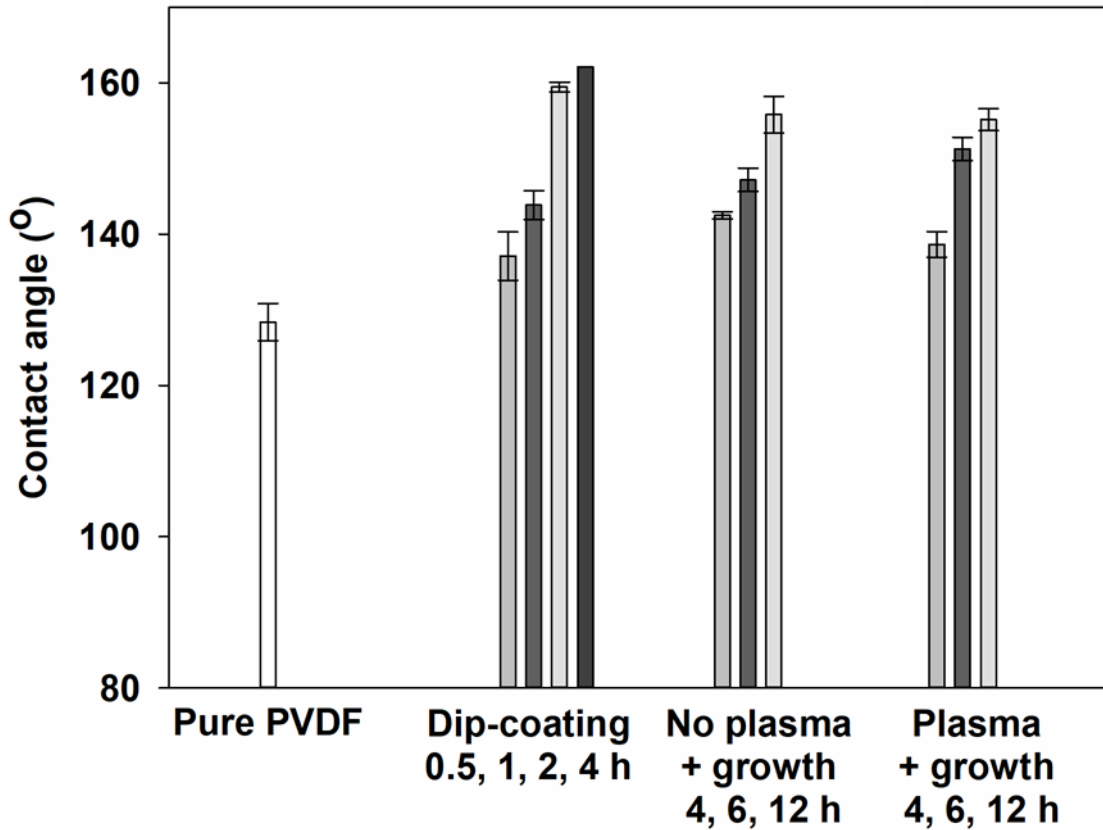
Figure 3. 15 CA value of the pure membrane and PVDF membranes modified with the dip-coating and NP growth methods with and without the plasma pretreatment.

Figure 3.15 shows that the pure PVDF membrane had a contact angle of 128°. The contact angle increased with the coating or growth time. Upon the 0.5 h of coating by the dip-coating method, the contact angle increased to 137°, while those after 1, 2, and 4 h were increased to 143, 159, and 162°, respectively. This shows the hydrophobicity increase as the hydrophobic NPs covered the surface. In addition, the contact angles between the coating times of 2 and 4 h were not significantly different; the surfaces were almost completely covered, as shown in the SEM images. The 4 h of NP growth increased the contact angle to 142°, while after 6 and 12 h, the contact angles increased to 147° and 157°, respectively. The SEM images suggest that the surface hydrophobicity increased as the surface was gradually covered with NPs. When the NPs were grown after the plasma pretreatment, the value was lower than that in the case of the coating treatment. The 4 h of treatment increased the contact angle of the membrane by 10°. The angle increased to 151 and 154° after 6 and 12 h, respectively. This shows that all the modification methods employed in this study increased the contact angle.

3.2.3 DCMD performances of the pure and surface modified PVDF membranes

Figure 3. 16 Water fluxes and SFs of the pure and modified PVDF membranes with coating method in the DCMD mode.

The performances of the pure and modified membranes were evaluated in the DCMD mode to investigate the effect of the omniphobicity change from the surface modification on the prevention of wetting phenomena in MD. When the flux was stabilized with the feed solution of 3.5 wt% NaCl at 70°C, 0.2 mM of SDS were added every 30 min to accelerate the wetting of the membranes and verify the omniphobicity of the membrane.

The flux of the pure PVDF membrane was stabilized after 2 h and maintained at 41 LMH (Figure 3.16). However, the flux immediately decreased, and the SF increased when SDS was spiked. Between the feed with the high temperature/concentration and permeate with the low temperature/concentration, differences in vapor pressure and osmotic pressure exist owing to the differences in temperature and concentration across the membrane, respectively. During the MD operation, water transports from the feed to the permeate due to the partial vapor pressure difference between the two sides of the membrane. However, when the membrane becomes wet, the DI water of the permeate with a low concentration moves to the feed due to the osmotic pressure difference. The reduction in flux and increase in SF in the pure PVDF membrane after the first spiking of SDS were due to the movement of water in the opposite direction, originated from the partial vapor pressure and osmotic pressure differences, which imply that the membrane was wet.

The same phenomenon was observed even when the dip-coating was carried out for 0.5 and 1 h. The fluxes of the membranes modified for 0.5 and 1 h were 31 and 25 LMH, respectively, lower than

that of the pure membrane. The gradual flux decrease with the increase in the coating time could be explained as the surface was gradually covered by NPs and thus the surface porosity of the membrane was reduced. As the SiO_2 NPs covered the membrane surface after 1 h, the increase in omniphobicity was confirmed by the contact angle measurement. However, it seems that the increase in the contact angle did not significantly contribute to the prevention of the wetting phenomenon when the DCMD operation was performed, as shown by the SF behavior. After the 2 h of dip-coating, most of the membrane surface was covered with hydrophobic particles, observed by SEM. The membrane was slightly more resistant to wetting than the membranes modified for 0.5 and 1 h. However, the flux began to decrease at approximately 8000 s. Similarly, the membrane coated for 4 h exhibited a flux of approximately 15 LMH, which decreased at approximately 8500 s. With the increase in the coating time, the surface was covered with the SiO_2 NPs and the wetting was gradually delayed even after adding the SDS solution. However, the SFs for the coating times of 2 and 4 h were slightly decreased compared to those at 0.5 and 1 h. The membranes modified for 0.5 and 1 h were completely wetted, and thus the salt passed through them in the liquid phase, not in the vapor phase, from the feed to the permeate and increased the SF. When the membranes were modified for 2 and 4 h, some pores of the membranes were slightly wetted leading to blockage of water vapor paths, but the condensed water-filled pores were not connected to each other from the feed surface to the permeate surface. With these results, dip-coating membrane showed that omniphobicity didn't increase enough to prevent the wetting while MD process.
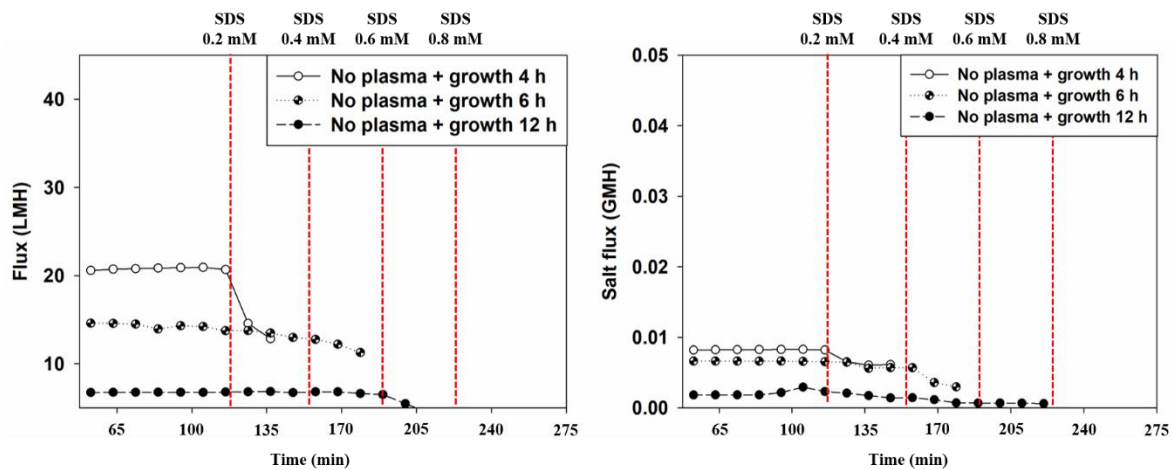
Figure 3. 17 Water fluxes and SFs of the pure and modified PVDF membranes with growing method in the DCMD mode.

When the membrane was modified by the NP growth on its surface, the flux of the membrane modified for 4 h was 21 LMH at the steady state, which decreased immediately after the addition of

SDS (Figure 3.17). The growth of NPs for 4 h was not sufficient to increase the membrane omniphobicity for preventing the wetting of the membrane. When the growth times increased to 6 and 12 h, the fluxes decreased to approximately 15 and 6 LMH, respectively; further, the fluxes slightly decreased after the second and third additions of SDS, respectively. This shows that the NPs generated on the surface reduced the flux due to the coverage and clogging of the surface pores, but increased the omniphobicity, preventing the wetting of the membrane for some period.
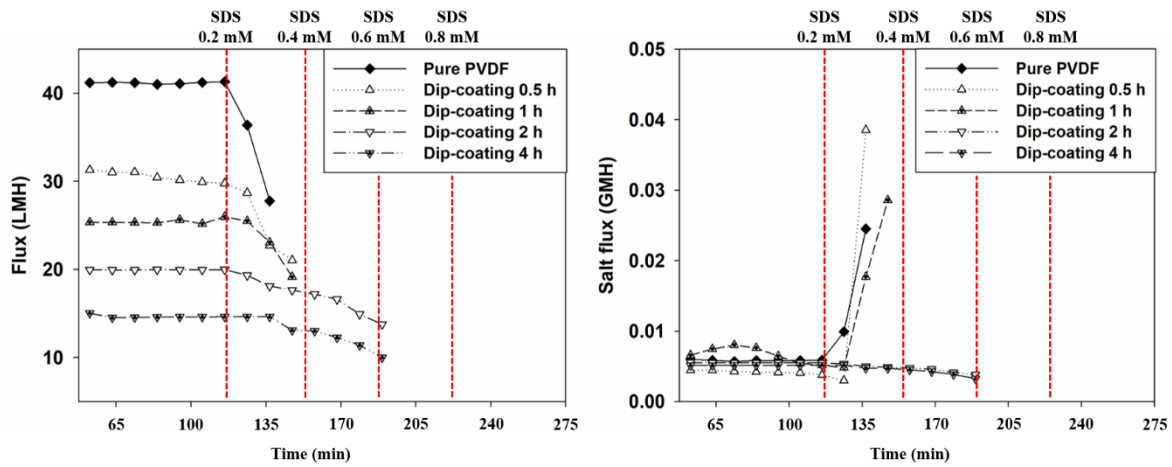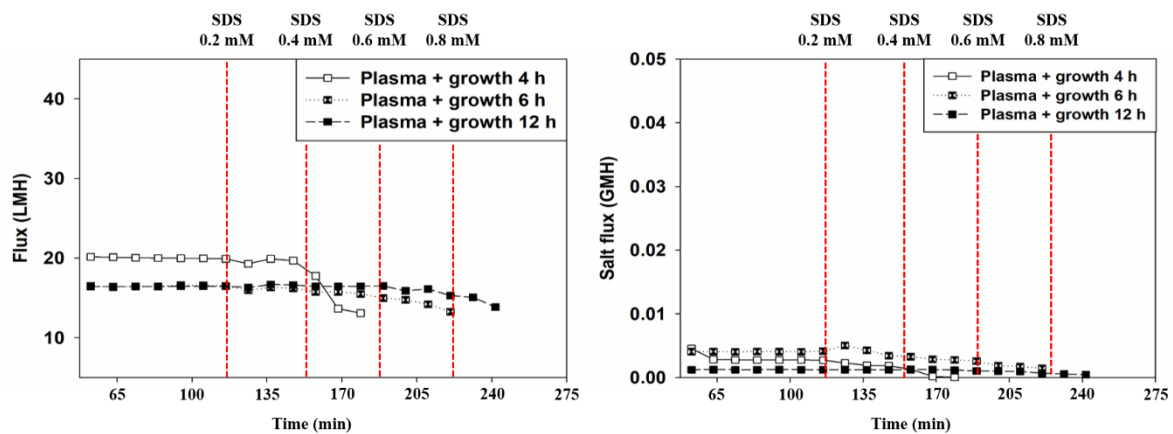

Figure 3. 18 Water fluxes and SFs of the pure and modified PVDF membranes with plasma and growing in the DCMD mode.

The performances of the membranes modified by enlarging the pores in their surfaces with the plasma treatment and growing the NPs in the pores to increase the stability of the NPs during the operation were investigated (Figure 3.18). The membrane modified for 4 h with the plasma pretreatment yielded a decreased flux after the two cycles of addition of SDS, leading to an enhanced wetting resistance compared with those of the pure membrane, membranes modified with the dip-coating, and membrane modified for 4 h without plasma treatment. For the membrane modified for 6 h, the initial flux of 16 LMH slightly decreased after the two cycles of addition and clearly decreased after the three cycles of addition. The flux of the membrane modified for 12 h was 16 LMH without any difference from that of the membrane modified for 6 h; the flux was maintained until the fourth addition of SDS. The change in SF was not noticeable in this case as the membrane was not wetted because of omniphobic property.

Furthermore, the membrane modified by the NP growth on its surface with the plasma pretreatment had a smaller thickness (0.2575 ± 0.0065 mm) than that of the membrane modified by the NP growth method without the plasma treatment (0.3421 ± 0.0076 mm), leading to the smaller decrease

in water flux owing to the smaller resistance during the passage of vaporized water. This implies that the SiO_2 NPs grown in the pores as well as on the surface significantly improved the omniphobicity of the PVDF membrane which lead to the stable performance without wetting even after adding the SDS solution [140].

3.2.4 Stabilities of the pure and surface modified PVDF membranes

The previous results showed that the hydrophobic modification through dip-coating had a remarkable effect increasing the hydrophobicity of the surface. However, as the hydrophobic NPs physically covered the membrane, the structural integrity was unstable during the DCMD operation. Compared with the dip-coating method, which involved the simple placing of NPs on the membrane surface, the NP growth method with the Fenton reaction effectively prevented the membrane from wetting in the DCMD operation by increasing the stability of the particles.
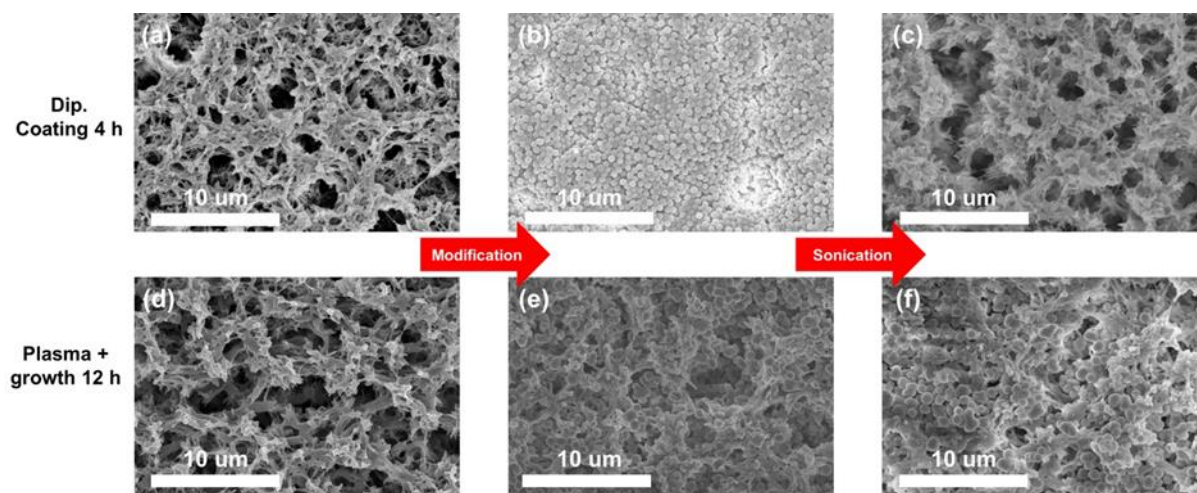
Figure 3. 19 Stability test through sonication for 30 min: (a) pure PVDF membrane, (b) membrane modified by dip-coating for 4 h, (c) membrane after 30 min of sonication of the sample in (b), (d) PVDF membrane after the plasma treatment, (e) membrane modified by the NP growth for 12 h (with the plasma pretreatment), and (f) membrane after 30 min of sonication of the sample in (e).

As a direct method to confirm the stability, the modified membranes were ultrasonically processed and investigated using SEM (Figure 3.19). With the membrane after dip-coating for 4 h, membrane has fully covered surface by NPs (Figure 3.19 (a) and (b)). Figure 3.19 (c) shows that the

NPs were completely detached from the membrane surface after the sonication of the membrane modified with the dip-coating method. This indicates that the membrane was physically covered with the NPs, and thus the modified membrane was not stable owing to the absence of adhesion force between the membrane and particles. On the other hand, the SEM image in Figure 3.19 (f) shows that the membrane after the plasma pretreatment followed by modification with the growth method did not exhibit any difference in surface morphology after the sonication. It is worth noting that not only the NPs grown inside the pores but also the NPs on the surface remained even after the sonication treatment. This study shows that the Fenton-reaction on the surface carried out to create reactive functional groups and enable NP formation at the generated reaction sites is effective to preserve the stability of the NPs during the operation. Furthermore, the stability could be further improved by the pore enlargement by the plasma pretreatment.
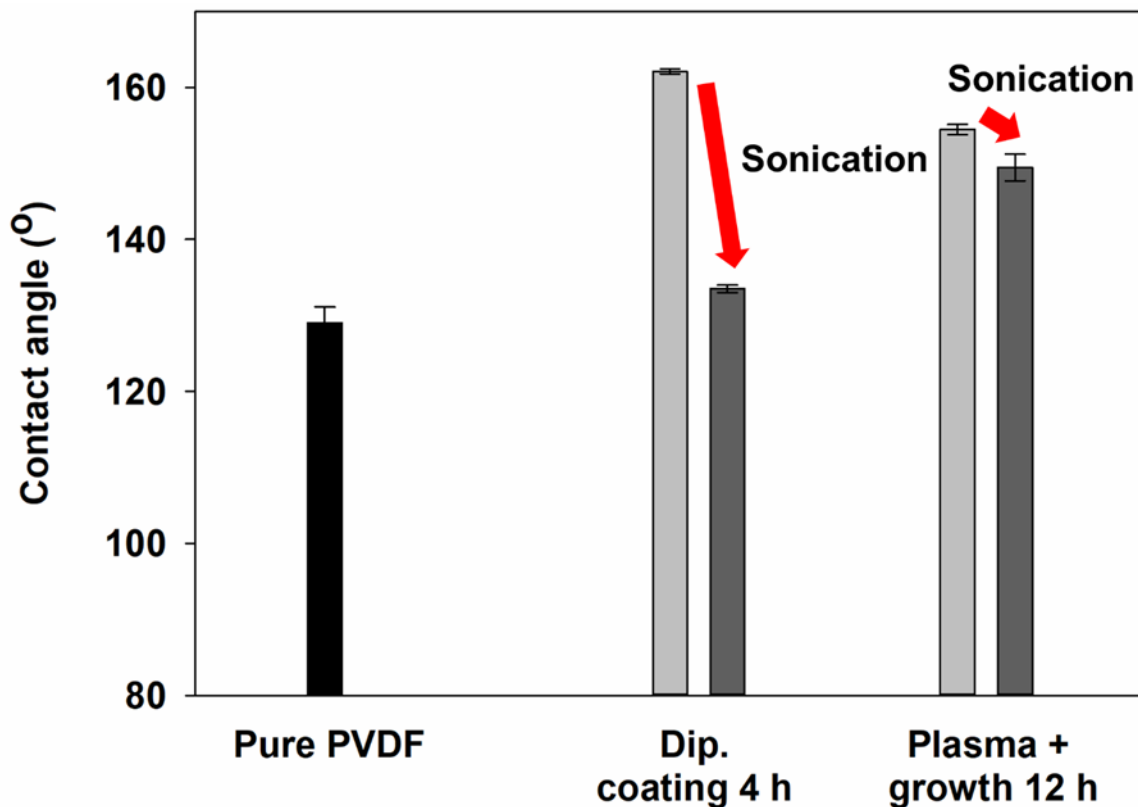
Figure 3. 20 Contact angle difference after sonication treatment.

Furthermore, the CA of the membrane surface was measured after sonication treatment to verify the stability of the NPs on the membrane (Figure 3.20). In the case of the dip-coated membrane, surface CA decreased to a similar value with pure PVDF membrane which can be explained with SEM

results in Figure 3.19 (c). During sonication, NPs on the membrane were detached which leads to loss of hydrophobicity. Instead of the dip-coated membrane, plasma + growing membrane showed excellent stability even after the sonication treatment. As can be seen in Figure 3. 19 (f), the membrane surface is still covered by NPs which are strongly stable because of chemical bonding between membrane and NPs.
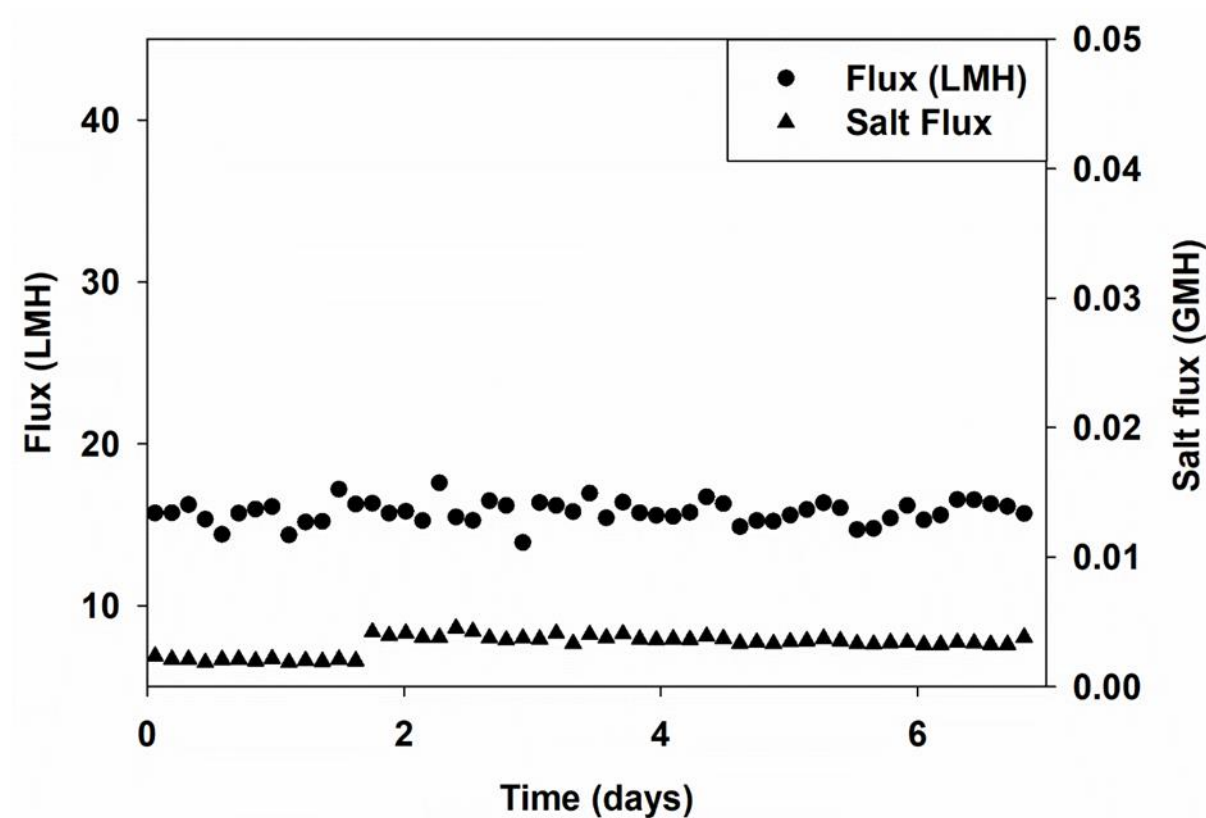
Figure 3. 21 Long-term DCMD test with plasma + growth 12 h membrane for 7 days.

For verifying the stability of the plasma + growing membrane, long-term process was conducted in the same method as the DCMD operating conditions in this chapter. In case of feed solution, 3.5 wt% NaCl solution of 70°C was prepared and flowed to the active layer with 1 LPM. DI as a permeate was maintained at 25°C and flowed to the opposite side of the feed with 1 LPM. The flux and SF were calculated by operating for 2 h. For feed solutions, DCMD was maintained at constant concentration during operation. Figure 3.21 shows that flux and SF remain constant during DCMD operation over 7 days.
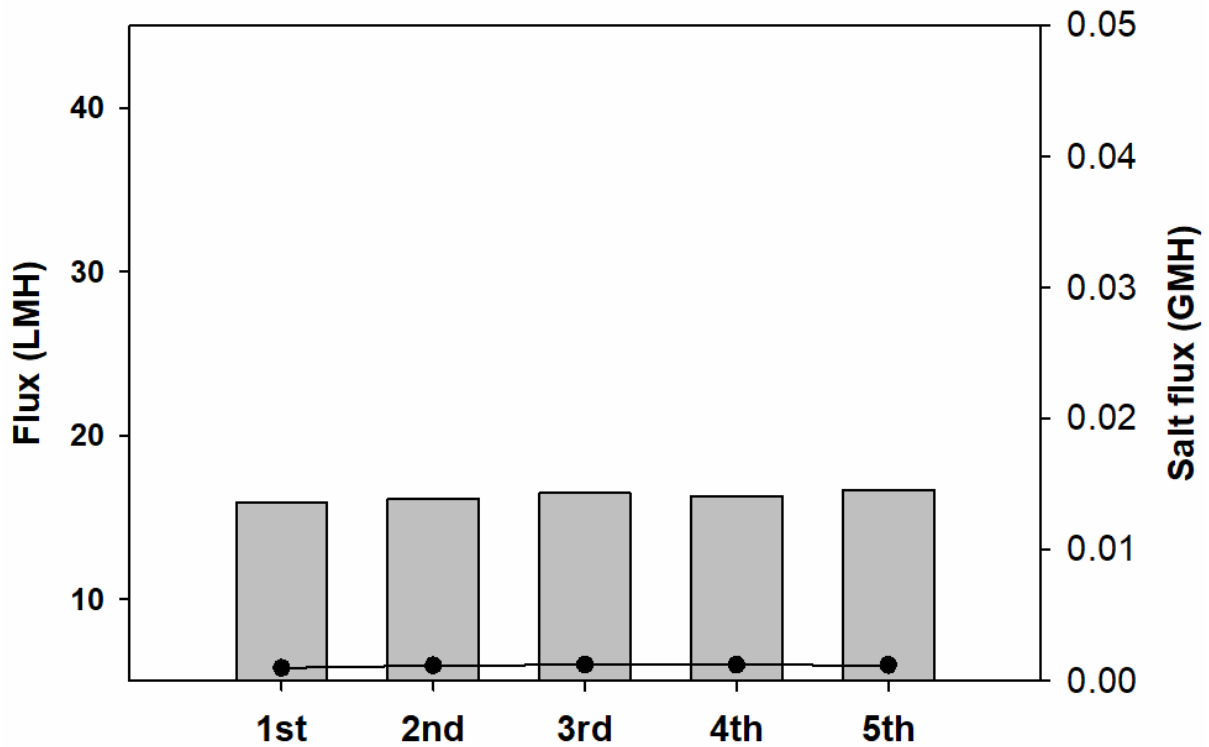
Figure 3. 22 Recycling DCMD experiment with plasma + growth 12 h.

For the recycling experiment, PVDF with plasma + growth 12 h modified membrane had been used for 5 times to confirm the stability of the hydorphobiity (Figure 3.22). As in the previous DCMD experiment, 3.5 wt% NaCl solution was used as a feed solution at 70°C, and DI was passed through the membrane at 25°C with 1 LPM each. After the experiment, the membrane was taken out from cell and immersed in ethanol and n-hexane for 1 hour each time. After removing from n-hexane, it was dried at room temperature and applied again to DCMD. Figure 3.22 shows that the flux and salt flux remain constant in the repeated experiment over 5 times.

3.3. Conclusions

In this chapter, PVDF membranes were modified through pore expansion, hydroxylation, and growth of hydrophobic NPs in the membrane pores to prevent the wetting phenomenon. The performances of the membranes were evaluated under accelerated wetting conditions. The efficiency of each step during the membrane preparation was evaluated by comparing the membranes fabricated by the three different methods. First, the surface of the PVDF membrane was modified by dip-coating to simply place the hydrophobic NPs on the membrane surface. Second, NPs were grown at the –OH functional groups of the PVDF membrane, produced by the Fenton reaction, to increase the stability of the particles. Third, NPs were grown in the PVDF membrane pores prepared by the plasma treatment to reduce the flux decrease and maximize the stability of the NPs.

The dip-coating using the SiO_2 NPs provided a contact angle of 162º, i.e., a superhydrophobic surface. However, the DCMD results showed that the coatings with the NPs physically placed on the surface did not have a significant effect to prevent the wetting, owing to the loss of NPs with no surface adhesion during the operation. Furthermore, after adding the SDS solution, surface showed that direct wetting because of low omniphobicity.

In the membranes with NPs grown on their surfaces where functional groups of OH were generated by the Fenton-reaction, the NPs were not detached during the operation and the hydrophobicity was maintained. This ensured the flux remained stable in the three cycles of addition of SDS which means that membrane has omniphobic surface. Consequently, the wetting phenomenon was prevented. However, the flux was reduced as the particles covered the pores and increased the total membrane thickness. When the plasma pretreatment was applied in addition to the modification method, the flux decrease was reduced by the reduction in the total thickness and the NPs grown inside the pores had an excellent stability during the operation and even under the sonication condition. This suggested that the omniphobicity increased not only on the surface but also inside the membrane.

Wetting resistance:

Patterning

Abstract

In this chapter, new technique was applied to prevent the wetting in MD. In the previous chapter, various methods were used to solve the limitations of the coating method which are low interaction between coating materials and membrane and decline of performance because of the pore blocking. However, to achieve the hydrophobic surface using the method describe in the former chapter, it requires an additional process, and these processes requires many procedures and time. To solve these problems and prevent wetting, in this chapter, patterned membrane was fabricated using a templet and further modified with chemical reaction to prevent wetting in MD. The polymer used in this chapter for chemical modification is PVDF-CTFE, which is similar in hydrophobicity to PVDF, but has a Cl functional group, which has the advantage of being very easy to chemically modify. For chemical modification, FAS was polymerized using ATRP process which makes membrane with low surface energy. The patterned surface after modification was compared with the non-patterned membrane to verify the anti-wetting property through MD. Furthermore, fouling issue caused by rough surface also compared by using foulant in feed solution. Because of the low surface energy after FAS polymerization, hydrophobic patterned membrane showed remarkable stability in fouling test.

4.1 Materials and Methods

4.1.1 Materials

In this study, PVDF-CTFE (SOLEF 31508/1001, Solvay) was dissolved in dimethylacetamide (DMAc) (Dajeong, 99.5%) and used as a casting solution. For surface modification of the membrane, 2-hydroxyethyl methacrylate (HEMA) (Sigma-Aldrich, 99%) and FOMA (Alfa aesar, 97%) were used. DI water and 1,4-dioxane (Sigma-Aldrich, 99.5%) were used for dissolving HEMA and FOMA, respectively. α-Bromoisobutyryl bromide (BiBB), triethanolamine (TEA, 99%), and dichloromethane (DCM, 99.5%) were utilized for BiBB reaction (Sigma-Aldrich), generating an initiating group for subsequent ATRP reaction. As a catalyst and ligand for ATRP reaction, CuBr, and N,N,N′,N″,N″-Pentamethyldiethylenetriamine (PMDETA, 99%) were obtained from Sigma-Aldrich. HA, AA, and BSA (Sigma-Aldrich) were used as foulants. NaCl (Alfa aesar, 99%) was used as a salt in feed stream solution.

4.1.2 Preparing patterned or flat membrane for MD
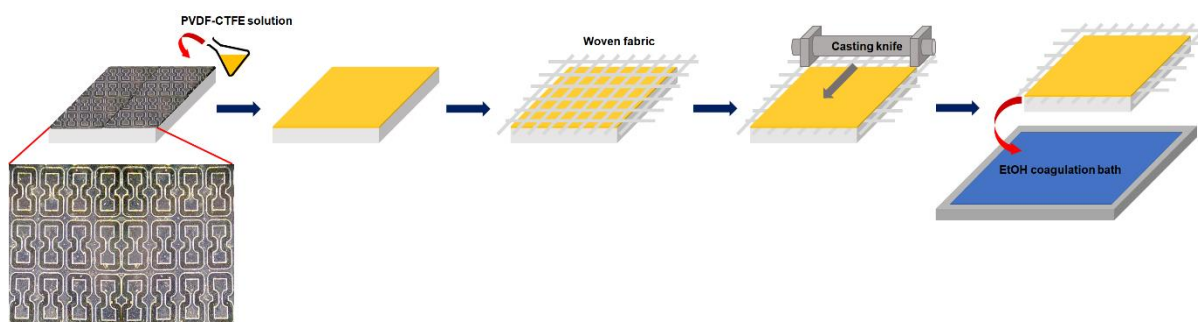
Figure 4. 1 Schematic diagram of casting patterned membrane on templet.

The preparation of the patterned PVDF-CTFE membrane (P-CTFE) is described in Figure. 14. Firstly, PVDF-CTFE solution was prepared by dissolving 25 wt% polymer in DMAc solvent. The solution was then poured onto a templet made of aluminum (Al). In this study, test piece's structures were engraved on the templet. These structures were uniformly arranged in a shape of number eight. Lines that made up the structure were connected continuously. The farthest distance of the line at the

top and the bottom on each structure was 200 μm. The middle part looking like a bottleneck had 60 μm. Each structure had a line thickness of 100 μm and a height of 40 μm. It was arranged at a constant distance of about 60 μm.

After that, the templet was covered with woven fabric. A constant thickness was maintained using a casting knife. The polymer-embedded woven fabric on the templet was soaked into EtOH solution immediately and kept it for 24 h at room temperature. After soaking in EtOH, the membrane was soaked again in n-hexane for 2 h. Finally, the membrane was taken out for drying at room temperature for 24 h. In the case of a flat PVDF-CTFE membrane (F-CTFE), the membrane was prepared using the same procedure with P-CTFE on a glass plate instead of the patterned templet.

4.1.3 Membrane modification
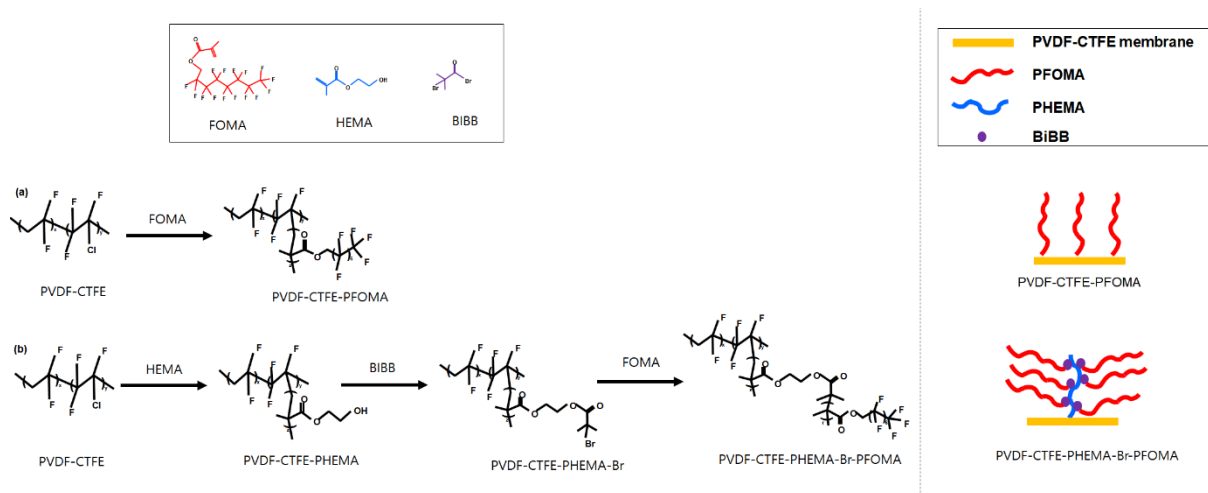
Figure 4. 2 Diagrammatic representation of chemical modification of PVDF-CTFE with (a) FOMA and (b) HEMA, BIBB, and FOMA in series.

The surface of the membrane was modified with FOMA to improve its hydrophobicity. Chemical modification was carried out in two ways through the ATRP method. First, the FOMA was directly grafted on the surface of the PVDF-CTFE membrane. FOMA was then polymerized by extending linearly from the surface (Figure 4.2 (a)). Second, to grow FOMA from the surface in the form of branch, the membrane was sequentially modified with HEMA, BIBB, and FOMA (Figure 4.2 (b)).

4.1.3.1 HEMA modification for OH functional group

HEMA was used to create -OH functional groups on the PVDF-CTFE membrane surface using the ATRP process, which caused the reaction between the Cl functional group of PVDF-CTFE and the C=C bond of HEMA [141]. Initially, 1 ml of PMDETA was added to 200 ml of DI water. The PVDF-CTFE membrane was then immersed in the above solution. After adding 1 g of CuBr, the mixture was purged with nitrogen and reacted at room temperature for 2 hours. After completion of the reaction, the membrane was taken out and rinsed thoroughly with DI. Due to this process, -OH functional groups were formed at the position of chlorine of PVDF-CTFE, making the membrane surface hydrophilic. This membrane was named PVDF-CTFE-PHEMA in Figure 4.2 (b).

4.1.3.2 BiBB modification for Br functional group

PVDF-CTFE-PHEMA was further modified with BiBB to generate Br on the surface [142]. For additional Br groups on the membrane surface, -OH functional groups on the PVDF-CTFE-PHEMA were reacted with BiBB (as shown in Figure 4.2 (b)). The prepared membrane was immersed in 200 ml of DCM. After that, 1 ml of TEA was added. The mixture was then stirred at 0°C. Next, 1 ml of BiBB was added and reacted for 1 hr. Thereafter, the temperature of the solution was adjusted to room temperature and reacted for an additional 12 hr. After this process, the membrane was taken out and washed with methanol thoroughly. Finally, the membrane was modified with FOMA according to the method described in 4.1.3.

4.1.3.3 FOMA modification for further hydrophobicity

In this study, FOMA with a long chain fluorine group was utilized as a chemical agent to make surface energy of the membrane low. Cl of PVDF-CTFE and double bond of FOMA reacted through ATRP bonding. Membranes prepared in section 4.1.2. were put into a mixture of 200 ml of 1,4-dioxane and DI solution (1:1). After that, 1 ml of PMDETA was added and purged with nitrogen. After increasing the temperature to 60°C, 1 g of CuBr was added and reacted for 12 hr. Thereafter, the modified membrane was washed with DI water thoroughly.

4.1.4 Membrane characterization

Scanning electron microscopy (SEM) (S-4800, Hitach High-Technology) was used to investigate surface morphologies and structures. The membrane was immersed in ethanol for 2 hr. It was then immersed in n-hexane for another 2 hr. After that, the membrane was dried at room temperature for 24 hr. The membrane surface was analyzed under various magnification. Porosity of the membrane was evaluated using a mercury porosimetry method (MicroActive AutoPore V 9600, Micrometrics. Co).

Regarding chemical analysis, an attenuated total reflectance Fourier-transform infrared (ATR-FTIR) (Nicolet 6700, Thermo Fisher, UK) was used to confirm chemical changes after modification of membrane surface. The prepared membrane was analyzed using a diamond ATR crystal. Spectra were measured in the range of 1000 to 1800 cm^{-1} at a resolution of 4 cm^{-1}. Chemical properties were confirmed using an X-ray photoelectron spectroscopy (XPS, Thermo Fisher, UK) with Kalpha (1486.6 eV). In XPS analysis, a double-focusing hemispherical analyzer was used. The pass energy was measured in a vacuum as 50 eV with a binding energy step size of 0.1 eV.

To evaluate hydrophobicity of the surface, a comparative study was performed using a contact angle (CA) measuring device. First, 5 µl of water droplet was placed on the membrane surface using a sessile-drop method. The contact angle of the water droplet was then recorded with a Phoenix 300Plus instrument (Surface & Electro Optics Co. Ltd., Korea). After the water droplet was kept on the membrane surface for 30 minutes, change in CA value was then measured. This experiment was performed 10 times for each sample to obtain an average value.

4.1.5 DCMD performance of membranes

DCMD was performed to evaluate performance of the membrane in terms of water flux and salt flux. Each membrane was mounted on a test cell with an effective area of 2.5 x 4 cm. As a feed solution, 3.5 wt% NaCl was used. Its temperature was maintained at 70°C. It was circulated to one side of the membrane at a rate of 0.5 LPM. For permeate stream, DI water at 25°C was used at a flow rate of 0.5 LPM to the opposite side of the membrane. Both streams flowed counter-currently. To determine wetting tendencies of pristine and modified membranes, membranes were operated for 7 days. Conductivity of the permeate was measured in real time simultaneously. During the DCMD process, it was found that the membrane was wet at the point where the salt permeated and the conductivity of permeate stream rapidly increased. The experimental run was continued until the salt permeated through the membrane. The wetting time was then compared. Salt flux (SF) was calculated based on the change

of volume (converted from mass, ΔVp) and concentration (converted from conductivity, ΔCp) of the permeate. Calculations for flux and SF were performed using Eq. (3) and (4):

$$Flux = \frac{\Delta\ \text{weight}}{\Delta\ \text{time} \times \text{effective membrane area}}\ \left(^{L}/_{m^2h}\ (\text{LMH})\right) \qquad \text{Eq. (3)}$$

$$SF = \left(\frac{\Delta\ Cp\ \Delta Vp}{\Delta\ \text{time} \times \text{effective membrane area}}\right)\ \left(^{g}/_{m^2h}\ (\text{GMH})\right) \qquad \text{Eq. (4)}$$

4.1.6 Fouling measurement

As the roughness of the membrane increases, fouling occurs easily. To confirm the effect of hydrophobicity, the fouling test was conducted using HA, BSA, and AA. DCMD is performed in the same condition as before instead of by preparing a 100 ppm foulant solution as a feed solution. The flux was calculated using Eq. (3), and the obtained values were compared by normalizing based on the maximum value.

4.2 Results and Discussion

4.2.1 Morphologies of the F-CTFE and P-CTFE membranes
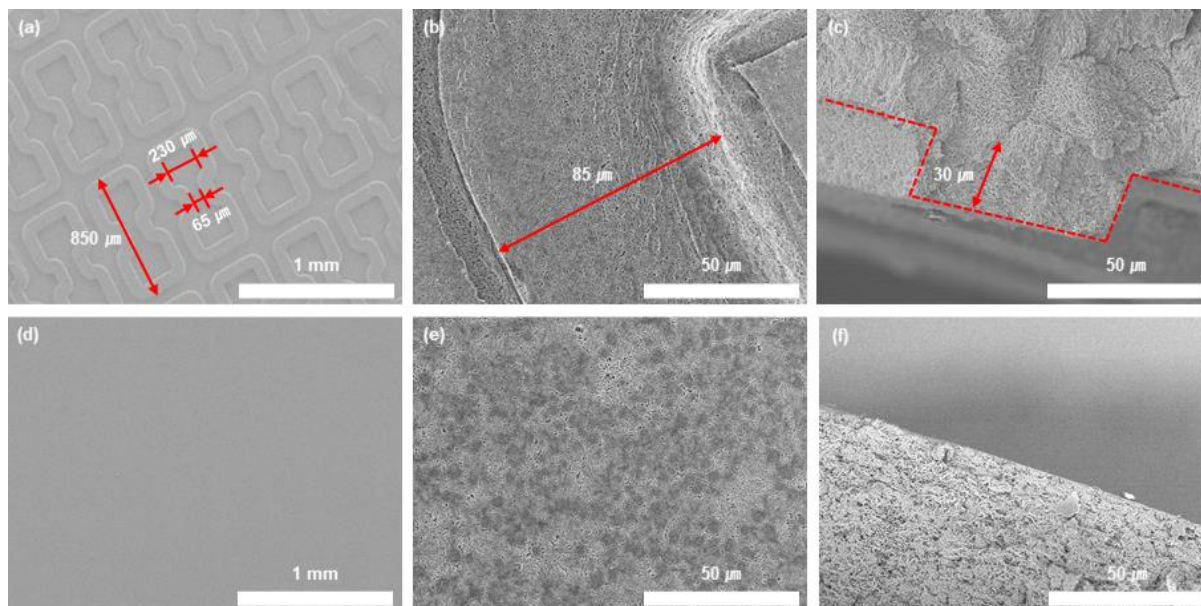
Figure 4. 3 SEM images of (a) P-CTFE surface, (b) magnified image of (a), (c) cross-sectional image of P-CTFE, (d) F-CTFE surface, (e) magnified image of (d), and cross-sectional image of F-CTFE.

F-CTFE and P-CTFE surface and cross-sectional images were observed by SEM (Figure 4.3). As shown in Figure 4.3 (a), structures on P-CTFE membrane surface had an internal distance of 230 μm at top and bottom. The distance between the center and membrane surface was 65 μm. Each structure had a line thickness of 85 μm (Figure 4.3 (b)) and 30 μm in height (Figure 4.3 (c)). The size of the structure of the P-CTFE membrane is smaller than the size of the Al templet. In general, when a polymer solution soaks into the non-solvent, shrinkage occurs due to phase separation. Due to this, the size of the structure is smaller than that of the templet, and the distance between the structures is increased. In general, hierarchical microstructures can increase the hydrophobicity of the surface by generating air layer (famously known as air pockets) at the membrane interface [143, 144]. However, when fabricating a micro-pillared structure using a patterned template, if the height of the structure is increased, the structure can get stuck in the template while peeling it off from the template, causing structure failure. To tackle these issues, the test piece structure shown in Figure 4.3 (a) was chosen in

this study. Micro-pillars were connected to each other to provide physical stability. Since many structures were arranged on the surface, the surface roughness would higher than that of a line-pattern structure. In contrast, F-CTFE had a smooth surface (Figure 4.3 (d) and (e)). Because of this test piece structure on the membrane, P-CTFE (62.4 nm) had rougher surface than F-CTFE (25.9 nm). Cross-section images (Figure 4.3 (c) and (f)) revealed that both membranes had a sponge-like structure. This sponge-like structure was the result of using EtOH as a coagulation bath [145]. Unlike a finger-like structure known to occur because of instantaneous de-mixing when DI was used as a coagulation bath, sponge-like structure of a constant size was formed throughout the membrane due to a delayed de-mixing between the solvent and the non-solvent. In addition, since the polymer solution of the same concentration was used to cast F and P-CTFE membranes, a sponge-like structure having a similar pore size was formed.
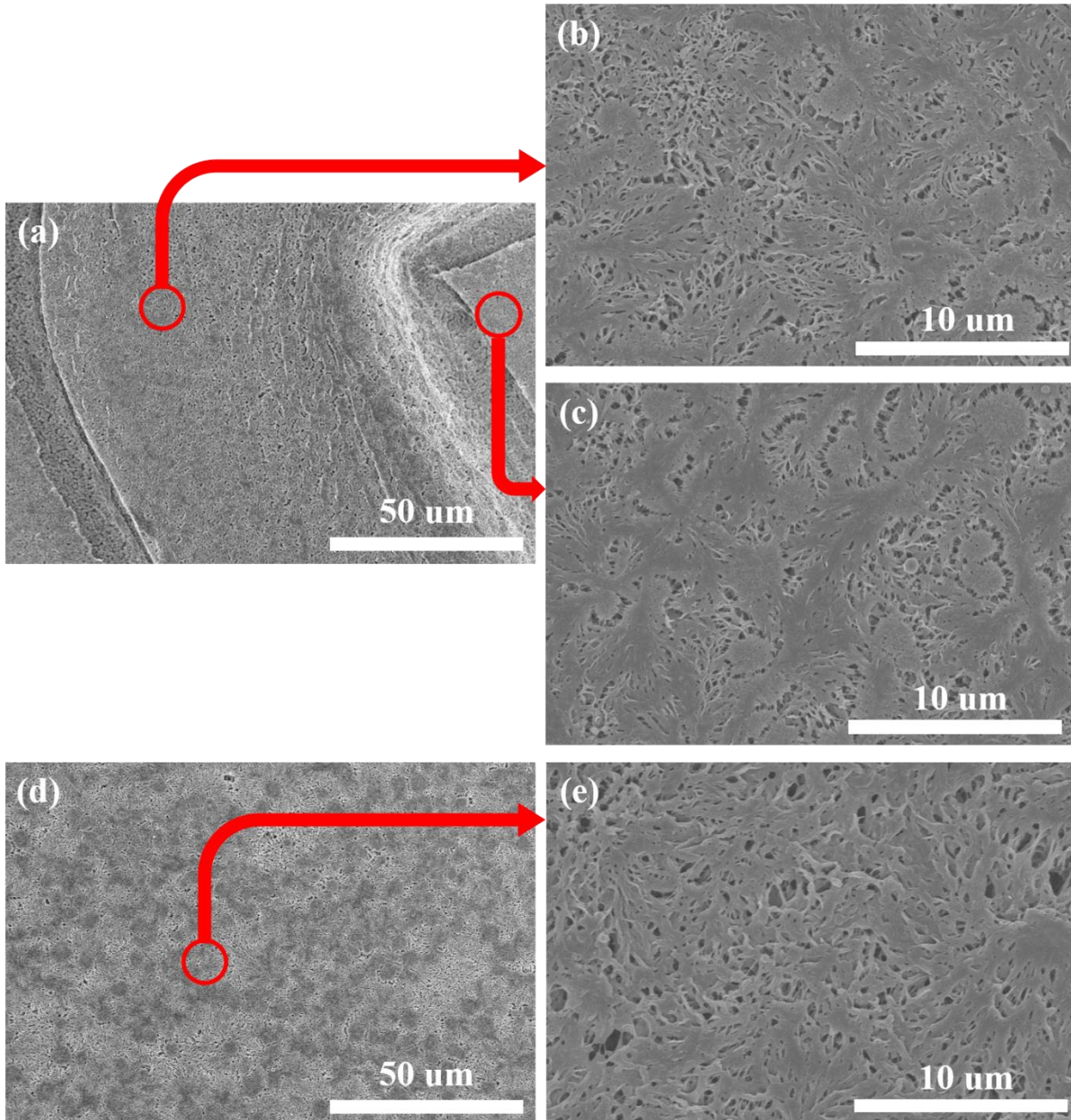
Figure 4. 4 SEM images of (a) P-CTFE surface, (b) magnified image of top side of pattern structure, (c) magnified image of bottom side of pattern structure, (d) F-CTFE surface, and (e) magnified image of (d).

In general, when preparing the patterned membrane using a template (mold), a pattern is generated on the surface where the polymer solution contact with the template, which causes a difference in the exchange rate between the solvent and the non-solvent (in Section 2.4. 3.6). Due to this speed difference, pores on the patterned side are relatively small, and large pores are formed on the side in contact with the coagulation bath solution, forming an asymmetric membrane. The VIPS method

is a one technique to solve this problem, but in this study, EtOH was used as a coagulation solution to prepare a symmetrical membrane by inducing delay-demixing (in Section 2.1.1.1). As can be seen in Figure 4.3 (c), pores of a uniform size are formed, and as in 4.4 (b) and (c), the surface pores at the top and bottom of the pattern structure are formed with similar sizes. In the case of the surface of the F-CTFE membrane prepared through a similar method with patterned membrane, it has similar pore size with P-CTFE (Figure 4.4 (e)). Through this, it can be expected that the hydrophobicity of the surface will be determined by the roughness, not by the pore size difference between F-CTFE and P-CTFE.

4.2.2 FTIR and XPS measurement of the pure and modified membranes
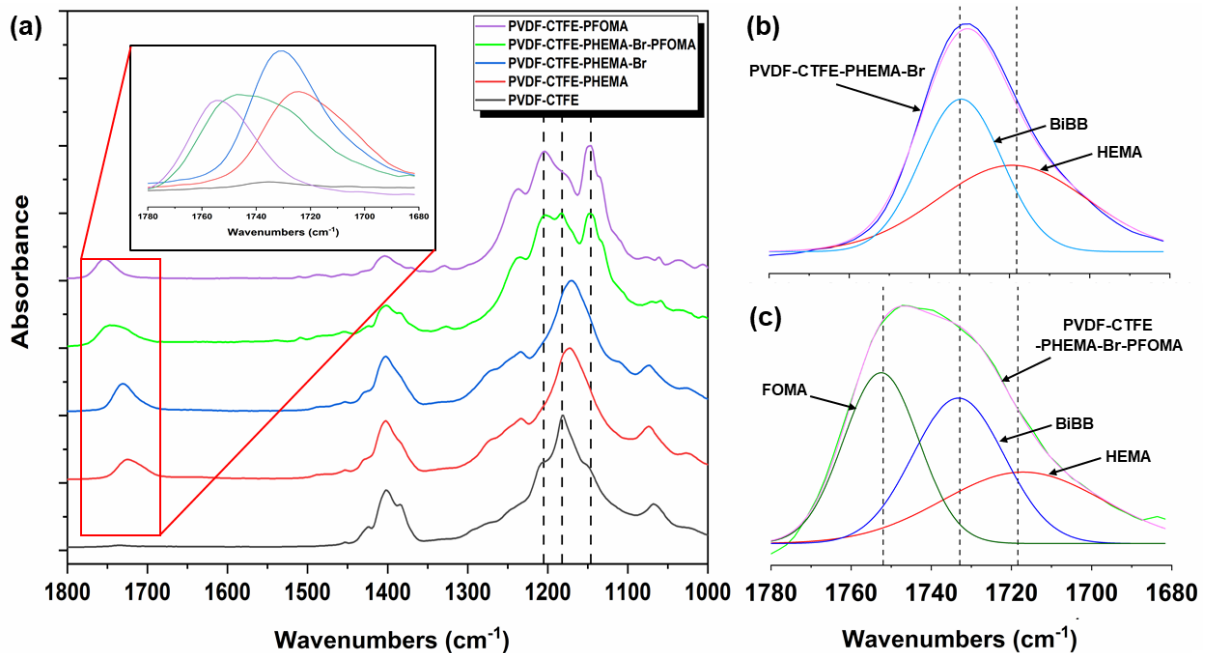
Figure 4. 5 FTIR spectra of (a) PVDF-CTFE, PVDF-CTFE-PHEMA, PVDF-CTFE-PHEMA-Br, PVDF-CTFE-PHEMA-Br-PFOMA, and PVDF-CTFE-PFOMA and analysis deconvoluted spectrum of (b) PVDF-CTFE-PHEMA-Br, and (c) PVDF-CTFE-PHEMA-Br-PFOMA for 1780-1680 cm^{-1} region.

FTIR was used to analyze chemical bonds on the prepared membrane's surfaces. As shown in Figure 4.5 (a), FTIR spectra of the PVDF-CTFE membrane modified with FOMA had a new peak formed at 1750 cm^{-1}. The membrane modified with HEMA (Figure 4.5 (a)) showed a peak corresponding to C=O bond from HEMA at 1720 cm^{-1} [146]. The PVDF-CTFE-PHEMA has OH

functional groups. To generate additional reacting sites for ATRP reaction, OH groups of HEMA were reacted with BiBB to produce Br functional groups at the end of grafting polymers. After reaction of BiBB onto PVDF-CTFE-PHEMA, the C=O peak shifted to 1730 cm^{-1} (Figure 4.5 (b)) [147]. This is because the carbonyl group of BiBB and the ester group of HEMA exist together [148, 149]. Due to this, the peak shifted to a high wavenumber, unlike PVDF-CTFE-PHEMA which showed a peak at 1720 cm^{-1}. This confirms the successful modification with HEMA and BiBB onto the membrane surface. After BiBB reaction, the membrane was modified with FOMA again through the ATRP reaction. It was found that the C=O peak shifted to 1750 cm^{-1}, confirming successful synthesis with FOMA (Figure 4.5 (c)). However, unlike PVDF-CTFE-PFOMA, PVDF-CTFE-PHEMA-Br-PFOMA had a broad peak from 1720 cm^{-1} to 1750 cm^{-1} (Figure 4.5 (c)). This is because PVDF-CTFE-PHEMA-Br-PFOMA has various C=O bonds resulting from HEMA, BiBB, and FOMA.

	C	O
Pure PVDF-CTFE	CF$_2$ / CH$_2$ / C-Cl Binding energy (eV) 294 292 290 288 286 284 282 280	Binding energy (eV) 544 542 540 538 536 534 532 530 528 526
PVDF-CTFE-PFOMA	C=O / C-C C-H Binding energy (eV) 294 292 290 288 286 284 282 280	C=O Binding energy (eV) 544 542 540 538 536 534 532 530 528 526
PVDF-CTFE-PHEMA-Br-PFOMA	CF$_2$ / C=O / C-C C-H / CF$_3$ Binding energy (eV) 294 292 290 288 286 284 282 280	C=O Binding energy (eV) 544 542 540 538 536 534 532 530 528 526

Figure 4. 6 XPS high resolution of C1s and O1s peaks of PVDF-CTFE, after synthesis with FOMA, and after synthesis with HEMA, Br, and FOMA.

To further investigate surface element composition, XPS analysis was performed. (Figure 4.6) In the case of PVDF-CTFE, only CF$_2$, CH$_2$, and C-Cl bonds can be identified, and the C-O bond cannot be confirmed [150]. In the subsequent analysis, to compare with PVDF-CTFE, PVDF-CTFE-PFOMA, and PVDF-CTFE-PHEMA-Br-PFOMA membranes were analyzed to confirm the chemical changes [151]. First, after synthesizing only FOMA with PVDF-CTFE, a new peak, C=O bond, is appeared at 288 and 532 eV. This is due to the O functional group present in FOMA, which is the result of

confirming that it is properly synthesized with PVDF-CTFE. In addition, when PHEMA, Br, and FOMA were sequentially reacted with PVDF-CTFE, it was confirmed that the C=O peak and the CF_3 peak increased [152]. This result shows that FOMA has successfully synthesized with Br presented at the end of PHEMA. In addition, the O functional group peak shifted from 532 eV to 533 eV when comparing PVDF-CTFE-PFOMA and PVDF-CTFE-PHEMA-Br-PFOMA. This is because the C=O bond of PVDF-CTFE-PHEMA-Br-PFOMA contains a C=O bond from HEMA, Br, and FOMA [153]. Through this chemical analysis, XPS and FTIR, it was confirmed that PVDF-CTFE was successfully synthesized with HEMA or BiBB or FOMA.

4.2.3 Surface hydrophobicity measurement through CA measurement
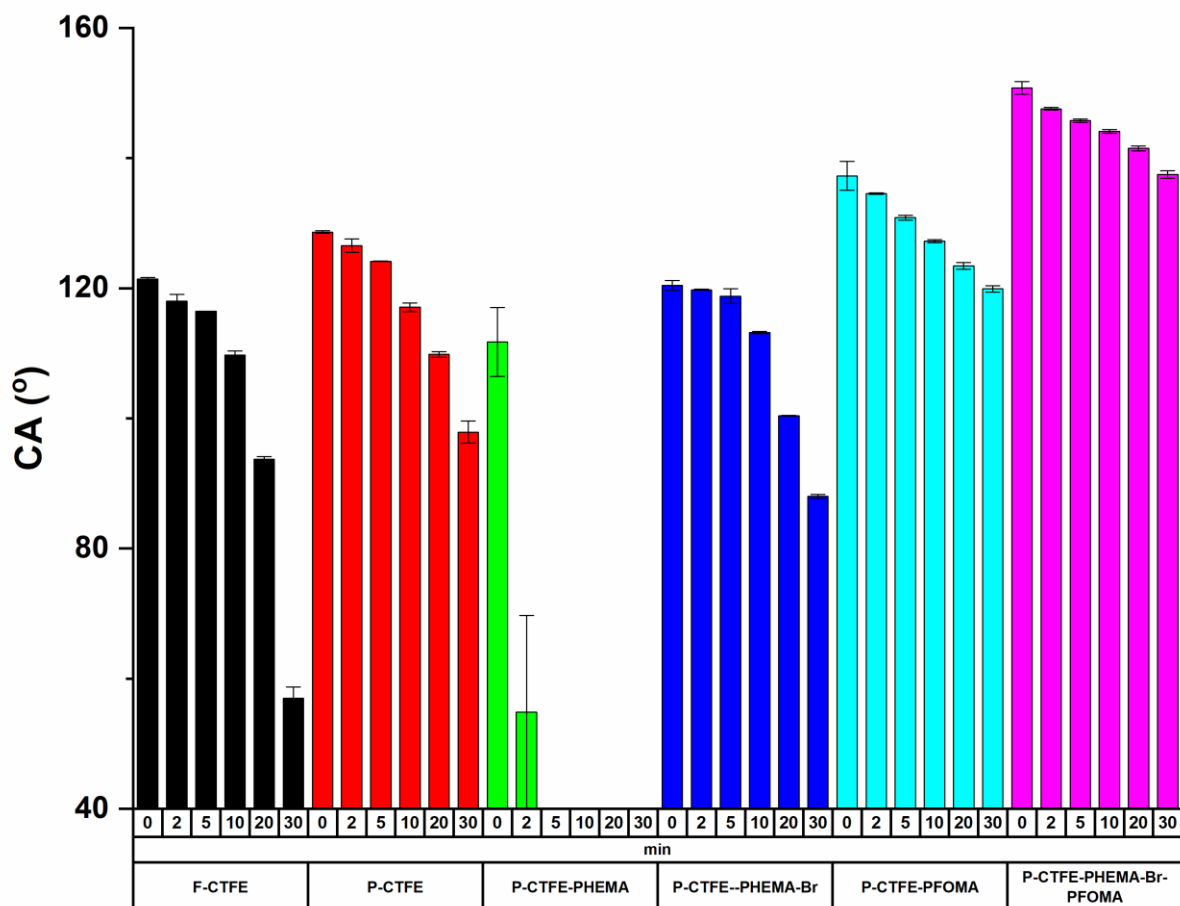
Figure 4. 7 CA value after exposing to DI for 30 min.

In CA measurement, the hydrophobicity was compared after exposure to water droplet for a duration of 30 min (Figure 4.7). In the case of F-CTFE, the CA was found to be 120°. It decreased rapidly after 20 min of exposure. It dropped to 60° at 30 min, indicating a loss of hydrophobicity. This rapid decrease in CA value is a phenomenon that occurs as water droplets become smaller due to evaporation [154]. In general, even on the same surface, the CA value changes depending on the size of the droplet. In this CA measurement, water droplets on the surface of the membrane evaporate and the size decreases rapidly decrease which leads to a decrease of CA value. In addition, due to the high surface tension of water, the surface got wet when droplet evaporates, and the CA value decreased dramatically.

In contrast, P-CTFE initially showed a higher contact angle (130°). The CA value decreased to 90° after 30 min of exposure to water droplet, exhibiting a higher stability than F-CTFE. This is due to an increase in surface roughness of the patterned structure, which increased the hydrophobicity by formation of hierarchical microstructures onto membrane surface (Figure 4.3 (a)) [155].

P-CTFE-PFOMA was found to be more stable in terms of hydrophobicity. P-CTFE-PFOMA showed a higher CA value of 140°. It only decreased about 20° after 30 min of exposure. It was more stable due to the hydrophobicity of FOMA.

In the case of PHEMA modification, hydrophilicity increased due to the formation of OH group, which reduced the CA to 0° within 5 min. After modification with BiBB, it had a similar tendency of decreasing CA to that of the P-CTFE. This confirmed the successful modification of OH group with BiBB. The hydrophilicity was again due to exchanges OH to Br. However, this CA value was slightly lower than that of P-CTFE due to the C=O functional groups of PHEMA and BiBB.

P-CTFE-PHEMA-Br-PFOMA exhibited a superhydrophobic feature, with an initial CA value of more than 150°, higher than that of P-CTFE-PFOMA due to branch-type growth of PFOMA on PHEMA (Figure 4.2 (b)). After 30 min of exposure, its CA value only decreased by about 15°.

These CA results indicated that the P-CTFE membrane possessed higher and stable CA value than F-CTFE when it was exposed to water droplet because a uniform structure on the surface caused a high roughness. Furthermore, P-FOMA or P-PHEMA-Br-PFOMA showed a stable CA value due to improvement in hydrophobicity. These results revealed that P-PFOMA or P-CTFE-PHEMA-Br-PFOMA showed anti-wetting characteristic when it was exposed to water droplet with wetting expected to occur later than F-CTFE when applied to a DCMD process.

Before soaking in DI | **After soaking in DI for 7 days**
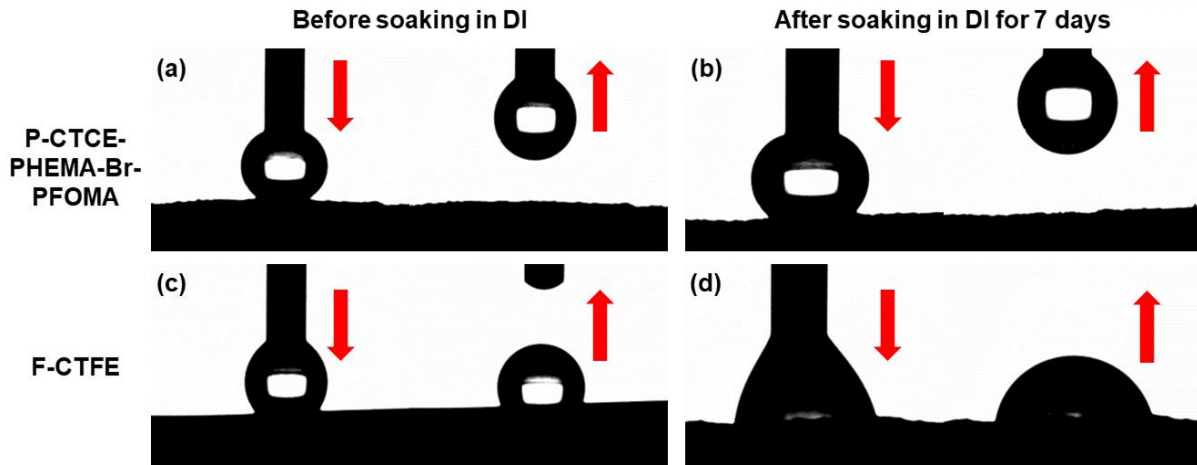
Figure 4. 8 Contact angle images of P-CTFE-Br-PFOM (a) before and (b) after soaking in DI for 7 days and contact angle images of F-CTFE (c) before and (d) after soaking in DI for 7 days.

In this chapter, a water droplet was placed on the membrane surface to measure CA, and the change in CA over time. It was confirmed that the CA value of the membrane surface could be changed because of the decrease in the size of the droplets due to the evaporation1. Also, evaporation cause the membrane wetting due to the high surface tension. In the case of the F-CTFE membrane, it was verified that CA value decreased rapidly after 30 min because of droplet size changes and wetting. In the case of the P-CTFE-PHEMA-Br-PFOMA membrane, the CA value decreases much less even when the water droplets evaporate, which shows advanced wetting resistance property.

The stability of the membrane hydrophobicity was confirmed by soaking in DI for 7 days. First, put F-CTFE and P-CTFE-PHEMA-Br-PFOMA membranes in DI and stirred vigorously for 7 days. After that, the membranes were taken out and the CA was measured immediately to compare hydrophobicity. In the case of the P-CTFE-PHEMA-Br-PFOMA membrane, and it was found that the water droplets could not adhere on the surface easily and the CA value maintained over 150° even after 7 days of soaking (Figure 4.8). However, in the case of F-CTFE, it had a CA value of more than 120°, but after soaking, it was confirmed that this value dropped to 75° and lost hydrophobicity. Through this soaking test, stability of the membrane can be verified.

4.2.4 Long-term DCMD performance
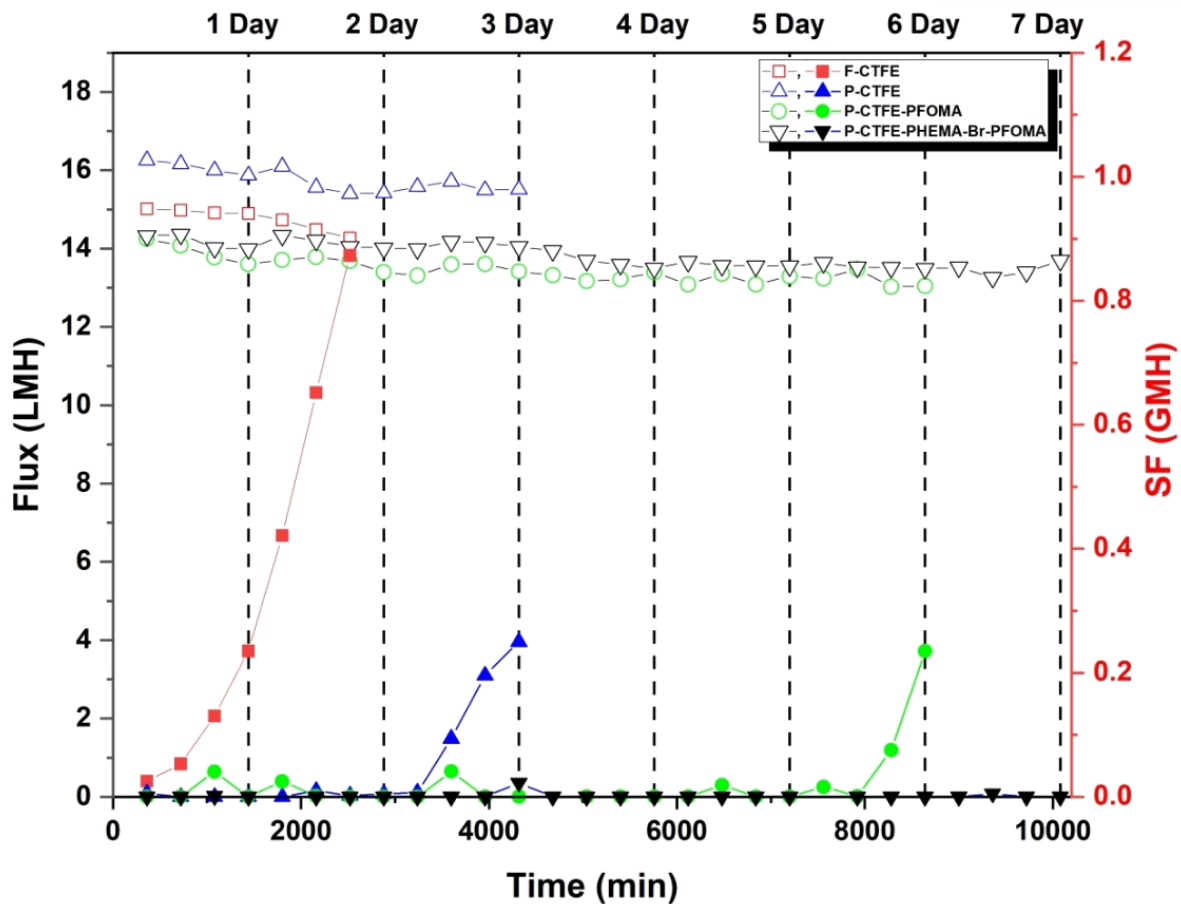
Figure 4. 9 Long-term DCMD process using 3.5 wt% of NaCl solution as a feed solution with flux (□, △, ○, ▽) and SF (■, ▲, ●, ▼) for each membrane.

To evaluate the anti-wetting characteristic, DCMD was performed until the membrane got wet. As shown in Figure 4.9, F-CTFE had a rapid SF increase within a day. It could be explained by CA results (as seen in Figure 4.7) which showed that the F-CTFE membrane with an initial CA value of 120° got wetted within 30 min of DI water exposure and ultimately CA value dropped below 60°, thus losing its hydrophobicity. In this study, it is worth to mention that membrane wetting was determined when the SF sharply increased. Although there was no flux change compared to the SF, an increase in SF indicated the passage of salts directly to the permeate stream due to pore wetting of the membrane.

On the other hand, P-CTFE had a patterned structure on its surface. It took more than two days to get wet. Such improved performance can be attributed to an enhancement of hydrophobicity due to presence of hierarchical microstructure on its surface. As shown in Figure 4.8, even after 30 minutes of DI exposure, the CA value only decreased slightly (from 130° to 90°), indicating a more stable performance than F-CTFE. In addition, P-CTFE showed slightly higher flux than F-CTFE due to its

higher surface area while forming a pattern on the membrane surface.

In the case of P-CTFE-PFOMA, hydrophobicity was improved due to formation of a long chain of FOMA on the surface which enhanced it anti-wetting characteristic. P-CTFE-PFOMA showed a stable performance for about five days without any significant SF change due to hydrophobicity of the membrane. Based on results shown in Figure 4.8, the stable CA value was maintained with DI exposure. The CA value only decreased by about 20° after 30 min of exposure. The membrane showed good stability. It can be explained by its surface roughness formed by patterned surface and a low surface energy by chemical modification with FOMA.

P-CTFE-PHEMA-Br-PFOMA membrane exhibited slightly lower flux than P-CTFE (14 LMH and 16 LMH, respectively) due to a reduction of porosity from 72.3% to 67.9% after chemical modification. It was observed that high temperature made membrane pores become slightly smaller, leading to a flux decline. However, P-CTFE-PHEMA-Br-PFOMA showed stable flux and SF for more than 7 days because of its superhydrophobic surface with an initial CA value of over 150°. It only showed a slight reduction of about 15° even after 30 minutes of DI water exposure.

Although the SF was found to be stable, the flux slightly decreased for all membranes during the DCMD process. This is because of partial pore wetting during DCMD [156]. The degree of flux reduction due to wetting was also less for P-CTFE compared to that for F-CTFE. It seems to be insignificant in case of P-CTFE-FOMA or P-CTFE-PHEMA-Br-PFOMA. It can also be explained by the surface roughness and low surface energy which could prevent wetting during a long-term operation of DCMD.

4.2.5 Fouling test using several types of foulants
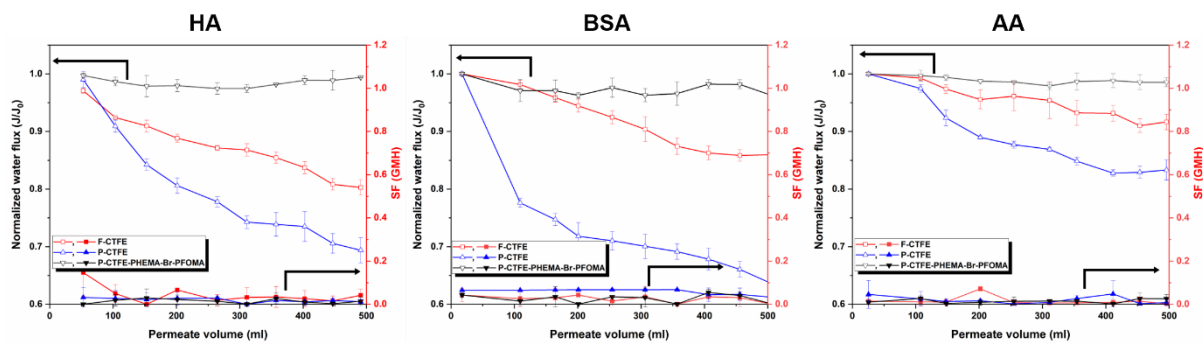
Figure 4. 10 Fouling test using 100 ppm of foulant solution as a feed solution.

It is well known that larger roughness of a membrane will make it more susceptible to membrane fouling [157]. In this experiment, a pattern structure was formed on the PVDF-CTFE membrane surface to increase its hydrophobicity. Furthermore, a superhydrophobic surface was achieved by modifying the surface with FOMA. To analyze the anti-fouling characteristic of the prepared membrane, DCMD was performed using 100 ppm of foulant solution as the feed solution (Figure 4.10). A decrease in flux was observed until 500 ml of permeate was collected. To compare the amount of flux reduction, normalized flux was calculated. Results of flux were compared. As shown in Figure 4.10, the flux of F-CTFE dropped to 80% with HA, 85% with BSA, and 91% with AA from the initial flux. On the other hand, the flux of P-CTFE dropped to 73% with HA, 63% with BSA, and 83% with AA. This difference was due to the formation of external fouling layer onto the rough surface [158]. However, the P-CTFE-PHEMA-Br-PFOMA membrane showed a constant flux (18, 15, and 17 LMH) during the collection of 500 ml of permeate. This could be attributed to the hydrophobic nature of FOMA coated on the membrane surface which provided a lower surface energy for foulant to adhere on the surface. Although the patterned membrane had a high roughness, flux data showed insignificant decreases during the DCMD process with a foulant.
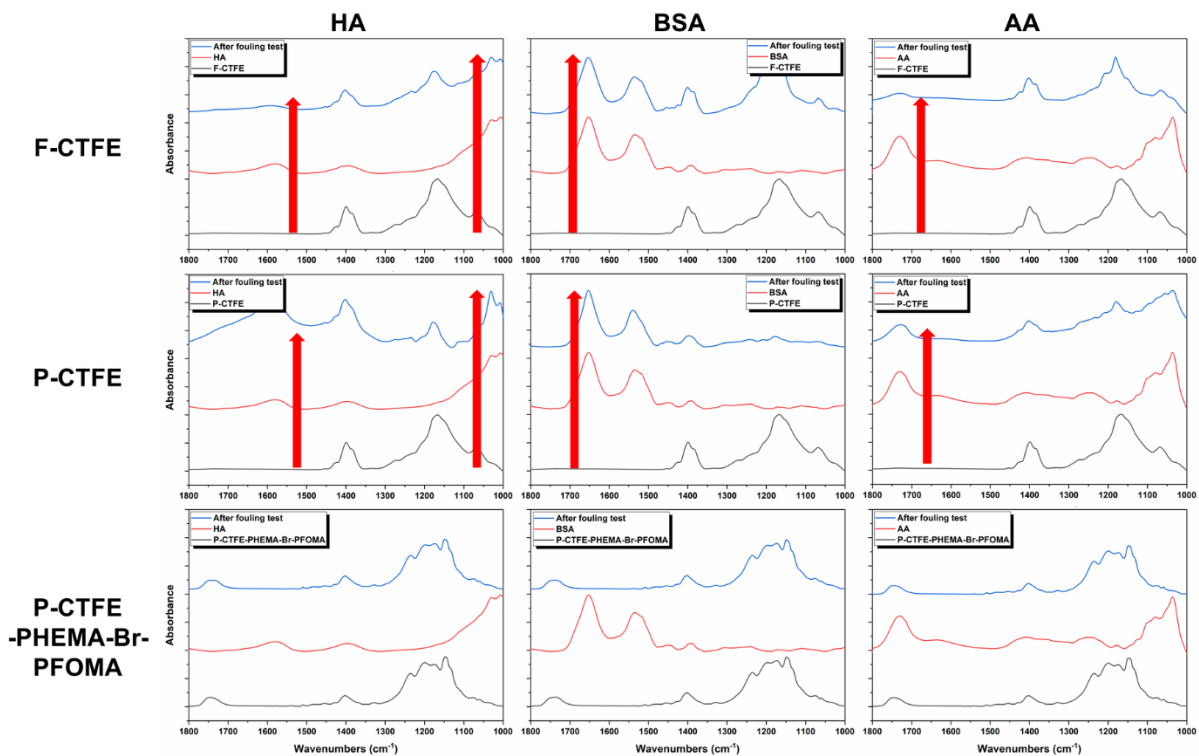
Figure 4. 11 FTIR spectra of F-CTFE, P-CTFE, and P-CTFE-PHEMA-Br-PFOMA after fouling test with foulants (HA, BSA, and AA).

In the fouling test with HA, BSA, and AA in Figure 4.11, DCMD was performed until 500 ml of permeate was collected. During fouling test, membranes showed flux decline and this flux decline could be caused by several factors. However, with the long-term DCMD test in Figure 4.10, there were no flux decline before membrane wetting. Besides, the fouling test was conducted until 500 ml of permeate was collected, which is not enough time for membrane wetting.

To confirm the flux decline caused by foulant on the surface, the change of the membrane surface after the fouling test was verified through FTIR. Fouling test was conducted with 100 ppm of HA or BSA or AA and membrane was dried after finishing the test. As can be seen in Figure 4.10, after the fouling test, all F-CTFE membranes showed peaks along with the foulant peaks. However, in the case of P-CTFE, surface was covered by foulant seriously compare with F-CTFE. Because of severe fouling layer on the surface, original peak was hard to find. Although, P-CTFE-PHEMA-Br-PFOMA showed that even after fouling test, peak showed almost same as before test which can explain no flux decline during fouling test in Figure 4.10.

4.3 Conclusions

In this chapter, hydrophobicity of the PVDF-CTFE membrane was improved by patterning the membrane surface using a templet. As far as hydrophobicity was concerned, P-CTFE possessed higher CA value (130°) than F-CTFE because of its hierarchical microstructures. In the DCMD process, F-CTFE membrane was wet within a day during the DCMD operation, while P-CTFE showed a stable performance over two days. However, due to the hierarchical microstructure, the rough surface of P-CTFE showed a rapid flux decline (73%, 63%, and 83% for HA, BSA, and AA, respectively) compared to that of F-CTFE (80%, 85%, and 91% for HA, BSA, and AA, respectively) due to deposition of foulants on the membrane surface. To prevent membrane fouling and wetting during the DCMD process, FOMA was polymerized on the membrane surface using an ATRP process with HEMA and BiBB. The ATRP process with HEMA was used to make -OH functional group on the surface. Simultaneously, BiBB was reacted with HEMA so that more reaction cites could be generated. Later, FOMA was utilized to form a network with P-CTFE-PHEMA-Br. P-CTFE-PHEMA-Br-PFOMA was found to be superhydrophobic (150°). It maintained stable flux and salt flux over 7 days in DCMD operation. Although P-CTFE-PHEMA-Br-PFOMA membrane had rough microstructures, it showed no significant flux decline during DCMD while using various foulants because of its superhydrophobic behavior. Therefore, it can be concluded that a combination of surface patterning and polymerization with FOMA on PVDF-CTFE membrane has potential to improve wetting and fouling resistance in DCMD for long term performance.

Wetting resistance:

Heating

Abstract

In this chapter, a technique to increase the temperature of the membrane itself was used to prevent wetting of the membrane. Until now, research has been conducted focusing on increasing the hydrophobicity of the membrane to prevent wetting in the MD process. This is because the vapor generated by the temperature difference between the feed and the permeate solution, which is the main reason for membrane wetting, coagulated as it passes through the membrane. However, in this chapter, to prevent this coagulation, the temperature of the membrane itself, not the hydrophobicity of the membrane, is kept higher than the feed solution. The higher temperature of the membrane could prevent condensation of the vapor, thereby preventing wetting and increasing the speed of vapor movement to improve performance. To increase the temperature of the membrane, in this study, a membrane can be manufactured using a copper mesh with high thermal conductivity, and to prevent MD performance and wetting, heat is applied to the membrane during MD operation to keep the temperature of the membrane higher than the feed solution.

5.1 Materials and Methods

5.1.1 Materials

PVDF polymer (Solef 1015/1001) was purchased from Solvay. Triethyl phosphate (TEP) used as a solvent was purchased from Sigma. Methanol, ethanol, and n-hexane were purchased from Daejeong. Carbon nanofibers (CNF) with 100 nm of diameter and 20 – 200 μm of length was purchased from Sigma. As a substrate for membrane, copper mesh was purchased from APEC (Korea) which has pore size of 200 mesh.

5.1.2 Preparing PVDF membrane on copper mesh

A dope solution was prepared by dissolving PVDF polymer (15, 17, and 19 wt%) in a TEP solvent. The dope solution was purged with nitrogen gas for 30 min to remove air bubbles trapped in the solution. Subsequently, the solution was mechanically stirred at 80ºC for 24 h to obtain a homogeneous solution. After the solution was prepared homogeneously, the polymer solution was cooled down at room temperature. The polymer dope solution was cast on a copper mesh (100 or 200 mesh) wrapped on a glass plate with a casting knife with a certain thickness, and then the solution cast on the PET was immediately put in an ethanol bath. The copper mesh was chosen because of its high thermal conductivity (Table 5.1). After the immersion for 12 h, the membrane was taken out and immediately soaked in methanol for 1 h, in 1-hexane for 1 h, and then taken out. The membrane was dried in an oven at a temperature of 60ºC.

Table 5. 1 Thermal conductivity of different type of metals.

Metals	Mass density, ρ (lb/ft³)	Heat capacity, c (Btu/lb·F)	Thermal conductivity, k (Btu/hr·ft·F)
Aluminum	169	0.208	117.0
Antinomy	415	0.049	10.6

Bismuth	**612**	**0.029**	**4.9**
Cadmium	**540**	**0.055**	**54.0**
Copper	**558**	**0.091**	**224.0**
Gold	**1203**	**0.030**	**169.0**
Iron	**491**	**0.104**	**35.8**
Inconel	**534**	**0.109**	**8.7**
Lead	**705**	**0.030**	**20.1**
Magnesium	**109**	**0.232**	**91.0**
Mercury	**849**	**0.033**	**4.8**
Molybdenum	**638**	**0.060**	**72.0**
Nickel	**556**	**0.106**	**52.0**
Palladium	**743**	**0.054**	**40.6**
Platinum	**1340**	**0.032**	**40.2**
Silver	**655**	**0.056**	**241.0**
Tin	**456**	**0.054**	**38.0**
Tungsten	**1208**	**0.032**	**94.0**
Zinc	**446**	**0.091**	**65.1**

5.1.3 Characterization

Scanning electron microscopy (SEM) (S-4800, Hitach High-Technology) was used to investigate surface morphologies and structures. The membrane was immersed in ethanol for 2 h. It was then immersed in n-hexane for another 2 h. After that, the membrane was dried at room temperature for 24 h. The membrane surface was analyzed under various magnification.

Regarding chemical analysis, an attenuated total reflectance Fourier-transform infrared (ATR-FTIR) (Nicolet 6700, Thermo Fisher, UK) was used to confirm chemical changes after modification of

membrane surface. The prepared membrane was analyzed using a diamond ATR crystal. Spectra were measured in the range of 1000 to 1800 cm^{-1} at a resolution of 4 cm^{-1}.

To evaluate hydrophobicity of the surface, a comparative study was performed using a contact angle (CA) measuring device. First, 5 µl of water droplet was placed on the membrane surface using a sessile-drop method. The contact angle of the water droplet was then recorded with a Phoenix 300Plus instrument (Surface & Electro Optics Co. Ltd., Korea). After the water droplet was kept on the membrane surface for 30 minutes, change in CA value was then measured. This experiment was performed 10 times for each sample to obtain an average value.

5.1.4 Performance test using SGMD

An operation in the SGMD mode was carried out to evaluate the performance of the heating membranes (Figure 5.1). Membrane samples were mounted in a cell with an effective area of 4×6 cm^2; the feed and permeate flowed counter-currently along the membrane. The feed solution of 1 M NaCl was circulated along the membrane surface using a gear pump at 1 Lmin^{-1} at 60˚C. As a permeate side, N$_2$ gas was flowing by contacting the other membrane surface at 1 Lmin^{-1}. To maintain the feed concentration after the start of the operation, DI water was added to the feed solution with an amount equal to that of the produced permeate. To compare the effect of heating, the membrane was performed with or without heating during SGMD. For increasing the temperature of the membrane, the heating tape was used to cover the part of the membrane revealed from the cell and maintained at 100˚C (Figure 5.1). The temperature of the membrane was monitored by a temperature meter which was mounted in a cell with the membrane in real time during the SGMD process. The flux was calculated using the change in weight of the permeate over the operating time, as shown in Eq. 5. In addition, the SF, which is the amount of salt passing from the feed to the permeate per unit area and time, was calculated using Eq. 6.

$$Flux = \frac{\Delta \text{ weight}}{\Delta \text{ time} \times \text{effective membrane area}} \left(L/_{m^2h} \text{ (LMH)} \right) \qquad \text{Eq. (5)}$$

$$SF = \left(\frac{\Delta \, Cp \, \Delta Vp}{\Delta \text{ time} \times \text{effective membrane area}} \right) \left(g/_{m^2h} \text{ (GMH)} \right) \qquad \text{Eq. (6)}$$
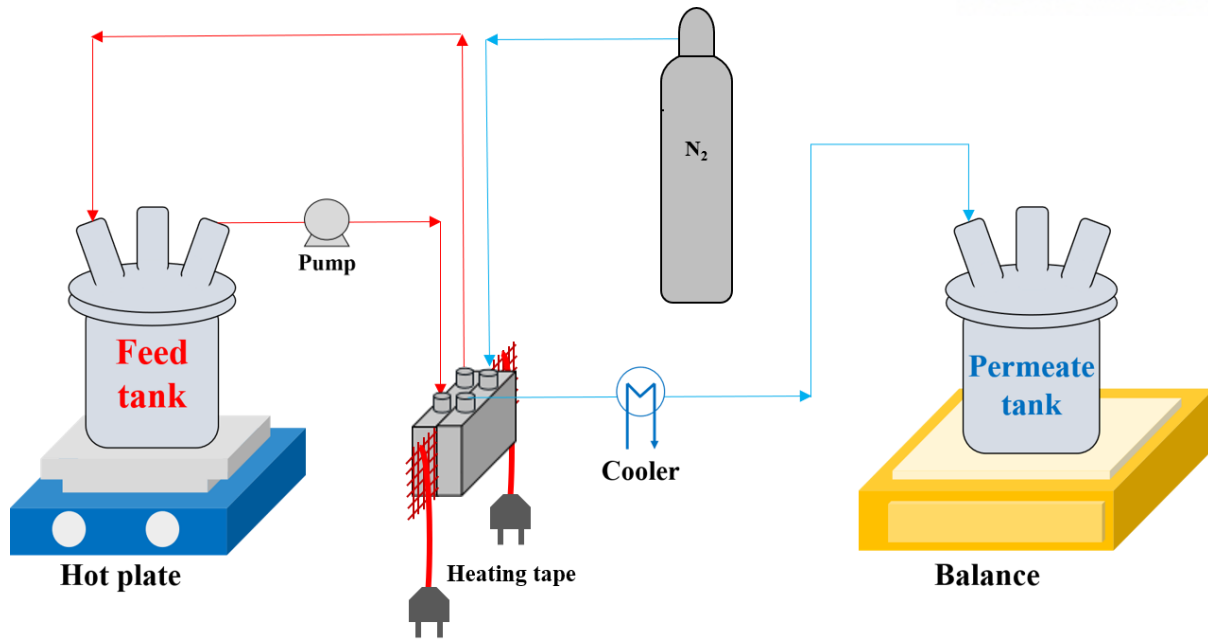
Figure 5. 1 Schematic diagram of lab scale SGMD system.

5.2 Results and Discussion

5.2.1 Morphologies of the membrane with copper mesh
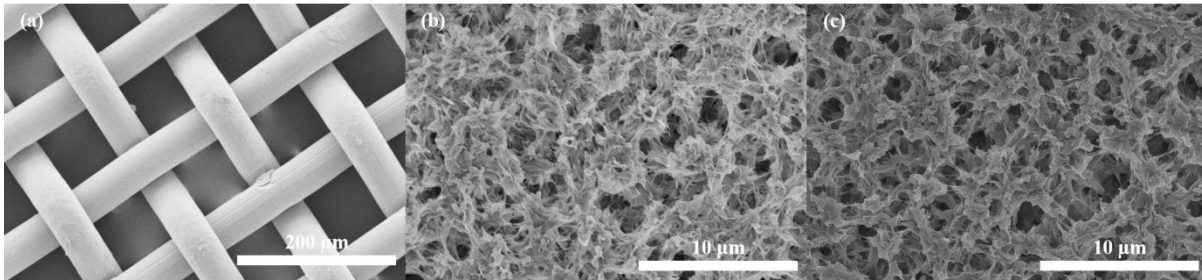
Figure 5. 2 SEM images of (a) copper mesh 200, (b) 19 wt% of PVDF on copper mesh, and (c) 18 wt% of PVDF with 1 wt% of CNF on copper mesh.

In Figure 5.2, the surface of the copper mesh, the membrane with 19 wt% of PVDF and 18 wt% of PVDF with 1 wt% of CNF was observed by SEM. As can be seen in Figure 5.2 (a), the copper mesh 200 has 75 µm of pore size. Using this copper mesh as a substrate, it was possible to fabricate a membrane with a certain thickness. Since casting was performed using a copper mesh, the PVDF solution penetrated the mesh to form a membrane. In addition, since the membrane was made using ethanol as a coagulation solution, the pores on the surface are large due to delay de-mixing (Figure 5.2 (b)). The membrane fabricated in this study, the copper mesh was in the center of the polymer layer, it would work effectively to prevent condensation when transferring heat during the MD process. Subsequently, in the case of the membrane which was fabricated by adding CNF to increase the thermal conductivity, it can be seen from Figure 5.2 (c) that CNF did not significantly affect the pore structure because it is buried in the polymer solution. Using the membrane prepared on copper mesh, it was possible to verify anti wetting performance in the SGMD process.

5.2.2 Contact angle measurement

90
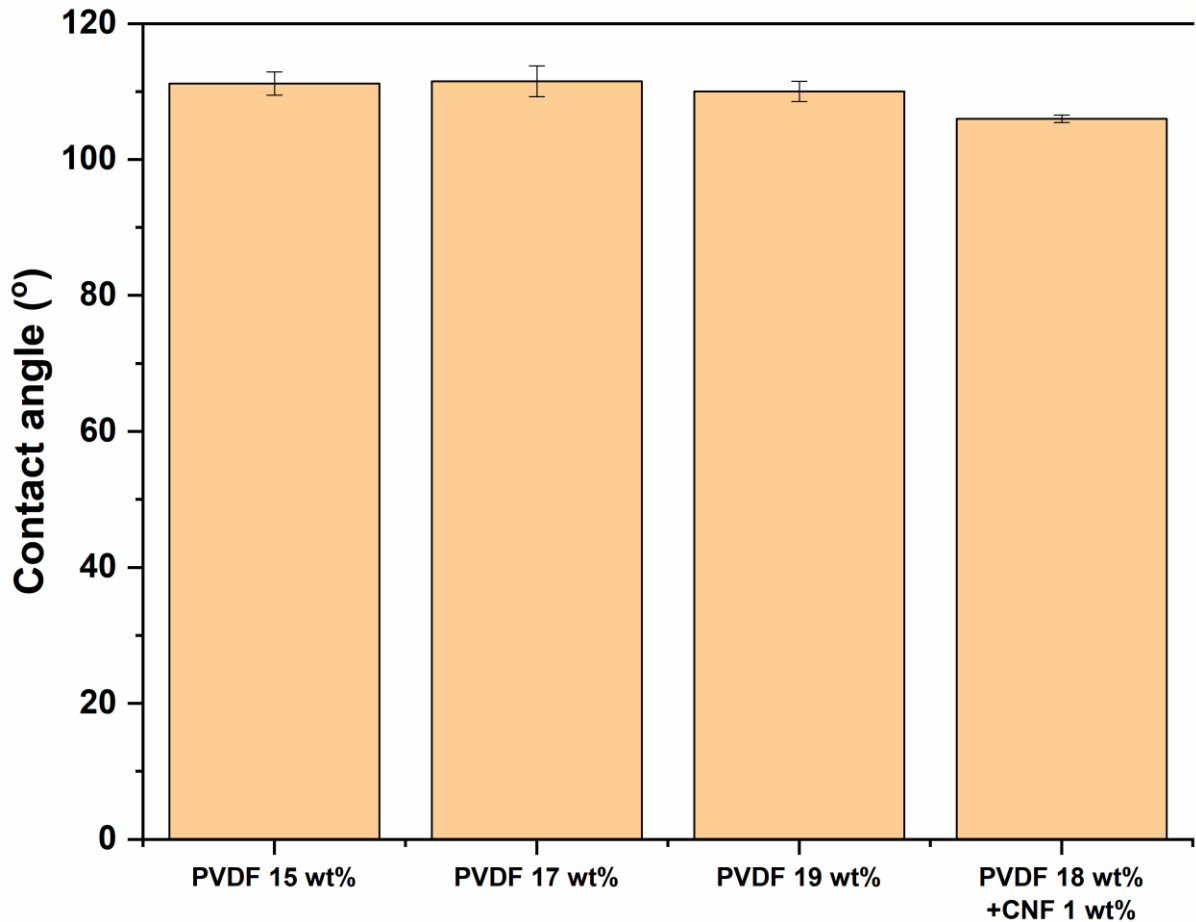
Figure 5. 3 Measurement of CA of different concentration of PVDF membranes and PVDF 18 wt% + CNF 1 wt% of membrane.

Since the hydrophobicity of the surface could influence preventing wetting during MD, the hydrophobicity of the surface was confirmed by measuring the CA. The CA according to the concentration of PVDF was verified, and the effect of CNF which was added to increase thermal conductivity was also confirmed. As can be seen in Figure 5.3, it was confirmed that there was no significant change in the CA value of the surface depending on the PVDF concentration, and it was confirmed that it had a value of about 110°. This can be considered because the hydrophobicity formed on the surface is determined by the properties of PVDF even when the PVDF concentration is increased. In addition, the surface hydrophobicity according to the addition of 1 wt% of CNF was also confirmed by CA measurement. Although a slight decrease was observed, it was confirmed that there was no significant difference in the surface hydrophobicity compare with 19 wt% of PVDF membrane. Through this, only the effect of the heating of the membrane could be confirmed without the effect of the hydrophobicity of the surface.

5.2.3 FTIR measurement of the pure and modified membranes
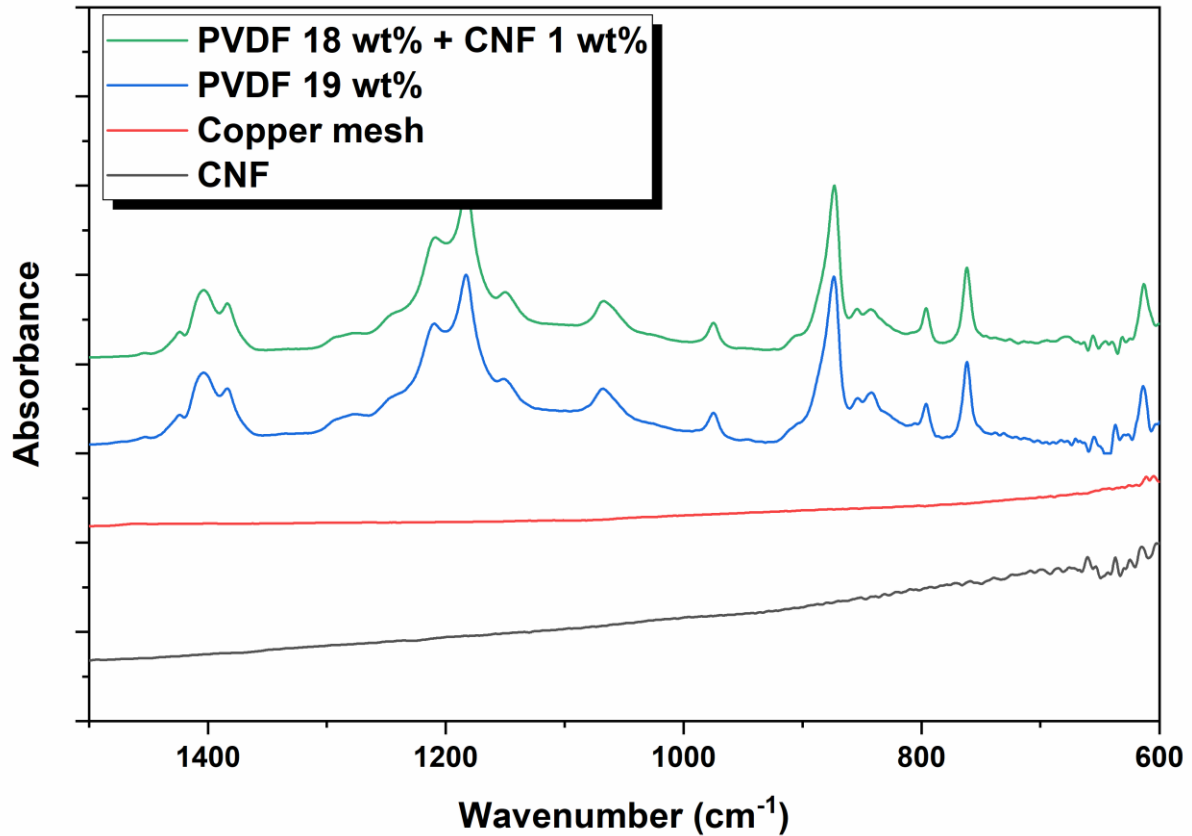
Figure 5. 4 FTIR spectra of CNF, copper mesh, PVDF 19 wt%, and PVDF 18 wt% + CNF 1 wt% for 1500-600 cm^{-1} region.

FTIR was used to analyze the chemical bonds of the previously prepared membrane surface. As shown in Figure 5.4, since PVDF completely covered the copper mesh, the peak of the copper mesh could not be found in the PVDF peak. After that, when CNF is added to increase the thermal conductivity of the membrane, the specific peak of CNF does not appear. This can be explained that CNF was well dispersed in PVDF dope solution, and the amount of CNF was too small.

5.2.4 Long-term SGMD performance with heating the membrane
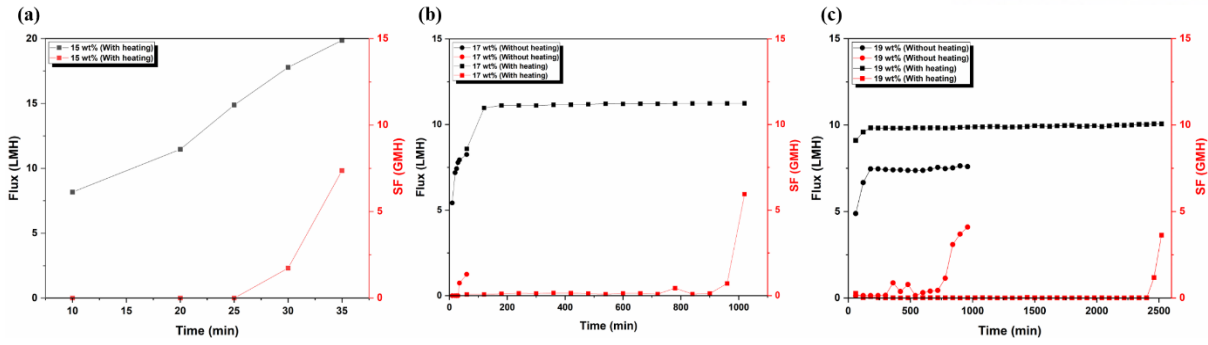
Figure 5. 5 Long-term SGMD process using 3.5 wt% of NaCl solution as a feed solution with (a) 15 wt% of PVDF, (b) 17 wt% of PVDF, and (c) 19 wt% of PVDF membranes.
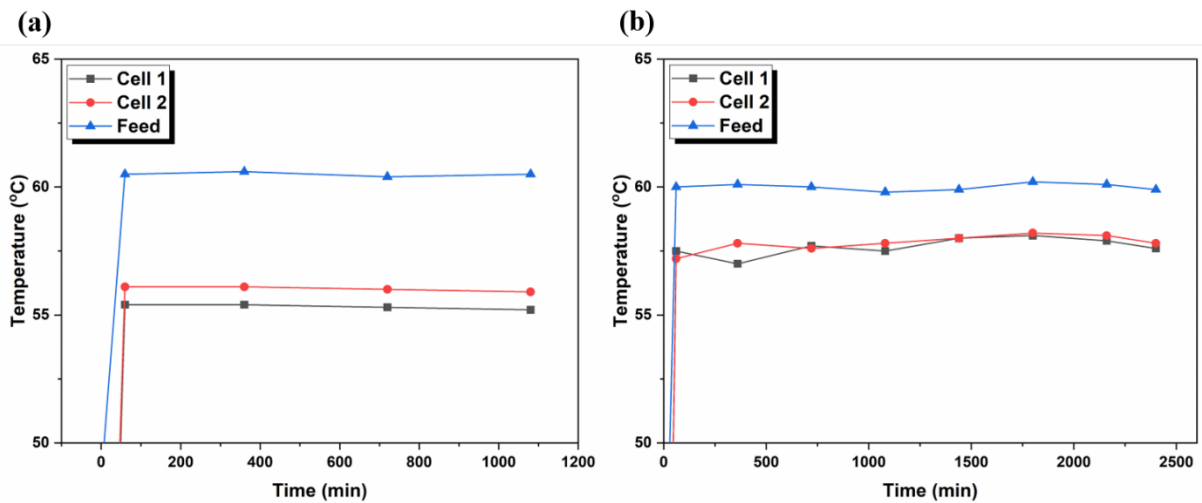
Figure 5. 6 Temperature differences between 19 wt% of PVDF membrane and feed solution (a) before heating and (b) after heating the membrane.

In previous CA measurements, it was confirmed that the concentration of PVDF and the addition of CNF into PVDF dope solution did not significantly affect the hydrophobicity of the membrane and chemical structure of the surface (Figures 5.5 and 5.6). To check the effect of high temperature on the wetting was confirmed by using the membrane prepared for each concentration of PVDF. As can be seen in Figure 5.5 (a), in the case of the 15 wt% of PVDF membrane, when the membrane was not heated, it was confirmed that the feed solution passed directly to the permeate side. However, if heated, it was possible to perform, but it was confirmed that the membrane did not perform properly because of the rapid increase of SF after getting wet in less than 30 min. In the case of the 17 wt% of PVDF membrane, the heating effect was confirmed. It can be seen from Figure 5.5 (b) that when the SGMD is operated with heating, the membrane was wetted after about 1000 min, compared

to the rapid increase of SF due to wet within about 60 min without heating. Furthermore, in the case of the 19 wt% of PVDF membrane, it was confirmed that heating was very effective in preventing wetting. Without heating, the membrane got wetted within 700 min but with heating, the membrane withstands almost 2500 min. To confirm this effect of heating, the temperature of the membrane and feed solution was compared while performing the SGMD (Figure 5.6). When the SGMD was operated without heating the membrane, the temperature of the feed solution was maintained at 60°, while the membrane temperature was about 55° (Figure 5.6 (a)). However, when the SGMD is operated with heating, there is only a difference of 2 to 3° between the feed solution and the membrane (Figure 5.6 (b)). In addition, the performance is higher when the membrane was heated because the generated vapor was transferred faster due to the high temperature when passing through the pores. Through this, it was confirmed that heating of the membrane affects not only preventing wetting but also improving performance.

5.2.5 Long-term SGMD performance with heating the CNF membrane
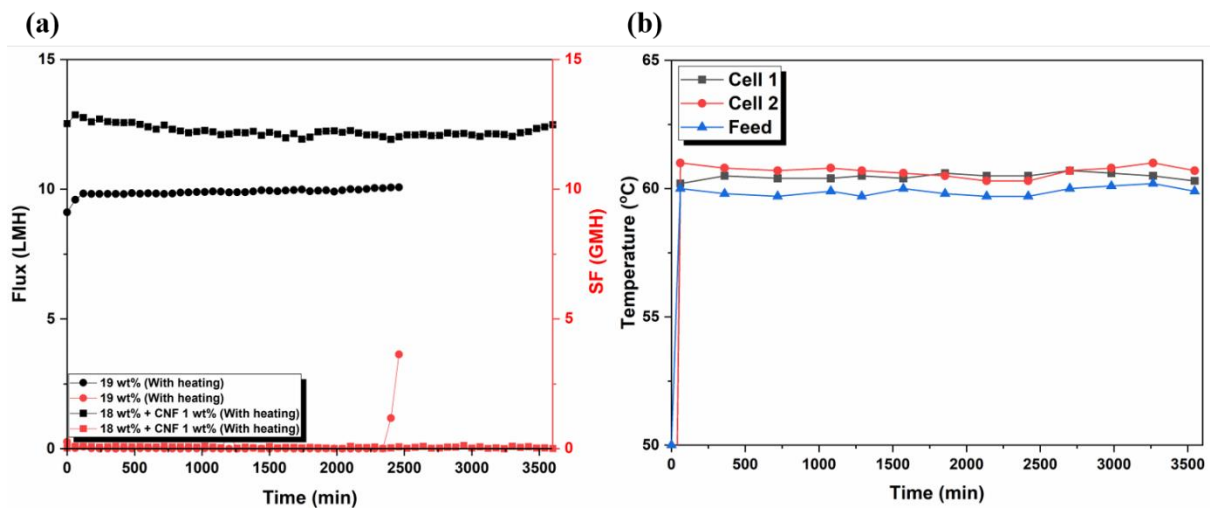
Figure 5. 7 Water fluxes and SF of the pure and modified PVDF membranes in the DCMD mode with addition of SDS solution.

In the case of the previous experiment, it was possible to prevent the wetting that occurs during MD by transferring heat to the copper mesh inside the PVDF membrane. To further improve the prevention of wetting through heating, a membrane was prepared by adding CNF. It can be seen from Figure 5.7 (b) that the heat transferred to the membrane is more effectively transferred through the PVDF membrane because of CNF dispersed inside of the membrane. In the previously conducted

SGMD, it was confirmed that the temperature of the membrane was lower than the temperature of the feed solution. However, it was confirmed that the membrane prepared by adding CNF maintained a higher temperature than the feed solution even during the operation of SGMD. In addition, it was confirmed that the SGMD showed stable performance for a longer period than when heating the general 19 wt% of PVDF during long-term operation and did not get wet after 3600 min (Figure 5.7 (a)). Through this, the effect of preventing wetting through heating could be confirmed, and the effect of heating could be further increased through an additive such as CNF.

5.3 Conclusions

In this study, as a next-generation technique to prevent wetting in MD, a membrane was prepared using copper mesh, a substrate with high thermal conductivity, and applied to SGMD to increase the temperature of the membrane. When the membrane was cast on the copper mesh using 15, 17, and 19 wt% of PVDF and applied to SGMD, the performance difference according to the concentration and the temperature of the membrane through heating were confirmed. In the case of 15 and 17 wt% of PVDF membranes, it was confirmed that the membrane did not perform properly, and in the case of 19 wt% PVDF membranes, the membrane performed for 1000 min without wetting. As a result of operating SGMD by directly applying heat to the copper mesh to keep the temperature of the membrane high, it was confirmed that even the case of 17 wt% of PVDF membrane performed for 900 min without wetting. Furthermore, when heating the 19 wt% of PVDF membrane, the membrane showed good performance for 2400 min without wetting. When the copper mesh is not heated, the temperature difference is about 5°, while the difference of 2.5° after heating can prevent the wetting effectively. To increase the heat transfer efficiency, when the membrane was prepared by adding CNF to the dope solution of PVDF, it was confirmed that the temperature of the membrane was higher than the temperature of the feed solution due to the high heat transfer efficiency. In addition, even when applied to SGMD, it was confirmed that it was more effective in preventing wetting by not getting wet for more than 3600 min.

Conclusions

6. Conclusions

As a new water treatment process using a membrane, many studies have been conducted on MD. MD is a process that does not require high pressure or high thermal energy and is a technology that utilizes the vapor generated by the temperature difference between two solutions. However, because of condensation of this vapor inside of the membrane pores, wetting occurs which should be prevented. So many studies have been conducted to solve this wetting using the various methods. In this study, the problems of the former methods that were conducted to prevent wetting in many studies could be improved and applied to MD, and the performance was verified through long-time operation on the lab scale.

6.1 Enlargement of pore and growing of NPs to prevent performance decline and to enhance the stability

In this chapter, serious issues of coating method such as performance decline and week interaction were improved by pore enlargement and NPs growing. For this, the PVDF membrane was modified in 4 steps: pore expansion by plasma treatment, hydroxylation through Fenton-reaction, and the growth of NPs, and hydrophobic modification using FAS. The performances of the membranes were evaluated under the accelerated condition in DCMD using SDS solution. Totally 3 types of the membrane were compared: dip-coated, NPs growth, plasma, and NPs growth membranes. First, the surface of the PVDF membrane was modified by dip-coating to simply place the hydrophobic NPs on the membrane surface. Second, NPs were grown at the –OH functional groups of the PVDF membrane which was pre-treated by the Fenton-reaction, to increase the stability of the NPs. Finally, NPs were grown in the PVDF membrane after plasma treatment to enhance the performance of the membrane and stability of the NPs.

The dip-coating using the hydrophobic NPs provided a contact angle of 162º, i.e., a superhydrophobic surface. However, the DCMD results showed that the coatings with the hydrophobic NPs physically placed on the surface did not have a significant effect to prevent the wetting, owing to the loss of hydrophobic NPs with no surface adhesion during the operation. In the membranes with NPs grown on their surfaces where functional groups of OH were generated by the Fenton-reaction, the NPs were not detached during the operation and the hydrophobicity was maintained. This ensured the flux remained stable in the three cycles of the addition of SDS. Consequently, the wetting phenomenon was

prevented. However, the flux was reduced as the particles covered the pores and increased the total membrane thickness. When the plasma pretreatment was applied in addition to the modification method, the flux decrease was reduced by the reduction in the total thickness and the NPs grown inside the pores had excellent stability during the operation and even under the sonication condition. This suggested that the hydrophobicity increased not only on the surface but also inside the membrane.

6.2 Patterning and polymerization to simplify the preparation of membrane and to prevent fouling

In many studies, membrane wetting was prevented by increasing hydrophobicity. As a new concept of the hydrophobic membrane, a patterned membrane has been utilized in MD. Because of the rough surface of the patterned membrane, the surface showed a hydrophobic property. Regarding hydrophobic patterned membrane, serious issues such as complex membrane preparation and fouling are the key point to apply in MD. To address these issues, in this chapter, a patterned membrane was prepared by using the template to simplify the fabrication process and by polymerization of hydrophobic materials to achieve low surface energy for preventing fouling on the surface.

For comparing the effect of patterning and polymerization of a hydrophobic material, a control membrane was prepared with a flat surface without polymerization. Compared to the F-CTFE (120°), P-CTFE-PHEMA-Br-PFOMA has a higher CA value (150°) caused by a combination of patterned surface and FOMA synthesis. Various characterization and measurements were conducted to prove successful reaction which was observed new C=O functional groups on the membrane. The effect on performance and anti-wetting was confirmed through long-term DCMD. In the case of the F-CTFE, it was wet within a day, but P-CTFE-PHEMA-Br-PFOMA shows stable flux and SF for more than 7 days. Due to the structure on the P-CTFE surface, it was confirmed that fouling easily occurred during the fouling test which reduces the flux to 70% (F-CTFE showed 80%). However, after hydrophobic modification with HEMA, BiBB, and FOMA, because of the many long FOMA chains on the membrane, the membrane maintains flux. Through this, it was confirmed that the uniform structure on the surface and chemical reaction with FOMA increase the hydrophobicity, and this improvement has the potential to prevent wetting and fouling during MD.

6.3 Heating the membrane for wetting prevention as a next generation concept

For the last concept for wetting prevention in MD, it was possible to control the thermal state of the membrane using copper mesh as a substrate. The basic reason for wetting in MD is the coagulation of vapor generated by the temperature difference between feed and permeate solution. If the membrane itself has a higher temperature than the feed solution, vapor coagulation cannot happen. To achieve the high temperature membrane, the copper mesh was chosen as the substrate for the membrane because of its high thermal conductivity. Through this, heat can be applied to the substrate, and condensation is expected to be prevented by maintaining the temperature inside the membrane higher than the temperature of the feed solution while the MD process.

PVDF was used to fabricate the membrane on copper mesh in this study. With a thermal conductive membrane, it was found that the membrane showed good performance without wetting over 2500 min when the heat was transferred by copper mesh (19 wt% of PVDF) meanwhile only withstand 700 min without heating. To enhance the efficiency of the heat transfer, CNF was chosen as an additive in the PVDF polymer solution. After adding the CNF, the membrane showed very stable performance over 3600 min without wetting even though there are no changes in hydrophobicity or chemical bonding.

References

[1]   "Water shortage set to boost membrane-based water and wastewater treatment market," *Membrane Technology,* vol. 2013, no. 8, pp. 1-16, 2013/08/01/ 2013, doi: https://doi.org/10.1016/S0958-2118(13)70154-X.

[2]   J. Kuylenstierna, P. Najlis, and G. Bjorklund, "The comprehensive assessment of the freshwater resources of the world - Policy options for an integrated sustainable water future," (in English), *Water Int.,* Article vol. 23, no. 1, pp. 17-20, Mar 1998, doi: 10.1080/02508069808686730.

[3]   M. G. Marcovecchio, S. F. Mussati, P. A. Aguirre, and N. J. Scenna, "Optimization of hybrid desalination processes including multi stage flash and reverse osmosis systems," (in English), *Desalination,* Article; Proceedings Paper vol. 182, no. 1-3, pp. 111-122, Nov 2005, doi: 10.1016/j.desal.2005.03.011.

[4]   Q. Schiermeier, "Purification with a pinch of salt," (in English), *Nature,* News Item vol. 452, no. 7185, pp. 260-261, Mar 2008, doi: 10.1038/452260a.

[5]   M. A. Shannon, P. W. Bohn, M. Elimelech, J. G. Georgiadis, B. J. Marinas, and A. M. Mayes, "Science and technology for water purification in the coming decades," (in English), *Nature,* Review vol. 452, no. 7185, pp. 301-310, Mar 2008, doi: 10.1038/nature06599.

[6]   A. D. Khawaji, I. K. Kutubkhanah, and J. M. Wie, "Advances in seawater desalination technologies," (in English), *Desalination,* Article; Proceedings Paper vol. 221, no. 1-3, pp. 47-69, Mar 2008, doi: 10.1016/j.desal.2007.01.067.

[7]   G. N. Tiwari, H. N. Singh, and R. Tripathi, "Present status of solar distillation," (in English), *Sol. Energy,* Article vol. 75, no. 5, pp. 367-373, 2003, doi: 10.1016/j.solener.2003.07.005.

[8]   L. F. Greenlee, D. F. Lawler, B. D. Freeman, B. Marrot, and P. Moulin, "Reverse osmosis desalination: Water sources, technology, and today's challenges," (in English), *Water Research,* Review vol. 43, no. 9, pp. 2317-2348, May 2009, doi: 10.1016/j.watres.2009.03.010.

[9]   K. Kalash, M. Kadhom, and M. Al-Furaiji, "Thin film nanocomposite membranes filled with MCM-41 and SBA-15 nanoparticles for brackish water desalination via reverse osmosis," *Environmental Technology & Innovation,* vol. 20, p. 101101, 2020/11/01/ 2020, doi: https://doi.org/10.1016/j.eti.2020.101101.

[10]   N. Kress, Y. Gertner, and E. Shoham-Frider, "Seawater quality at the brine discharge site from two mega size seawater reverse osmosis desalination plants in Israel (Eastern

Mediterranean)," (in English), *Water Research,* Article vol. 171, p. 12, Mar 2020, Art no. 115402, doi: 10.1016/j.watres.2019.115402.

[11] K. Lee, T. Arnot, and D. Mattia, "A review of reverse osmosis membrane materials for desalination--Development to date and future potential," *Journal of Membrane Science,* vol. 370, pp. 1-22, 03/01 2011, doi: 10.1016/j.memsci.2010.12.036.

[12] E. Curcio and E. Drioli, "Membrane distillation and related operations - A review," (in English), *Sep. Purif. Rev.,* Review vol. 34, no. 1, pp. 35-86, Jan-Jun 2005, doi: 10.1081/spm-200054951.

[13] S. S. Ray, H. K. Lee, and Y. N. Kwon, "Review on Blueprint of Designing Anti-Wetting Polymeric Membrane Surfaces for Enhanced Membrane Distillation Performance," (in English), *Polymers,* Review vol. 12, no. 1, p. 35, Jan 2020, Art no. 23, doi: 10.3390/polym12010023.

[14] R. A. Tufa, "Perspectives on environmental ethics in sustainability of membrane based technologies for water and energy production," *Environmental Technology & Innovation,* vol. 4, pp. 182-193, 2015/10/01/ 2015, doi: https://doi.org/10.1016/j.eti.2015.07.003.

[15] J. F. Kong and K. Li, "An improved gas permeation method for characterising and predicting the performance of microporous asymmetric hollow fibre membranes used in gas absorption," (in English), *Journal of Membrane Science,* Article vol. 182, no. 1-2, pp. 271-281, Feb 2001, doi: 10.1016/s0376-7388(00)00573-1.

[16] M. Gryta, "Influence of polypropylene membrane surface porosity on the performance of membrane distillation process," (in English), *Journal of Membrane Science,* Article vol. 287, no. 1, pp. 67-78, Jan 2007, doi: 10.1016/j.memsci.2006.10.011.

[17] M. Khayet and T. Matsuura, "Preparation and Characterization of Polyvinylidene Fluoride Membranes for Membrane Distillation," *Industrial & Engineering Chemistry Research,* vol. 40, no. 24, pp. 5710-5718, 2001/11/01 2001, doi: 10.1021/ie010553y.

[18] Z. Q. Dong, X. H. Ma, Z. L. Xu, and Z. Y. Gu, "Superhydrophobic modification of PVDF-SiO2 electrospun nanofiber membranes for vacuum membrane distillation," (in English), *RSC Adv.,* Article vol. 5, no. 83, pp. 67962-67970, 2015, doi: 10.1039/c5ra10575g.

[19] X. J. Feng, Y. L. Shi, Y. S. Wang, G. R. Yue, and W. Yang, "Preparation of superhydrophobic silver nano coatings with feather-like structures by electroless galvanic deposition," (in English), *Chin. Sci. Bull.,* Article vol. 58, no. 16, pp. 1887-1891, Jun 2013, doi: 10.1007/s11434-013-5755-9.

[20] J. E. Efome, M. Baghbanzadeh, D. Rana, T. Matsuura, and C. Q. Lan, "Effects of superhydrophobic SiO2 nanoparticles on the performance of PVDF flat sheet membranes for vacuum membrane distillation," (in English), *Desalination,* Article vol. 373, pp. 47-57, Oct 2015, doi: 10.1016/j.desal.2015.07.002.

[21] J. A. Prince, G. Singh, D. Rana, T. Matsuura, V. Anbharasi, and T. S. Shanmugasundaram, "Preparation and characterization of highly hydrophobic poly(vinylidene fluoride) – Clay nanocomposite nanofiber membranes (PVDF–clay NNMs) for desalination using direct contact membrane distillation," *Journal of Membrane Science,* vol. 397-398, pp. 80-86, 2012/04/15/ 2012, doi: https://doi.org/10.1016/j.memsci.2012.01.012.

[22] Y. Liao, C. H. Loh, R. Wang, and A. G. Fane, "Electrospun Superhydrophobic Membranes with Unique Structures for Membrane Distillation," (in English), *ACS Appl. Mater. Interfaces,* Article vol. 6, no. 18, pp. 16035-16048, Sep 2014, doi: 10.1021/am503968n.

[23] J. Zhang, Z. Song, B. Li, Q. Wang, and S. Wang, "Fabrication and characterization of superhydrophobic poly (vinylidene fluoride) membrane for direct contact membrane distillation," *Desalination,* vol. 324, pp. 1-9, 2013/09/02/ 2013, doi: https://doi.org/10.1016/j.desal.2013.05.018.

[24] W. Zhang, Y. Li, J. Liu, B. Li, and S. Wang, "Fabrication of hierarchical poly (vinylidene fluoride) micro/nano-composite membrane with anti-fouling property for membrane distillation," *Journal of Membrane Science,* vol. 535, pp. 258-267, 2017/08/01/ 2017, doi: https://doi.org/10.1016/j.memsci.2017.04.051.

[25] X. Li *et al.*, "Evolution of Polyvinylidene Fluoride (PVDF) Hierarchical Morphology during Slow Gelation Process and Its Superhydrophobicity," *ACS Appl. Mater. Interfaces,* vol. 5, no. 12, pp. 5430-5435, 2013/06/26 2013, doi: 10.1021/am401412a.

[26] D. M. Warsinger *et al.*, "Combining air recharging and membrane superhydrophobicity for fouling prevention in membrane distillation," (in English), *Journal of Membrane Science,* Article vol. 505, pp. 241-252, May 2016, doi: 10.1016/j.memsci.2016.01.018.

[27] G. X. Dong, H. Y. Li, and V. K. Chen, "Challenges and opportunities for mixed-matrix membranes for gas separation," (in English), *J. Mater. Chem. A,* Article vol. 1, no. 15, pp. 4610-4630, 2013, doi: 10.1039/c3ta00927k.

[28] J. D. Mackenzie, "Applications of the sol-gel process," *Journal of Non-Crystalline Solids,* vol. 100, no. 1, pp. 162-168, 1988/03/01/ 1988, doi: https://doi.org/10.1016/0022-3093(88)90013-0.

[29] A. Schneider, X. Y. Wang, D. L. Kaplan, J. A. Garlick, and C. Egles, "Biofunctionalized electrospun silk mats as a topical bioactive dressing for accelerated wound healing," *Acta Biomaterialia,* vol. 5, no. 7, pp. 2570-2578, 2009/09/01/ 2009, doi: https://doi.org/10.1016/j.actbio.2008.12.013.

[30] E. Fontananova, J. C. Jansen, A. Cristiano, E. Curcio, and E. Drioli, "Effect of additives in the casting solution on the formation of PVDF membranes," (in English), *Desalination,* Article; Proceedings Paper vol. 192, no. 1-3, pp. 190-197, May 2006, doi:

10.1016/j.desal.2005.09.021.

[31] M. Gryta, "Fouling in direct contact membrane distillation process," (in English), *Journal of Membrane Science,* Article vol. 325, no. 1, pp. 383-394, Nov 2008, doi: 10.1016/j.memsci.2008.08.001.

[32] M. S. El-Bourawi, Z. Ding, R. Ma, and M. Khayet, "A framework for better understanding membrane distillation separation process," (in English), *Journal of Membrane Science,* Review vol. 285, no. 1-2, pp. 4-29, Nov 2006, doi: 10.1016/j.memsci.2006.08.002.

[33] A. C. M. Franken, J. A. M. Nolten, M. H. V. Mulder, D. Bargeman, and C. A. Smolders, "Wetting criteria for the applicability of membrane distillation," *Journal of Membrane Science,* vol. 33, no. 3, pp. 315-328, 1987/10/01/ 1987, doi: https://doi.org/10.1016/S0376-7388(00)80288-4.

[34] Y. Shin *et al.*, "Application of response surface methodology (RSM) in the optimization of dewetting conditions for flat sheet membrane distillation (MD) membranes," (in English), *Desalin. Water Treat.,* Article vol. 57, no. 22, pp. 10020-10030, May 2016, doi: 10.1080/19443994.2015.1038114.

[35] Y. Sui, Z. N. Wang, X. L. Gao, and C. J. Gao, "Antifouling PVDF ultrafiltration membranes incorporating PVDF-g-PHEMA additive via atom transfer radical graft polymerizations," (in English), *Journal of Membrane Science,* Article vol. 413, pp. 38-47, Sep 2012, doi: 10.1016/j.memsci.2012.03.055.

[36] Y. H. Teow, A. A. Latif, J. K. Lim, H. P. Ngang, L. Y. Susan, and B. S. Ooi, "Hydroxyl functionalized PVDF-TiO2 ultrafiltration membrane and its antifouling properties," (in English), *J. Appl. Polym. Sci.,* Article vol. 132, no. 21, p. 13, Jun 2015, Art no. 41844, doi: 10.1002/app.41844.

[37] Y. Sui, Z. N. Wang, and C. J. Gao, "A new synthetical process of PVDF derivatives via atom transfer radical graft polymerizations and its application in fabrication of antifouling and antibacterial PVDF ultrafiltration membranes," (in English), *Desalin. Water Treat.,* Article vol. 52, no. 34-36, pp. 6377-6388, Oct 2014, doi: 10.1080/19443994.2013.822185.

[38] B. D. Tompkins, J. M. Dennison, and E. R. Fisher, "H2O plasma modification of track-etched polymer membranes for increased wettability and improved performance," (in English), *Journal of Membrane Science,* Article vol. 428, pp. 576-588, Feb 2013, doi: 10.1016/j.memsci.2012.10.037.

[39] L. D. Tijing, Y. C. Woo, J.-S. Choi, S. Lee, S.-H. Kim, and H. K. Shon, "Fouling and its control in membrane distillation—A review," *Journal of Membrane Science,* vol. 475, pp. 215-244, 2015/02/01/ 2015, doi: https://doi.org/10.1016/j.memsci.2014.09.042.

[40] S. Mu *et al.*, "Effect of the relative degree of foulant "hydrophobicity" on membrane fouling," *Journal of Membrane Science,* vol. 570-571, pp. 1-8, 2019/01/15/ 2019, doi: https://doi.org/10.1016/j.memsci.2018.10.023.

[41] G. Naidu, S. Jeong, S.-J. Kim, I. S. Kim, and S. Vigneswaran, "Organic fouling behavior in direct contact membrane distillation," *Desalination,* vol. 347, pp. 230-239, 2014/08/15/ 2014, doi: https://doi.org/10.1016/j.desal.2014.05.045.

[42] D. Hou, D. Lin, C. Zhao, J. Wang, and C. Fu, "Control of protein (BSA) fouling by ultrasonic irradiation during membrane distillation process," *Separation and Purification Technology,* vol. 175, pp. 287-297, 2017/03/24/ 2017, doi: https://doi.org/10.1016/j.seppur.2016.11.047.

[43] M. Laqbaqbi, J. Sanmartino, M. Khayet, M. C. García-Payo, and M. Chaouch, "Fouling in Membrane Distillation, Osmotic Distillation and Osmotic Membrane Distillation," *Applied Sciences,* vol. 7, p. 334, 03/29 2017, doi: 10.3390/app7040334.

[44] S. Srisurichan, R. Jiraratananon, and A. G. Fane, "Humic acid fouling in the membrane distillation process," *Desalination,* vol. 174, no. 1, pp. 63-72, 2005/04/01/ 2005, doi: https://doi.org/10.1016/j.desal.2004.09.003.

[45] C. Kahrs and J. Schwellenbach, "Membrane formation via non-solvent induced phase separation using sustainable solvents: A comparative study," *Polymer,* vol. 186, p. 122071, 2020/01/09/ 2020, doi: https://doi.org/10.1016/j.polymer.2019.122071.

[46] F. Tasselli, "Non-solvent Induced Phase Separation Process (NIPS) for Membrane Preparation," in *Encyclopedia of Membranes*, E. Drioli and L. Giorno Eds. Berlin, Heidelberg: Springer Berlin Heidelberg, 2015, pp. 1-3.

[47] J. Jung, J. Kim, H. Wang, E. Di Nicolò, E. Drioli, and Y. M. Lee, "Understanding the non-solvent induced phase separation (NIPS) effect during the fabrication of microporous PVDF membranes via thermally induced phase separation (TIPS)," *Journal of Membrane Science,* vol. 514, 05/01 2016, doi: 10.1016/j.memsci.2016.04.069.

[48] C. Kahrs, T. Gühlstorf, and J. Schwellenbach, "Influences of different preparation variables on polymeric membrane formation via nonsolvent induced phase separation," *J. Appl. Polym. Sci.,* https://doi.org/10.1002/app.48852 vol. 137, no. 28, p. 48852, 2020/07/20 2020, doi: https://doi.org/10.1002/app.48852.

[49] S. Ashtiani *et al.*, "Fabrication of a PVDF membrane with tailored morphology and properties via exploring and computing its ternary phase diagram for wastewater treatment and gas separation applications," *RSC Adv.,* 10.1039/D0RA07592B vol. 10, no. 66, pp. 40373-40383, 2020, doi: 10.1039/D0RA07592B.

[50] A. Figoli, "Thermally Induced Phase Separation (TIPS) for Membrane Preparation," in *Encyclopedia of Membranes*, E. Drioli and L. Giorno Eds. Berlin, Heidelberg: Springer

Berlin Heidelberg, 2016, pp. 1-2.

[51] N. Ismail, A. Venault, J.-P. Mikkola, D. Bouyer, E. Drioli, and N. Tavajohi Hassan Kiadeh, "Investigating the potential of membranes formed by the vapor induced phase separation process," *Journal of Membrane Science,* vol. 597, p. 117601, 2020/03/01/ 2020, doi: https://doi.org/10.1016/j.memsci.2019.117601.

[52] K. Scott, "INTRODUCTION TO MEMBRANE SEPARATIONS," in *Handbook of Industrial Membranes*, K. Scott Ed. Amsterdam: Elsevier Science, 1995, pp. 3-185.

[53] J. M. S. Henis and M. K. Tripodi, "Composite hollow fiber membranes for gas separation: the resistance model approach," *Journal of Membrane Science,* vol. 8, no. 3, pp. 233-246, 1981/01/01/ 1981, doi: https://doi.org/10.1016/S0376-7388(00)82312-1.

[54] S. Bragg-Sitton, "13 - Hybrid energy systems (HESs) using small modular reactors (SMRs)," in *Handbook of Small Modular Nuclear Reactors*, M. D. Carelli and D. T. Ingersoll Eds.: Woodhead Publishing, 2015, pp. 319-350.

[55] W. Suwaileh, N. Pathak, H. Shon, and N. Hilal, "Forward osmosis membranes and processes: A comprehensive review of research trends and future outlook," *Desalination,* vol. 485, p. 114455, 2020/07/01/ 2020, doi: https://doi.org/10.1016/j.desal.2020.114455.

[56] J. E. Cadotte, "Evolution of Composite Reverse Osmosis Membranes," in *Materials Science of Synthetic Membranes*, vol. 269, (ACS Symposium Series, no. 269): American Chemical Society, 1985, ch. 12, pp. 273-294.

[57] M. Li *et al.*, "Concentration and Recovery of Dyes from Textile Wastewater Using a Self-Standing, Support-Free Forward Osmosis Membrane," *Environ. Sci. Technol.,* vol. 53, no. 6, pp. 3078-3086, 2019/03/19 2019, doi: 10.1021/acs.est.9b00446.

[58] J. K. Beasley, "The evaluation and selection of polymeric materials for reverse osmosis membranes," *Desalination,* vol. 22, no. 1, pp. 181-189, 1977/12/01/ 1977, doi: https://doi.org/10.1016/S0011-9164(00)88374-5.

[59] A. Al Mayyahi, "Important Approaches to Enhance Reverse Osmosis (RO) Thin Film Composite (TFC) Membranes Performance," (in eng), *Membranes,* vol. 8, no. 3, p. 68, 2018, doi: 10.3390/membranes8030068.

[60] J. E. Cadotte, R. J. Petersen, R. E. Larson, and E. E. Erickson, "A new thin-film composite seawater reverse osmosis membrane," *Desalination,* vol. 32, pp. 25-31, 1980/01/01/ 1980, doi: https://doi.org/10.1016/S0011-9164(00)86003-8.

[61] A. Hussain, A. Janson, J. M. Matar, and S. Adham, "Membrane distillation: recent technological developments and advancements in membrane materials," *Emergent Materials,* 2021/01/05 2021, doi: 10.1007/s42247-020-00152-8.

[62] K. Lu and T.-S. Chung, "Introduction to Membrane Distillation," 2019, pp. 3-14.

[63] M. R. Shirzad Kebria and A. Rahimpour, "Membrane Distillation: Basics, Advances, and

Applications," 2020.

[64] K. W. Lawson and D. R. Lloyd, "Membrane distillation," *Journal of Membrane Science,* vol. 124, no. 1, pp. 1-25, 1997/02/05/ 1997, doi: https://doi.org/10.1016/S0376-7388(96)00236-0.

[65] L. Camacho *et al.*, "Advances in Membrane Distillation for Water Desalination and Purification Applications," *Water,* vol. 5, pp. 94-196, 03/01 2013, doi: 10.3390/w5010094.

[66] P. Pal, "Chapter 5 - Arsenic Removal by Membrane Distillation," in *Groundwater Arsenic Remediation*, P. Pal Ed.: Butterworth-Heinemann, 2015, pp. 179-270.

[67] M. Tomaszewska, "Sweep Gas Membrane Distillation (SGMD)," in *Encyclopedia of Membranes*, E. Drioli and L. Giorno Eds. Berlin, Heidelberg: Springer Berlin Heidelberg, 2015, pp. 1-3.

[68] M. R. Bilad and I. Vankelecom, "Vibrating Membranes," in *Encyclopedia of Membranes*, E. Drioli and L. Giorno Eds. Berlin, Heidelberg: Springer Berlin Heidelberg, 2016, pp. 1966-1967.

[69] S. Bandini and G. C. Sarti, "Heat and mass transport resistances in vacuum membrane distillation per drop," *AIChE Journal,* https://doi.org/10.1002/aic.690450707 vol. 45, no. 7, pp. 1422-1433, 1999/07/01 1999, doi: https://doi.org/10.1002/aic.690450707.

[70] M. Rezaei, D. M. Warsinger, J. H. Lienhard V, M. C. Duke, T. Matsuura, and W. M. Samhaber, "Wetting phenomena in membrane distillation: Mechanisms, reversal, and prevention," *Water Research,* vol. 139, pp. 329-352, 2018/08/01/ 2018, doi: https://doi.org/10.1016/j.watres.2018.03.058.

[71] S. Lin, S. Nejati, C. Boo, Y. Hu, C. O. Osuji, and M. Elimelech, "Omniphobic Membrane for Robust Membrane Distillation," *Environmental Science & Technology Letters,* vol. 1, no. 11, pp. 443-447, 2014/11/11 2014, doi: 10.1021/ez500267p.

[72] C. S. Fernandes *et al.*, "Explication of hydrophobic silica as effective pore former for membrane fabrication," *Applied Surface Science Advances,* vol. 3, p. 100051, 2021/03/01/ 2021, doi: https://doi.org/10.1016/j.apsadv.2020.100051.

[73] M. Khayet, C. García-Payo, and T. Matsuura, "Superhydrophobic nanofibers electrospun by surface segregating fluorinated amphiphilic additive for membrane distillation," *Journal of Membrane Science,* vol. 588, p. 117215, 2019/10/15/ 2019, doi: https://doi.org/10.1016/j.memsci.2019.117215.

[74] S. J. Hardman *et al.*, "Electrospinning Superhydrophobic Fibers Using Surface Segregating End-Functionalized Polymer Additives," *Macromolecules,* vol. 44, no. 16, pp. 6461-6470, 2011/08/23 2011, doi: 10.1021/ma200852z.

[75] Z.-Q. Dong, X.-h. Ma, Z.-L. Xu, W.-T. You, and F.-b. Li, "Superhydrophobic PVDF–PTFE electrospun nanofibrous membranes for desalination by vacuum membrane distillation,"

Desalination, vol. 347, pp. 175-183, 2014/08/15/ 2014, doi: https://doi.org/10.1016/j.desal.2014.05.015.

[76] C. Su, Y. Li, Y. Dai, F. Gao, K. Tang, and H. Cao, "Fabrication of three-dimensional superhydrophobic membranes with high porosity via simultaneous electrospraying and electrospinning," *Materials Letters,* vol. 170, pp. 67-71, 2016/05/01/ 2016, doi: https://doi.org/10.1016/j.matlet.2016.01.133.

[77] Y. C. Woo *et al.*, "Water desalination using graphene-enhanced electrospun nanofiber membrane via air gap membrane distillation," *Journal of Membrane Science,* vol. 520, pp. 99-110, 2016/12/15/ 2016, doi: https://doi.org/10.1016/j.memsci.2016.07.049.

[78] E. Gontarek *et al.*, "Adsorption-assisted transport of water vapour in super-hydrophobic membranes filled with multilayer graphene platelets," *Nanoscale,* 10.1039/C9NR02581B vol. 11, no. 24, pp. 11521-11529, 2019, doi: 10.1039/C9NR02581B.

[79] A. K. An, E.-J. Lee, J. Guo, S. Jeong, J.-g. Lee, and N. Ghaffour, "Enhanced vapor transport in membrane distillation via functionalized carbon nanotubes anchored into electrospun nanofibres," *Sci Rep,* vol. 7, 2017.

[80] L. N. Nthunya *et al.*, "Superhydrophobic PVDF nanofibre membranes coated with an organic fouling resistant hydrophilic active layer for direct-contact membrane distillation," *Colloids and Surfaces A: Physicochemical and Engineering Aspects,* vol. 575, pp. 363-372, 2019/08/20/ 2019, doi: https://doi.org/10.1016/j.colsurfa.2019.05.031.

[81] F. Yang, J. E. Efome, D. Rana, T. Matsuura, and C. Lan, "Metal–Organic Frameworks Supported on Nanofiber for Desalination by Direct Contact Membrane Distillation," *ACS Appl. Mater. Interfaces,* vol. 10, no. 13, pp. 11251-11260, 2018/04/04 2018, doi: 10.1021/acsami.8b01371.

[82] A. L. McGaughey, P. Karandikar, M. Gupta, and A. E. Childress, "Hydrophobicity versus Pore Size: Polymer Coatings to Improve Membrane Wetting Resistance for Membrane Distillation," *ACS Applied Polymer Materials,* vol. 2, no. 3, pp. 1256-1267, 2020/03/13 2020, doi: 10.1021/acsapm.9b01133.

[83] K. Wang, D. Hou, J. Wang, Z. Wang, B. Tian, and P. Liang, "Hydrophilic surface coating on hydrophobic PTFE membrane for robust anti-oil-fouling membrane distillation," *Applied Surface Science,* vol. 450, pp. 57-65, 2018/08/30/ 2018, doi: https://doi.org/10.1016/j.apsusc.2018.04.180.

[84] J.-C. Han *et al.*, "Modification of regenerated cellulose ultrafiltration membranes with multi-walled carbon nanotubes for enhanced antifouling ability: Field test and mechanism study," *Science of The Total Environment,* vol. 780, p. 146657, 2021/08/01/ 2021, doi: https://doi.org/10.1016/j.scitotenv.2021.146657.

[85] X. Gong *et al.*, "Construct a stable super-hydrophobic surface through acetonitrile

extracted lignin and nano-silica and its application in oil-water separation," *Industrial Crops and Products,* vol. 166, p. 113471, 2021/08/01/ 2021, doi: https://doi.org/10.1016/j.indcrop.2021.113471.

[86]   J. Zhang, N. Li, D. Wang, J. Li, Y. Chen, and Z. Wang, "Omniphobic palygorskite coated Janus membrane with enhanced fouling and wetting resistance for direct contact membrane distillation," *Desalination,* vol. 505, p. 114986, 2021/06/01/ 2021, doi: https://doi.org/10.1016/j.desal.2021.114986.

[87]   M. Yang *et al.*, "Superhydrophobic and Corrosion-Resistant Electrospun Hybrid Membrane for High-Efficiency Electromagnetic Interference Shielding," *ACS Applied Electronic Materials,* vol. 3, no. 5, pp. 2067-2078, 2021/05/25 2021, doi: 10.1021/acsaelm.1c00076.

[88]   T. G. Kim, G. S. An, J. S. Han, J. U. Hur, B. G. Park, and S.-C. Choi, "Synthesis of Size Controlled Spherical Silica Nanoparticles via Sol-Gel Process within Hydrophilic Solvent," *J. Korean Ceram. Soc,* vol. 54, no. 1, pp. 49-54, 1 2017, doi: 10.4191/kcers.2017.54.1.10.

[89]   I. A. Rahman and V. Padavettan, "Synthesis of Silica Nanoparticles by Sol-Gel: Size-Dependent Properties, Surface Modification, and Applications in Silica-Polymer Nanocomposites—A Review," *Journal of Nanomaterials,* vol. 2012, p. 132424, 2012/05/10 2012, doi: 10.1155/2012/132424.

[90]   F. Norazmi, K. Chaudhary, E. Mazalan, Z. Hader, and J. Ali, "Effect of various amount of ammonium hydroxide on morphology of silica nanoparticles grown by sol-gel," *Malaysian Journal of Fundamental and Applied Sciences,* vol. 14, pp. 482-484, 10/25 2018, doi: 10.11113/mjfas.v14n0.1278.

[91]   J. H. Zhang, P. Zhan, Z. L. Wang, W. Y. Zhang, and N. B. Ming, "Preparation of monodisperse silica particles with controllable size and shape," *Journal of Materials Research,* vol. 18, no. 3, pp. 649-653, 2003, doi: 10.1557/JMR.2003.0085.

[92]   K. Nozawa *et al.*, "Smart Control of Monodisperse Stöber Silica Particles: Effect of Reactant Addition Rate on Growth Process," *Langmuir,* vol. 21, no. 4, pp. 1516-1523, 2005/02/01 2005, doi: 10.1021/la048569r.

[93]   N. I. Vazquez, Z. Gonzalez, B. Ferrari, and Y. Castro, "Synthesis of mesoporous silica nanoparticles by sol–gel as nanocontainer for future drug delivery applications," *Boletín de la Sociedad Española de Cerámica y Vidrio,* vol. 56, no. 3, pp. 139-145, 2017/05/01/ 2017, doi: https://doi.org/10.1016/j.bsecv.2017.03.002.

[94]   G. De, B. Karmakar, and D. Ganguli, "Hydrolysis–condensation reactions of TEOS in the presence of acetic acid leading to the generation of glass-like silica microspheres in solution at room temperature," *Journal of Materials Chemistry,* 10.1039/B003221M vol.

10, no. 10, pp. 2289-2293, 2000, doi: 10.1039/B003221M.

[95]   J. Verma, "Analysis on Synthesis of Silica Nanoparticles and its Effect on Growth of T. Harzianum & Rhizoctonia Species," *Biomedical Journal of Scientific & Technical Research,* vol. 10, 10/29 2018, doi: 10.26717/BJSTR.2018.10.001972.

[96]   K. S. Rao, K. El-Hami, T. Kodaki, K. Matsushige, and K. Makino, "A novel method for synthesis of silica nanoparticles," *Journal of Colloid and Interface Science,* vol. 289, no. 1, pp. 125-131, 2005/09/01/ 2005, doi: https://doi.org/10.1016/j.jcis.2005.02.019.

[97]   C. Picard, A. Larbot, F. Guida-Pietrasanta, B. Boutevin, and A. Ratsimihety, "Grafting of ceramic membranes by fluorinated silanes: hydrophobic features," *Separation and Purification Technology,* vol. 25, no. 1, pp. 65-69, 2001/10/01/ 2001, doi: https://doi.org/10.1016/S1383-5866(01)00091-0.

[98]   O. Burtovyy, V. Klep, H. C. Chen, R. K. Hu, C. C. Lin, and I. Luzinov, "Hydrophobic Modification of Polymer Surfaces via "Grafting to" Approach," *Journal of Macromolecular Science, Part B,* vol. 46, no. 1, pp. 137-154, 2007/02/01 2007, doi: 10.1080/00222340601044326.

[99]   M. Khemakhem, S. Khemakhem, and R. Ben Amar, "Emulsion separation using hydrophobic grafted ceramic membranes by," *Colloids and Surfaces A: Physicochemical and Engineering Aspects,* vol. 436, pp. 402-407, 2013/09/05/ 2013, doi: https://doi.org/10.1016/j.colsurfa.2013.05.073.

[100]   C. C. Wei and K. Li, "Preparation and Characterization of a Robust and Hydrophobic Ceramic Membrane via an Improved Surface Grafting Technique," *Industrial & Engineering Chemistry Research,* vol. 48, no. 7, pp. 3446-3452, 2009/04/01 2009, doi: 10.1021/ie801639d.

[101]   W.-T. Xu, Z.-P. Zhao, M. Liu, and K.-C. Chen, "Morphological and hydrophobic modifications of PVDF flat membrane with silane coupling agent grafting via plasma flow for VMD of ethanol–water mixture," *Journal of Membrane Science,* vol. 491, pp. 110-120, 2015/10/01/ 2015, doi: https://doi.org/10.1016/j.memsci.2015.05.024.

[102]   V. H. Nguyen and J.-J. Shim, "Ionic liquid-mediated synthesis and self-assembly of poly(ethylene glycol)-block-polystyrene copolymer by ATRP method," *Colloid and Polymer Science,* vol. 293, no. 2, pp. 617-623, 2015/02/01 2015, doi: 10.1007/s00396-014-3431-5.

[103]   F. Yu, W. Yang, J. Song, Q. Wu, and L. Chen, "Investigation on hydrophobic modification of bamboo flour surface by means of atom transfer radical polymerization method," *Wood Science and Technology,* vol. 48, no. 2, pp. 289-299, 2014/03/01 2014, doi: 10.1007/s00226-013-0596-x.

[104]   Z. Liu, J. Gao, and C. Xiao, "Preparation and vacuum membrane distillation

performance of a superhydrophobic polypropylene hollow fiber membrane modified via ATRP," *Desalination,* vol. 512, p. 115130, 2021/09/15/ 2021, doi: https://doi.org/10.1016/j.desal.2021.115130.

[105] I. V. Korolkov, Y. G. Gorin, A. B. Yeszhanov, A. L. Kozlovskiy, and M. V. Zdorovets, "Preparation of PET track-etched membranes for membrane distillation by photo-induced graft polymerization," *Materials Chemistry and Physics,* vol. 205, pp. 55-63, 2018/02/01/ 2018, doi: https://doi.org/10.1016/j.matchemphys.2017.11.006.

[106] S. S. Hussein, S. S. Ibrahim, M. A. Toma, Q. F. Alsalhy, and E. Drioli, "Novel chemical modification of polyvinyl chloride membrane by free radical graft copolymerization for direct contact membrane distillation (DCMD) application," *Journal of Membrane Science,* vol. 611, p. 118266, 2020/10/01/ 2020, doi: https://doi.org/10.1016/j.memsci.2020.118266.

[107] S. Al-Gharabli, J. Kujawa, M. O. Mavukkandy, T. A. Agbaje, E. M. Hamad, and H. A. Arafat, "Covalent surface entanglement of polyvinylidene fluoride membranes with carbon nanotubes," *European Polymer Journal,* vol. 100, pp. 153-164, 2018/03/01/ 2018, doi: https://doi.org/10.1016/j.eurpolymj.2018.01.027.

[108] M. M. Puppolo *et al.*, "Plasma modification of microporous polymer membranes for application in biomimetic dissolution studies," *AAPS Open,* vol. 3, no. 1, p. 9, 2017/10/24 2017, doi: 10.1186/s41120-017-0019-4.

[109] S. Jeong, B. Shin, W. Jo, H.-Y. Kim, M.-W. Moon, and S. Lee, "Nanostructured PVDF membrane for MD application by an O2 and CF4 plasma treatment," *Desalination,* vol. 399, pp. 178-184, 2016/12/01/ 2016, doi: https://doi.org/10.1016/j.desal.2016.09.001.

[110] M. Yue *et al.*, "Switchable hydrophobic/hydrophilic surface of electrospun poly (l-lactide) membranes obtained by CF4 microwave plasma treatment," *Applied Surface Science,* vol. 327, pp. 93-99, 2015/02/01/ 2015, doi: https://doi.org/10.1016/j.apsusc.2014.11.149.

[111] M. Iqbal, D. K. Dinh, Q. Abbas, M. Imran, H. Sattar, and A. Ul Ahmad, "Controlled Surface Wettability by Plasma Polymer Surface Modification," *Surfaces,* vol. 2, no. 2, 2019, doi: 10.3390/surfaces2020026.

[112] L. Liu *et al.*, "A novel plasma-induced surface hydrophobization strategy for membrane distillation: Etching, dipping and grafting," *Journal of Membrane Science,* vol. 499, pp. 544-554, 2016/02/01/ 2016, doi: https://doi.org/10.1016/j.memsci.2015.11.003.

[113] S. Jeong, B. Shin, W. Jo, H.-Y. Kim, M. Moon, and S. Lee, "Nanostructured PVDF membrane for MD application by an O2 and CF4 plasma treatment," *Desalination,* vol. 399, pp. 178-184, 2016.

[114] Y. Chen *et al.*, "Anti-wetting behavior of negatively charged superhydrophobic PVDF membranes in direct contact membrane distillation of emulsified wastewaters," *Journal of Membrane Science,* vol. 535, pp. 230-238, 2017/08/01/ 2017, doi:

https://doi.org/10.1016/j.memsci.2017.04.040.

[115] H. Wu, F. Shen, Y. Su, X. Chen, and W. Yinhua, "Modification of polyacrylonitrile membranes via plasma treatment followed by polydimethylsiloxane coating for recovery of ethyl acetate from aqueous solution through vacuum membrane distillation," *Separation and Purification Technology,* vol. 197, 05/31 2018, doi: 10.1016/j.seppur.2018.01.011.

[116] H. Şakalak, K. Yılmaz, M. Gürsoy, and M. Karaman, "Roll-to roll initiated chemical vapor deposition of super hydrophobic thin films on large-scale flexible substrates," *Chemical Engineering Science,* vol. 215, p. 115466, 2020/04/06/ 2020, doi: https://doi.org/10.1016/j.ces.2019.115466.

[117] F. Guo, A. Servi, A. Liu, K. K. Gleason, and G. C. Rutledge, "Desalination by Membrane Distillation using Electrospun Polyamide Fiber Membranes with Surface Fluorination by Chemical Vapor Deposition," *ACS Appl. Mater. Interfaces,* vol. 7, no. 15, pp. 8225-8232, 2015/04/22 2015, doi: 10.1021/acsami.5b01197.

[118] T. Pan *et al.*, "ZnO Nanowires@PVDF nanofiber membrane with superhydrophobicity for enhanced anti-wetting and anti-scaling properties in membrane distillation," *Journal of Membrane Science,* vol. 621, p. 118877, 2021/03/01/ 2021, doi: https://doi.org/10.1016/j.memsci.2020.118877.

[119] M. Zhu and Y. Mao, "Large-pore-size membranes tuned by chemically vapor deposited nanocoatings for rapid and controlled desalination," *RSC Adv.,* 10.1039/D0RA07629E vol. 10, no. 66, pp. 40562-40568, 2020, doi: 10.1039/D0RA07629E.

[120] N. Beauregard *et al.*, "Enhancing iCVD Modification of Electrospun Membranes for Membrane Distillation Using a 3D Printed Scaffold," (in eng), *Polymers (Basel),* vol. 12, no. 9, Sep 12 2020, doi: 10.3390/polym12092074.

[121] A. Asatekin and K. K. Gleason, "Polymeric Nanopore Membranes for Hydrophobicity-Based Separations by Conformal Initiated Chemical Vapor Deposition," *Nano Letters,* vol. 11, no. 2, pp. 677-686, 2011/02/09 2011, doi: 10.1021/nl103799d.

[122] Z. Zheng, Z. Gu, R. Huo, and Y. Ye, "Superhydrophobicity of polyvinylidene fluoride membrane fabricated by chemical vapor deposition from solution," *Applied Surface Science,* vol. 255, no. 16, pp. 7263-7267, 2009/05/30/ 2009, doi: https://doi.org/10.1016/j.apsusc.2009.03.084.

[123] X. Zhou *et al.*, "Robust and Durable Superhydrophobic Cotton Fabrics for Oil/Water Separation," *ACS Appl. Mater. Interfaces,* vol. 5, no. 15, pp. 7208-7214, 2013/08/14 2013, doi: 10.1021/am4015346.

[124] N. U. Barambu, M. R. Bilad, Y. Wibisono, J. Jaafar, T. M. I. Mahlia, and A. L. Khan, "Membrane Surface Patterning as a Fouling Mitigation Strategy in Liquid Filtration: A

Review," (in eng), *Polymers,* vol. 11, no. 10, p. 1687, 2019, doi: 10.3390/polym11101687.

[125] M. Xie, W. Luo, and S. R. Gray, "Surface pattern by nanoimprint for membrane fouling mitigation: Design, performance and mechanisms," *Water Research,* vol. 124, pp. 238-243, 2017/11/01/ 2017, doi: https://doi.org/10.1016/j.watres.2017.07.057.

[126] M. Bikel, I. G. M. Pünt, R. G. H. Lammertink, and M. Wessling, "Micropatterned Polymer Films by Vapor-Induced Phase Separation Using Permeable Molds," *ACS Appl. Mater. Interfaces,* vol. 1, no. 12, pp. 2856-2861, 2009/12/30 2009, doi: 10.1021/am900594p.

[127] W. Liu, F. Sun, L. Jiang, J. C. Meredith, and Y. Deng, "Surface Structure Patterning for Fabricating Non-fluorinated Superhydrophobic Cellulosic Membranes," *ACS Applied Polymer Materials,* vol. 1, no. 5, pp. 1220-1229, 2019/05/10 2019, doi: 10.1021/acsapm.9b00215.

[128] W.-C. Lin and N. A. Mohd Razali, "Temporary Wettability Tuning of PCL/PDMS Micro Pattern Using the Plasma Treatments," (in eng), *Materials (Basel),* vol. 12, no. 4, p. 644, 2019, doi: 10.3390/ma12040644.

[129] C. Carlborg, F. Moraga, F. Saharil, W. Wijngaart, and T. Haraldsson, "Rapid permanent hydrophilic and hydrophobic patterning of polymer surfaces via off-stoichiometry thiol-ene (OSTE) photografting," *Proceedings of the 16th International Conference on Miniaturized Systems for Chemistry and Life Sciences, MicroTAS 2012,* pp. 677-679, 01/01 2012.

[130] Z. Wang *et al.*, "Patterned, anti-fouling membrane with controllable wettability for ultrafast oil/water separation and liquid–liquid extraction," *Chemical Communications,* 10.1039/D0CC04804F vol. 56, no. 80, pp. 12045-12048, 2020, doi: 10.1039/D0CC04804F.

[131] J. Wang, Z. Yuan, X. Wu, Y. Li, J. Chen, and Z. Jiang, "Beetle-Inspired Assembly of Heterostructured Lamellar Membranes with Polymer Cluster–Patterned Surface for Enhanced Molecular Permeation," *Advanced Functional Materials,* https://doi.org/10.1002/adfm.201900819 vol. 29, no. 23, p. 1900819, 2019/06/01 2019, doi: https://doi.org/10.1002/adfm.201900819.

[132] A. Osman *et al.*, "Patterned Membrane in an Energy-Efficient Tilted Panel Filtration System for Fouling Control in Activated Sludge Filtration," (in eng), *Polymers (Basel),* vol. 12, no. 2, Feb 12 2020, doi: 10.3390/polym12020432.

[133] M. H. Yildirim, J. te Braake, H. C. Aran, D. F. Stamatialis, and M. Wessling, "Micro-patterned Nafion membranes for direct methanol fuel cell applications," *Journal of Membrane Science,* vol. 349, no. 1, pp. 231-236, 2010/03/01/ 2010, doi: https://doi.org/10.1016/j.memsci.2009.11.050.

[134] J. A. Kharraz and A. K. An, "Patterned superhydrophobic polyvinylidene fluoride (PVDF) membranes for membrane distillation: Enhanced flux with improved fouling and wetting

resistance," *Journal of Membrane Science,* vol. 595, p. 117596, 2020/02/01/ 2020, doi: https://doi.org/10.1016/j.memsci.2019.117596.

[135] H. H. Chang, L. K. Chang, C. D. Yang, D. J. Lin, and L. P. Cheng, "Effect of solvent on the dipole rotation of poly(vinylidene fluoride) during porous membrane formation by precipitation in alcohol baths," (in English), *Polymer,* Article vol. 115, pp. 164-175, Apr 2017, doi: 10.1016/j.polymer.2017.03.044.

[136] E. J. Lee, B. J. Deka, J. X. Guo, Y. C. Woo, H. K. Shon, and A. K. An, "Engineering the Re-Entrant Hierarchy and Surface Energy of PDMS-PVDF Membrane for Membrane Distillation Using a Facile and Benign Microsphere Coating," (in English), *Environ. Sci. Technol.,* Article vol. 51, no. 17, pp. 10117-10126, Sep 2017, doi: 10.1021/acs.est7b01108.

[137] X. M. Lu, Y. L. Peng, H. R. Qiu, X. R. Liu, and L. Ge, "Anti-fouling membranes by manipulating surface wettability and their anti-fouling mechanism," (in English), *Desalination,* Article vol. 413, pp. 127-135, Jul 2017, doi: 10.1016/j.desal.2017.02.022.

[138] H. Yamazaki *et al.*, "The Influence of Fluorinated Silicon Nitride Gate Insulator on Positive Bias Stability toward Highly Reliable Amorphous InGaZnO Thin-Film Transistors," (in English), *ECS J. Solid State Sci. Technol.,* Article vol. 3, no. 2, pp. Q20-Q23, 2014, doi: 10.1149/2.014402jss.

[139] R. B. Viana, A. B. F. da Silva, and A. S. Pimentel, "Infrared Spectroscopy of Anionic, Cationic, and Zwitterionic Surfactants %J Advances in Physical Chemistry," vol. 2012, p. 14, 2012, Art no. 903272, doi: 10.1155/2012/903272.

[140] Y. Liao, R. Wang, and A. G. Fane, "Engineering superhydrophobic surface on poly(vinylidene fluoride) nanofiber membranes for direct contact membrane distillation," (in English), *Journal of Membrane Science,* Article vol. 440, pp. 77-87, Aug 2013, doi: 10.1016/j.memsci.2013.04.006.

[141] A. C. Pauly *et al.*, "ATRP-based synthesis and characterization of light-responsive coatings for transdermal delivery systems," *Science and Technology of Advanced Materials,* vol. 16, no. 3, p. 034604, 2015/06/20 2015, doi: 10.1088/1468-6996/16/3/034604.

[142] G. Zhao and W. N. Chen, "Design of poly(vinylidene fluoride)-g-p(hydroxyethyl methacrylate-co-N-isopropylacrylamide) membrane via surface modification for enhanced fouling resistance and release property," *Applied Surface Science,* vol. 398, pp. 103-115, 2017/03/15/ 2017, doi: https://doi.org/10.1016/j.apsusc.2016.11.138.

[143] Z. Xiao *et al.*, "Slippery for scaling resistance in membrane distillation: A novel porous micropillared superhydrophobic surface," *Water Research,* vol. 155, pp. 152-161, 2019/05/15/ 2019, doi: https://doi.org/10.1016/j.watres.2019.01.036.

[144] L. Vogelaar *et al.*, "Phase Separation Micromolding: A New Generic Approach for Microstructuring Various Materials," *Small,* vol. 1, no. 6, pp. 645-655, 2005/06/01 2005,

doi: 10.1002/smll.200400128.

[145] H. Yi *et al.*, "Constructing high-performance 3D porous self-standing electrodes with various morphologies and shapes by a flexible phase separation-derived method," *J. Mater. Chem. A,* 10.1039/C9TA08845H vol. 7, no. 39, pp. 22550-22558, 2019, doi: 10.1039/C9TA08845H.

[146] M. F. Passos, M. Fernández-Gutiérrez, B. Vázquez-Lasa, J. S. Román, and R. M. Filho, "PHEMA-PLLA semi-interpenetrating polymer networks: A study of their swelling kinetics, mechanical properties and cellular behavior," *European Polymer Journal,* vol. 85, pp. 150-163, 2016/12/01/ 2016, doi: https://doi.org/10.1016/j.eurpolymj.2016.10.023.

[147] S. Chen and W. Zhao, "Adsorption of Pb2+ from Aqueous Solutions Using Novel Functionalized Corncobs via Atom Transfer Radical Polymerization," *Polymers,* vol. 11, p. 1715, 10/19 2019, doi: 10.3390/polym11101715.

[148] S. V. Araújo, B. S. Rocha, F. M. T. Luna, E. M. Rola, D. C. S. Azevedo, and C. L. Cavalcante, "FTIR assessment of the oxidation process of castor oil FAME submitted to PetroOXY and Rancimat methods," *Fuel Processing Technology,* vol. 92, no. 5, pp. 1152-1155, 2011/05/01/ 2011, doi: https://doi.org/10.1016/j.fuproc.2010.12.026.

[149] N. Saxena, N. Pal, K. Ojha, S. Dey, and A. Mandal, "Synthesis, characterization, physical and thermodynamic properties of a novel anionic surfactant derived from Sapindus laurifolius," *RSC Adv.,* vol. 8, pp. 24485-24499, 07/02 2018, doi: 10.1039/C8RA03888K.

[150] J. Zheng *et al.*, "Production of Graphite Chloride and Bromide Using Microwave Sparks," *Sci Rep,* vol. 2, no. 1, p. 662, 2012/09/17 2012, doi: 10.1038/srep00662.

[151] Z. Lyu, Q. An, P. Qin, W. Li, and X. Wang, "Preparation and characterization of POSS-containing poly(perfluoropolyether)methacrylate hybrid copolymer and its superhydrophobic coating performance," *RSC Adv.,* 10.1039/C8RA10490E vol. 9, no. 9, pp. 4765-4770, 2019, doi: 10.1039/C8RA10490E.

[152] N. Vandencasteele and F. Reniers, "Plasma-modified polymer surfaces: Characterization using XPS," *Journal of Electron Spectroscopy and Related Phenomena,* vol. 178-179, pp. 394-408, 2010/05/01/ 2010, doi: https://doi.org/10.1016/j.elspec.2009.12.003.

[153] X. T. Cao, N. T. T. Nguyen, V. C. Nguyen, T. T. K. Tu, and K. T. Lim, "Preparation and characterization of silica-polymer/Ag hybrid nanocomposites via surface-initiated single electron transfer living radical polymerization," *Molecular Crystals and Liquid Crystals,* vol. 679, no. 1, pp. 102-110, 2019/01/22 2019, doi: 10.1080/15421406.2019.1597552.

[154] G. McHale, N. J. Shirtcliffe, and M. I. Newton, "Contact-Angle Hysteresis on Super-Hydrophobic Surfaces," *Langmuir,* vol. 20, no. 23, pp. 10146-10149, 2004/11/01 2004, doi: 10.1021/la0486584.

[155] Y. Yuan, M. P. Hays, P. R. Hardwidge, and J. Kim, "Surface characteristics influencing

bacterial adhesion to polymeric substrates," *RSC Adv.,* 10.1039/C7RA01571B vol. 7, no. 23, pp. 14254-14261, 2017, doi: 10.1039/C7RA01571B.

[156] L. N. Nthunya, L. Gutierrez, A. R. Verliefde, and S. D. Mhlanga, "Enhanced flux in direct contact membrane distillation using superhydrophobic PVDF nanofibre membranes embedded with organically modified SiO2 nanoparticles," *Journal of Chemical Technology & Biotechnology,* vol. 94, no. 9, pp. 2826-2837, 2019/09/01 2019, doi: 10.1002/jctb.6104.

[157] M. Zhang, J. Chen, Y. Ma, L. Shen, Y. He, and H. Lin, "Fractal reconstruction of rough membrane surface related with membrane fouling in a membrane bioreactor," *Bioresource Technology,* vol. 216, pp. 817-823, 2016/09/01/ 2016, doi: https://doi.org/10.1016/j.biortech.2016.06.034.

[158] S. Park, E. Yang, H. Park, and H. Choi, "Fabrication of functionalized halloysite nanotube blended ultrafiltration membranes for high flux and fouling resistance," *Environmental Engineering Research,* vol. 25, no. 5, pp. 771-778, 10 2020, doi: 10.4491/eer.2019.402.